Technical Report Documentation Page

1. Report No.	2. Government Accession No.	3. Recipient's Catalog No.
TX - 96 / 2921-1F		

4. Title and Subtitle	5. Report Date
EXPERIMENTAL DESIGN, PLANNING, AND ANALYSIS OF PAVEMENT TEST SECTIONS FOR THE TEXAS MOBILE LOAD SIMULATOR	December 1995
	6. Performing Organization Code

7. Author(s)	8. Performing Organization Report No.
C. C. Pilson, W. R. Hudson, and V. Anderson	Research Report 2921-1F

9. Performing Organization Name and Address	10. Work Unit No. (TRAIS)
Center for Transportation Research The University of Texas at Austin 3208 Red River, Suite 200 Austin, Texas 78705-2650	11. Contract or Grant No. Research Study 7-2921
	13. Type of Report and Period Covered
12. Sponsoring Agency Name and Address Texas Department of Transportation Research and Technology Transfer Office P. O. Box 5080 Austin, Texas 78763-5080	Final
	14. Sponsoring Agency Code

15. Supplementary Notes
Study conducted in cooperation with the Texas Department of Transportation.
Research study title: Experimental Design, Planning, and Analysis of Pavement Test Sections for the Texas Mobile Load Simulator

16. Abstract

This project was undertaken to assist with the design, planning, and analysis of pavement test sections for future use with the newly developed Texas Mobile Load Simulator. It specifically addresses the type, number, and positions for strain and pressure sensors in test sections. In the project, we conducted two full factorial experiments on test sections built by the Texas Department of Transportation (TxDOT) in Victoria, Texas. Using a conventional dump truck, we collected data from various makes of strain and pressure sensors embedded in the pavement at different positions and depths. These data were analyzed to determine variability characteristics by constructing a quadratic response surface model estimated by least squares regression. This analysis was then used to assess precision of measurements, with the model used to compare measured values with theoretically predicted values for an assessment of accuracy. In this way, conclusions with regard to the make, number, and position of sensors for future experimental test sections could be drawn.

We found that HBM DA3 strain gauges and Kulite pressure cells gave the most precise and most accurate results; these are therefore recommended for future experiments. It is recommended that between 9 and 17 strain and pressure sensors be used per section. While HBM sensors appear to give reasonably accurate results, it appears that other types of strain gauge tested adequately under measured strain.

17. Key Words	18. Distribution Statement
Texas Mobile Load Simulator, accelerated pavement testing, test section design, pavement instrumentation	No restrictions. This document is available to the public through the National Technical Information Service, Springfield, Virginia 22161.

19. Security Classif. (of this report)	20. Security Classif. (of this page)	21. No. of Pages	22. Price
Unclassified	Unclassified	131	

Form DOT F 1700.7 (8-72) Reproduction of completed page authorized

EXPERIMENTAL DESIGN, PLANNING, AND ANALYSIS OF PAVEMENT TEST SECTIONS FOR THE TEXAS MOBILE LOAD SIMULATOR

C. C. Pilson
W. R. Hudson
and
V. Anderson

Research Report 2921-1F

Research Project 7-2921
Experimental Design, Planning, and Analysis of Pavement Test Sections
for the Texas Mobile Load Simulator

conducted for the

Texas Department of Transportation

by the

CENTER FOR TRANSPORTATION RESEARCH
Bureau of Engineering Research
THE UNIVERSITY OF TEXAS AT AUSTIN

December 1995

IMPLEMENTATION STATEMENT

The recommendations of this project will be very useful, if not vital, in deciding on types, numbers, and placement of strain and pressure sensors in future experiments with the Mobile Load Simulator. Such guidelines will ensure that measurements obtained are statistically significant. In addition, many other aspects of future experiment design are discussed and guidelines are given regarding the sample rate for data collection, the possible range of waveform characteristics that can be collected, and the number of load applications that should be measured at one time. Finally, guidelines provided for the possible development of a dedicated database will certainly provide a sound basis for its implementation.

Prepared in cooperation with the Texas Department of Transportation.

DISCLAIMERS

W. R. Hudson, P.E. (Texas No. 16821)
Research Supervisor

TABLE OF CONTENTS

SUMMARY

This project was undertaken to assist with the design, planning, and analysis of pavement test sections for future use with the newly developed Texas Mobile Load Simulator. It specifically addresses the type, number, and positions for strain and pressure sensors in test sections. In the project, we conducted two full factorial experiments on test sections built by the Texas Department of Transportation (TxDOT) in Victoria, Texas. Using a conventional dump truck, we collected data from various makes of strain and pressure sensors embedded in the pavement at different positions and depths. These data were analyzed to determine variability characteristics by constructing a quadratic response surface model estimated by least squares regression. This analysis was then used to assess precision of measurements, with the model used to compare measured values with theoretically predicted values for an assessment of accuracy. In this way, conclusions with regard to the make, number, and position of sensors for future experimental test sections could be drawn.

We found that HBM DA3 strain gauges and Kulite pressure cells gave the most precise and most accurate results; these are therefore recommended for future experiments. It is recommended that between 9 and 17 strain and pressure sensors be used per section. While HBM sensors appear to give reasonably accurate results, it appears that other types of strain gauge tested adequately under measured strain.

CHAPTER 1. INTRODUCTION AND BACKGROUND

1.1 BACKGROUND

1.1.1 Accelerated Pavement Testing Using TxMLS

Accelerated pavement testing (APT) is just one of the methods used in the transportation industry to study factors that affect pavement performance [McNerney 94]. Other methods range from simple engineering judgment, to laboratory testing, to small in-situ road tests, and, ultimately, to large studies like the AASHO Road Test [Carey 62] and the Strategic Highway Research Program's (SHRP's) Long-Term Pavement Performance Program (LTPP).

It is generally accepted [Haas 94] that, among pavements and their life cycles, there are four broad classes of variables that can be observed (objectively or subjectively). The first and most basic class is comprised of the material properties themselves. These properties include elastic moduli, Poisson's ratio, shear moduli, and creep compliance. Other dimensional characteristics, such as layer thickness, also fall within this class. The next class is that pertaining to behavior. This is generally defined as the pavement's direct response to loading and typical variables, including such things as deflections and strains. Pavement distress, the third class, is a measure of such things as rutting and cracking. Finally, pavement performance, the fourth variable, is considered to be a measure of the serviceability of the pavement over time.

The ultimate goal of almost all studies involving pavements is to predict pavement performance. If the future performance of the pavement can be predicted, then initial design and construction, as well as ongoing rehabilitation and maintenance, can be optimized in terms of life cycle or, more generally, long-term total costs. This prediction is presently carried out through fairly subjective methods (e.g., visual condition surveys of current distress) or through reasonably sophisticated methods (e.g., theoretical and mechanistic 3-D finite element modeling). Without exception, however, all methods have as their fundamental building block some form of "prediction model." Figure 1.1 illustrates the numerous different routes that the prediction of pavement performance might take. A large portion of pavement research is dedicated to finding new models to link various variables, and then calibrating these (or previously proposed) models.

These prediction models may be purely mathematical or theoretical. For instance, linear elastic layer theory and Westergaard's equations have contributed substantially to pavement behavior theory. The theoretical models themselves may vary in how exactly they represent real conditions, however, and doubts have been expressed for some time [Zafir 94] about how applicable linear elastic theory really is to the prediction of long-term performance. In addition, dynamic behavior is only now being more comprehensively addressed and modeled.

Models may also be purely empirical. They may, for example, serve to relate distress and performance directly, purely by utilizing some basic initial pavement variables and historical databases containing distress data to generate "performance curves" without any knowledge of

the fundamental, underlying processes being needed. Ultimately, until the theoretical models (and the means to measure their required input variables) are developed to the point where models relating current response or distress to future performance may be *derived*, a combination of approaches where theoretical models are empirically calibrated to actual results will be needed. These have been termed mechanistic-empirical methods [AASHTO 93].

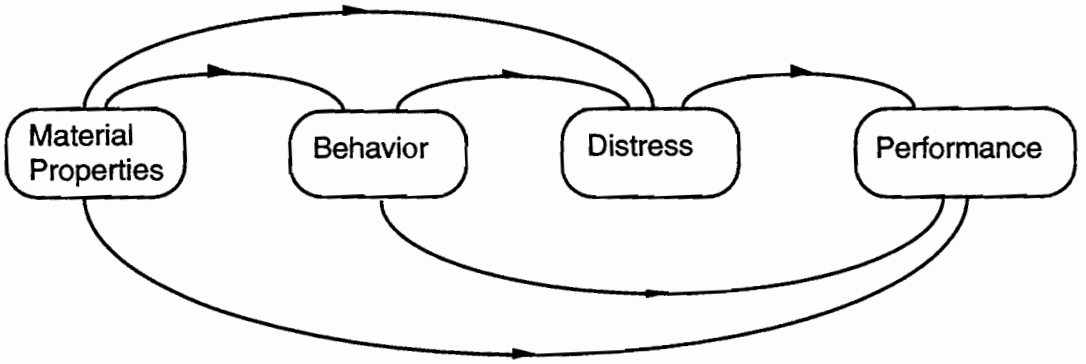

Figure 1.1 Prediction models for pavement variables

With APT, almost the whole range of variable classes may be measured to some extent, since APT sets out to model actual pavement loading conditions as closely as possible, while still retaining a measure of control over most input variables. This is especially true of the newly built Texas Mobile Load Simulator (MLS), which attempts to overcome the perceived limitations of previous APT devices — that of the dynamic aspect of pavement/vehicle interaction. With the versatility of, and the closer conformance to real conditions obtained by, the MLS, engineers and researchers now theoretically have the ability to pursue any of the models in the network shown in Figure 1.1. The fundamental necessity is, of course, that the variables not only be measured, but that the variability of the measurements be observed as well. It is vital, therefore, that the stochastic nature of both input and output variables be recognized and assessed, whether these be micro-variations in pavement thickness, normal changes in instantaneous loading, or macro-variations in PSI derived from visual condition surveys.

It is difficult to classify the many different variables as "input" or "output" variables within the "behavior" and "distress" classes, since the input for one model may be either measured directly or be the output from some other model. It is probably correct to say, however, that there are numerous fundamental input variables. These may be categorized as initial physical characteristics of the pavement, and as loading and environmental variables. These are shown in Table 1.1. It should, however, be stressed that many of the physical characteristics do change during a pavement's life. Changes in layer thickness resulting in rutting or loss of stiffness (fatigue) are obvious examples.

Table 1.1 Input variables

Material Properties	Physical Characteristics	Load	Environmental
Resilient Modulus Poisson's Ratio Plasticity Complex Shear Modulus Friction between layers, etc.	Pavement layer thickness Surface profile, etc.	Magnitude of load Position of load Speed of load Direction of load Micro Variability of load, etc.	Temperature Moisture, etc.

We may then define a class of "intermediate" variables consisting of behavior and distress variables, which we will need to measure for the purposes of calibration or checking of output from fundamental (and most often theoretical) models, or as input to final stage performance prediction (often empirical) models. These are shown in Table 1.2.

Table 1.2 Intermediate variables

Behavior / Response	Distress
Deflection Stress Strain Permanent Deformation	Cracking Rutting Surface Roughness Surface Friction

The true output variables for the process as a whole are related to the serviceability as seen by the road user, and the maintenance and rehabilitation measures required of the agency. The combination of the two is vital, since the ultimate goal of pavement research is improved overall efficiency in the management of pavement networks; and one of the ways of accomplishing this is to minimize overall, long-term costs as an objective function using minimum serviceability to the road user as a constraint. Since pavement serviceability is largely a function of roughness and has only a relatively small "distress" component, we also need to classify roughness as a major variable. While not normally the case, roughness should probably be considered as a form of distress under this system.

Table 1.3 Output variables

Performance	Pavement Management
Pavement Serviceability Index Safety	Maintenance, Rehabilitation, and Reconstruction Strategies and Timing

Having described many of the variables involved, we may now go on to briefly mention ways of measuring them. Variables from the first category are generally measured using various

laboratory tests. They may, of course, also be "backcalculated" from measurements of response or even distress variables with varying degrees of success. Distress is more difficult to measure objectively, though various image processing, ultrasonic, and radar techniques are being investigated and used in such units as the "ARAN" vehicles to measure longitudinal and transverse profiles and to detect voids under rigid pavement [Lu 91]. Mainly because of the prohibitive cost of these technologies, however, distress is still measured largely through visual surveys. Direct response variables, such as strain or deflection, are also commonly measured in both research and field environments, with deflection measurements obtained through the falling weight deflectometer (FWD) being the best known example. Response can be measured either just at the surface (FWD) or at various depths in the pavement, though this is generally only possible under experimental conditions.

Another area of interest is the dynamic behavior of pavements, a subject currently being investigated through the Spectral Analysis of Surface Waves (SASW) method. Nonetheless, it is the measurement of such basic response variables as strain and deflection at various depths in the pavement *under real (or at least realistic) loads* that is most desirable, both when quantitative assessment of fundamental deterministic models is sought and when successive empirical models to predict performance directly are being developed. Continuous (instantaneous at a reasonably high sampling rate) measurement of load, load position, strain and deflection is thus a vital research tool in the overall investigation of pavements using APT. While load and load position are vital, these are "input variables," and will generally be measured from the MLS itself. The response variables, for instance, deflection and strain, will, however, be measured from within the pavement; this is generally termed "pavement instrumentation."

1.2 OBJECTIVES

1.2.1 General Objectives of Pavement Instrumentation

For this project, it is necessary to think in terms of a general method for designing future experiments. Since these experiments could potentially cover a huge range in terms of scope and objective, we need to define a general objective that would encompass as much of that range as possible.

As was discussed in the previous section, pavement sensors measure the direct response or behavior of the pavement; APT devices are a good way of generating this response with a fair degree of accuracy, since experiments are largely controllable and repeatable. In the case of an APT device such as the MLS, what is measured is, in fact, a cross section of the three-dimensional dynamic strain, pressure, or deflection profile across the pavement. This is illustrated in Figure 1.2.

If all input variables are assumed to remain constant longitudinally, then having a wheel load pass over a measurement point in the pavement (i.e., the sensor) is basically equivalent to holding the wheel stationary and measuring along the line of the sensor relative to the wheel load in the pavement. It is important to note, however, that the profile measured would still be the profile for the dynamic case, and might be expected to be asymmetric either side of the load

owing to visco-elastic effects and to the momentum of the pavement layers. If dynamic effects were neglected and the pavement response was assumed to be axi-symmetric around the load point (as various simpler theoretical models imply), we would need only a single sensor at the center of the wheel path to be able to construct the entire 3-D response profile for a particular depth (that is, response as a function of both the longitudinal and transverse distances from the load). If we do not wish to neglect the fact that the load is moving, however, it might still be possible to construct the entire behavior surface by assuming longitudinal linear symmetry and by using a suitable transition function to generate the polar transition between the response wave shape preceding the load and that following the load.

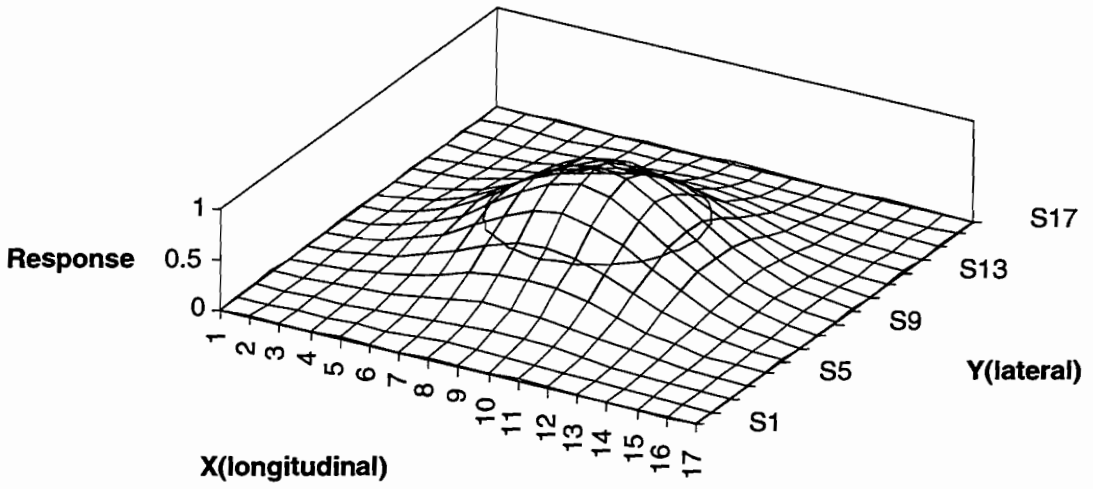

Figure 1.2 Example of a 3-D behavior profile

A major reason, however, for not using a single sensor is the expected variability; accordingly, a certain number of observations (the number will depend on the magnitude of that variability) is needed to obtain an expected value (mean) with reasonable reliability for the measurement based on the sample.

The general objectives of pavement instrumentation are:

- to measure the 3-D profile of a particular pavement response for a set of controlled test variables; and
- to do this in such a way that the profile constructed from the measurements is as close as possible to the actual profile with a known confidence range.

Finally, having summarized the objectives above, the *reasons* for measuring this 3-D profile are twofold. As discussed in the first section, the response variables lie in the middle of the overall progression from fundamental material properties to pavement performance. They therefore serve, first, as checks of output from preceding models (as well as input for backcalculation using the same models) and, second, as input for succeeding models seeking to predict distress or performance from measured pavement behavior.

1.2.2 Specific Project Objectives and Scope of Study

The general objectives in instrumenting pavements were summarized above as the need to measure pavement response as accurately as possible. While this is easily defined, it is very difficult to accomplish in practice for two reasons: we cannot tell how accurate the measurements are unless we know exactly what they should be, and, unless we know the expected variance in our measurements, we cannot even adequately define what our initial measurements are.

Taking the above two problems in reverse order, it is therefore evident that we would normally need to assess two things:

1. *Precision of measurements:* We need to assess the variability in individual measurements in order to identify the necessary sample size (number and location of sensors to install in pavement test section, as well as number of measurements to take) so a measured profile can be constructed to a chosen reliability.
2. *Accuracy of measurements:* We need to assess how close this measured profile is to the real or actual profile for the purpose of calculating a systematic error correction ("calibration factor"), which may be applied to the measured profile to obtain the real profile.

The concepts of precision and accuracy are illustrated in Figure 1.3. It is evident that the precision may be determined by setting up a controlled factorial experiment so that the variability in the individual readings from a fairly large sample may be calculated, after which the necessary sample size for future experiments may be calculated to obtain the final measured response within a chosen tolerance to a chosen reliability.

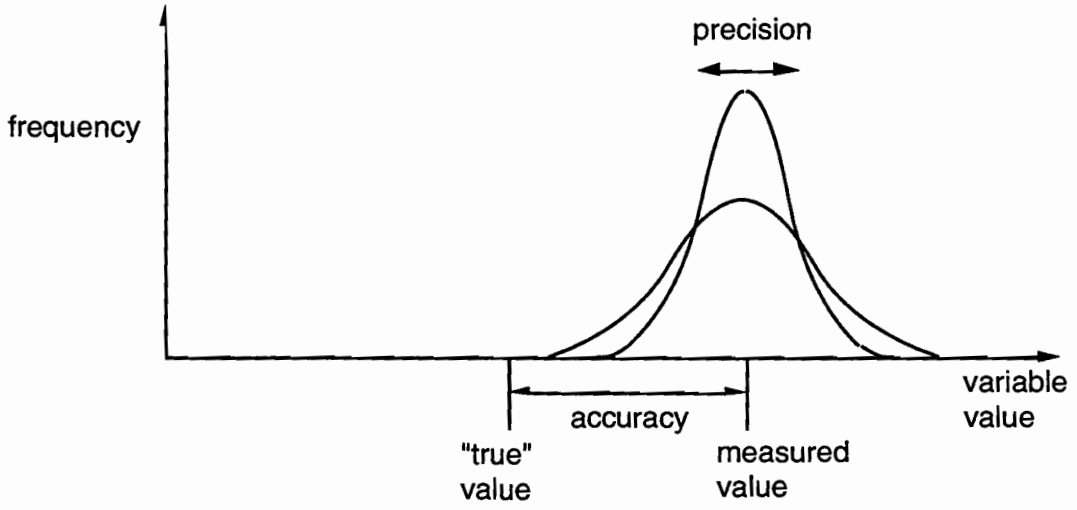

Figure 1.3 Illustration of precision and accuracy

It is also evident that determining accuracy is difficult, since just the act of installing a sensor itself affects the subsequent behavior of the pavement at that point. In essence, the act of measuring affects the measurement. This effect will vary depending on, for instance, whether the sensor is installed during construction or retrofitted. It will also depend on numerous properties of the sensor itself (e.g., the stiffness, length, etc.). The basic problem is, however, that *some* effect will always be present and, therefore, the only possible way of obtaining the real value for comparison with measured values is by calculating it from theory. This introduces a paradox, since one of the basic reasons we wish to measure the response is to test our theories! Nonetheless, if we can identify and minimize the factors likely to produce this systematic error (for instance, by choosing very light sensors having very low stiffnesses), we can at least assume that we will be minimizing the systematic error.

Because the statistical evaluation of the precision or variation in the individual measurements *must* precede any assessment of accuracy, it is the evaluation of this variation that is the main objective of this project. Some very subjective assessment of the accuracy will need to be included, however, in order to get a feeling for the accuracy (assessing the accuracy of the measurements in detail represents a worthwhile subject for future study). In practice, it should often be the case that data are collected from sensors of only one particular type, with all installed using the same method. What will then be important to researchers will be differences and trends in these data, and these may be assessed without necessarily needing to know the absolute magnitudes to a high degree of accuracy.

The objectives of the study can therefore be summarized as the following:

1. Assess the variability in sensor measurements not due to any intended changes in the input variables listed in Table 1.1.
2. Use the variance evaluated above to assess required sample sizes for future experiments using the MLS.
3. Develop a generalized systematic method for accomplishing 1 and 2.
4. Provide this information to TxDOT by means of documents and reports.

1.3. GENERAL METHODOLOGY

1.3.1 Sources of Variation

Quite evidently there are a great many sources for variation in response measurements, and some estimation of these is vital for accomplishing the objectives laid out above. Most obviously, variation in measured response will result from the construction (type) and installation of the sensors themselves. In addition, variation will obviously exist owing to variations in any of the input variables from Table 1.1 (in the first section), whether they are quantified and intended or unintended microvariations. In terms of ultimately constructing all or part of the 3-D response profile discussed in the previous section, we theoretically need to determine variance caused by unmeasured microvariations in pavement thickness, profile,

material properties, and bogie-pavement interaction as a function of the known *mean* input variables from Table 1.1. These microvariations may occur through time, position in the pavement, or through both. In other words, there may be variation at a specified point as well as between two points in any MLS test section. A sample therefore needs to be taken both of different points in time and at different positions (points in space).

Finally, there will probably be a "noise" variation associated with each sensor owing to electronic interference and digitization of the signal. This may be dependent on which sensor or type of sensor the measurement comes from, but is likely to be largely independent of other variables.

In order to evaluate variation at a number of representative points in the response profile as a function of mean input variables, a factorial experiment is required that will cover the basic ranges of input variables and will give a large enough sample size to assess variation relatively accurately. This is discussed in detail in a later section.

Prior to this full factorial experiment, however, it is necessary to perform a pilot experiment to check which sensors were still working and obtain an initial estimate of the initial variation as input for the design of the final factorial experiment. This was carried out and is discussed in more detail in a later section.

1.3.2 Data Collection and Storage

It is obviously possible with modern technology to collect data at an extremely high sample rate (e.g., rates of 10,000 samples per second are not uncommon). This can result in a virtually continuous profile being generated, though at the cost of huge volumes of data. While much has been said about the ultimate objective of measuring the complete 3-D response profile, it has been suggested that this could be roughly and relatively easily constructed from a single continuous longitudinal profile taken at the center of the wheel path. This is the most readily collected; a typical strain profile for a single moving load is shown below in Figure 1.4.

Looking ahead to the eventual creation of a dedicated response measurement database for the MLS, it will probably be necessary to simplify this single profile even further. In this study, it is suggested that the storage of a few relevant points on the profile should be adequate for the foreseeable future. This is in line with practice elsewhere and, for instance, in the Organization for Economic Cooperation and Development (OECD) tests in Nantes, France, in 1989, [OECD 91] three characteristics of the strain response were stored. These were the first compressive peak, the tensile peak, and the distance between them.

These peaks are evident from Figure 1.4. Although the strain profile possesses a number of maximums and minimums, much valuable analysis has been accomplished using only the maximum tensile strains in the past; accordingly, only the maximums are used for statistical analysis in this study. For future study, however, it is suggested that there may well be merit in storing more than just the maximum; this is discussed in more detail under the section dealing with data collection and reduction methods.

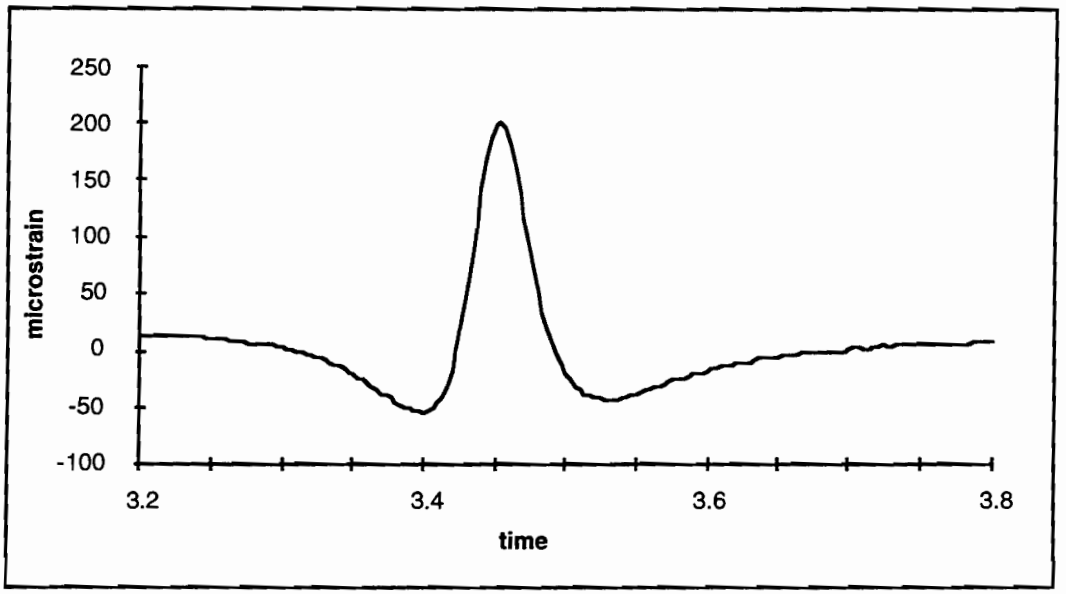

Figure 1.4 Typical measured strain profile for a single moving load

1.3.3 Data Analysis

Once the data have been collected and reduced, a variety of analyses may be performed to investigate changes in response caused by intentional input variable changes. The main objective in this study, however, is assessing changes *not* due to intentional input variable changes. By investigating variability in the data, recommendations can be made for future MLS experiment designs, the most specific being the type, number, and placement of sensors needed to attain chosen levels of reliability.

1.3.4 Deliverables

The main deliverable for this study is intended to be a generalized experiment design procedure for future MLS experiments. This report, therefore, provides the background and a foundation for this procedure; in addition, it provides numerous specific guidelines for use when designing future experiments. Recommendations regarding the type of sensor that should be used in the future, the number and placement of these sensors, and the number of load passes that should be measured at a time are all therefore well documented. Finally, a systematic method for data collection, reduction, and storage is proposed based on a brief discussion of the stated objectives for the MLS, and the resulting possible areas for future experiments.

CHAPTER 2. SENSORS

2.1 DESCRIPTION OF SENSORS

2.1.1 Strain Gauges

The strains in flexible pavements have historically been among the most interesting to researchers concerned with pavement behavior variables [Rauhut 82, Rowe 95, Scazziga 87]. This is largely because they are generally considered easier to measure and are related to stress through elastic modulus; moreover, both fatigue failure and rutting appear to be almost always closely related to strain in the surface layer. Rutting and permanent deformations are related to vertical compressive and shear strains, while fatigue cracking is related to high lateral strains, normally at the bottom of the surface layer. The disadvantage of measuring strains, while closely related to deflections, appears to be that it is rarely possible to measure absolute strains, as is possible for deflections with linear variable differential transformer (LVDT) instruments (e.g., multidepth deflectometers). This limits measurement to dynamic comparative observations only during the loading and unloading cycles of the pavement. Maximum compressive and tensile strains may then be compared to an assumed zero strain for the case with no load applied. This is generally enforced by "balancing" the strain to zero before loading and measurement are begun.

Measurement of strains in flexible pavements is usually accomplished by placing strain gauges at the point at which measurement is desired in the pavement. Since the critical strains (at least for fatigue cracking) are generally found at the bottom of the asphalt layer, the vast majority of strain gauges in test pavements have been installed laterally at this interface between the surface layer and the base. The numerous different types of strain gauges available commercially can either be installed as the pavement is constructed or can be retrofitted later.

Methods of measuring strain include various mechanical, acoustical, optical, pneumatic and electrical techniques. The most common and applicable method for use in pavements are the electric techniques. These include capacitance and inductance strain gauges, piezoelectric gauges, and gauges based on the change in electrical resistance with strain. The vast majority of gauges use this last effect and are termed "bonded resistance strain gauges." This term can be applied to non-metallic (semiconductor) gauges, or to metallic (wire or foil) gauges. While semiconductor gauges are generally more sensitive, they unfortunately do not exhibit a linear change in resistance with strain. Both foil and semiconductor gauges are also temperature sensitive. This temperature sensitivity, however, is generally not a major problem if extremes in temperature are avoided. The Kyowa KM gauges, for instance, undermeasure by a maximum of 1.8 microstrain per degree centigrade on either side of 20°C down to 10°C and up to 40°C [Omega 92]. In time, if other variation is reduced to the extent that this becomes important, this effect may generally be relatively easily corrected for either in the data acquisition software or in post processing.

Because gauges as manufactured are not generally considered suitable for use in pavements, researchers often assemble their own. The most common method of doing this is to

enclose the foil gauge between two layers of plastic material and then to attach stiff (mostly brass) anchors to the ends. This results in the family of gauges known as "H-gauges." A notable exception to this is the HBM DA3 gauge, which is manufactured specifically for use in pavements.

Three flexible pavement test pads were constructed in Victoria, Texas, for the testing of the MLS and associated instrumentation. Five different types of strain sensors were selected for installation in these test pads and for further testing (based on the literature and experience in other road tests). Particular attention was paid to the recent work by Sebaaly et al. [Sebaaly 89, Sebaaly 92] on instrumentation for flexible pavements for the FHWA Accelerated Loading Facility (ALF), as well as to the OECD tests at Nardo, Italy, in 1984, and Nantes, France, in 1989 [Scazziga 87, OECD 91]. From initial tests of construction-placed sensors, one or possibly two types were to be chosen for use in retrofit experiments. The five different types are described in more detail below.

HBM DA3 Gauges

Made by:	Hottinger Baldwin Measurements
	139 Newbury Street, P. O. Box 1500
	Framingham, MA 01701 USA
	Tel. (617) 875-8282/3/4/5
Dist. by:	Austin Measurement Technologies
	9218 Balcones Club Drive #1322
	Austin, TX 78750
Contact:	Jon Sutherland
Temp. Sensitivity:	NA (Suggest using compensation gauge)

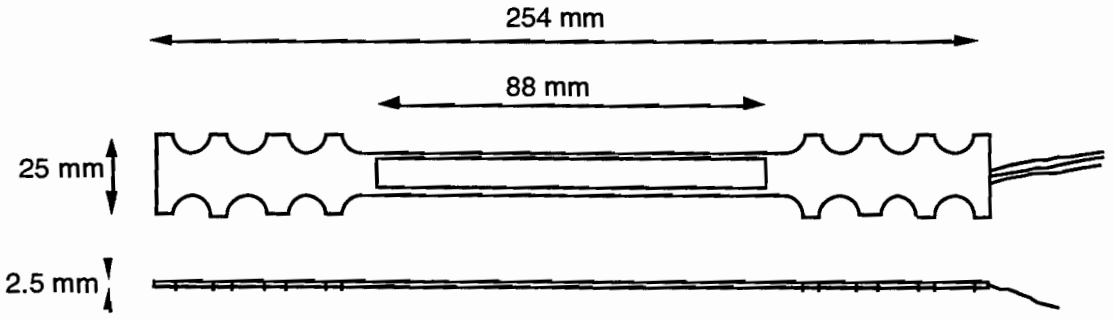

Figure 2.1 Dimensions of HBM strain gauge

Tokyo Sokki PML 60 Gauges

Made by: Tokyo Sokki Kenkyujo Co., Ltd.
Dist. by: Texas Measurements
P. O. Box 2618
College Station, TX 77841
Tel. (409) 764-0422
Contact: Susan Harris
Temp. Sensitivity: (See Figure)

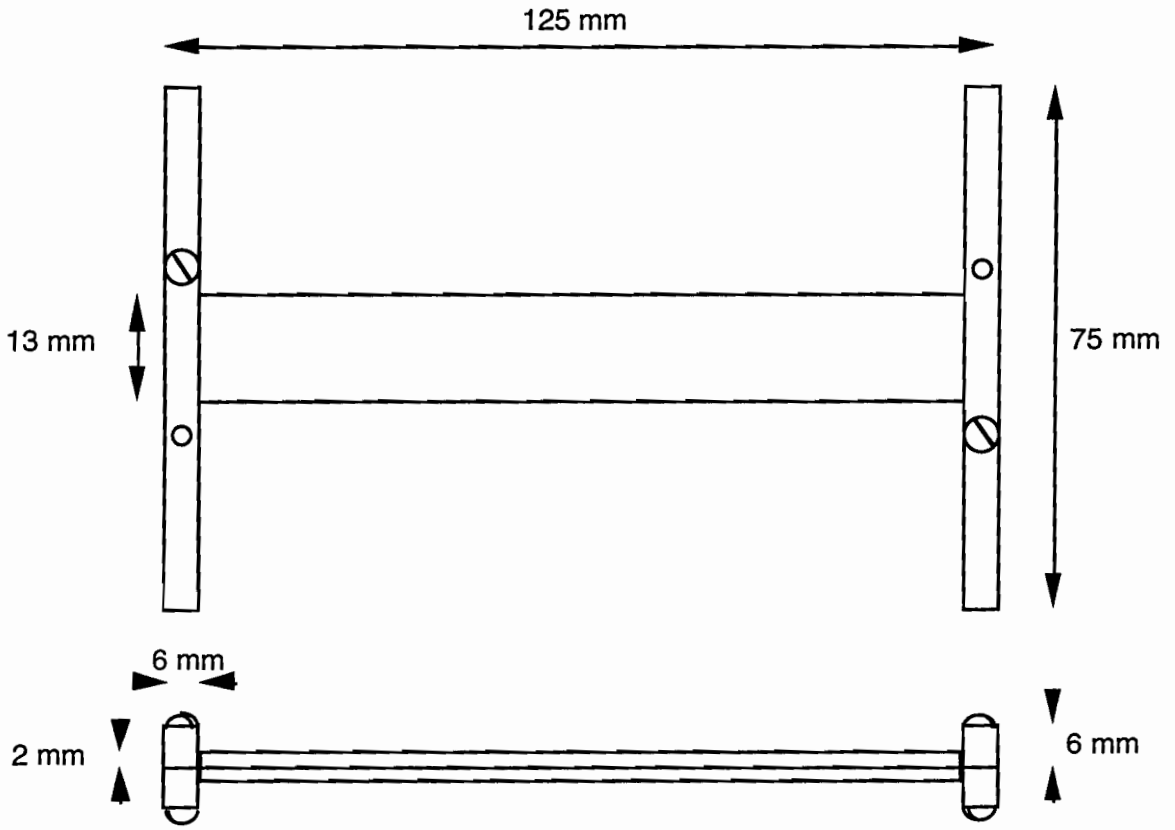

Figure 2.2 Dimensions of Tokyo Sokki PML 60 gauges

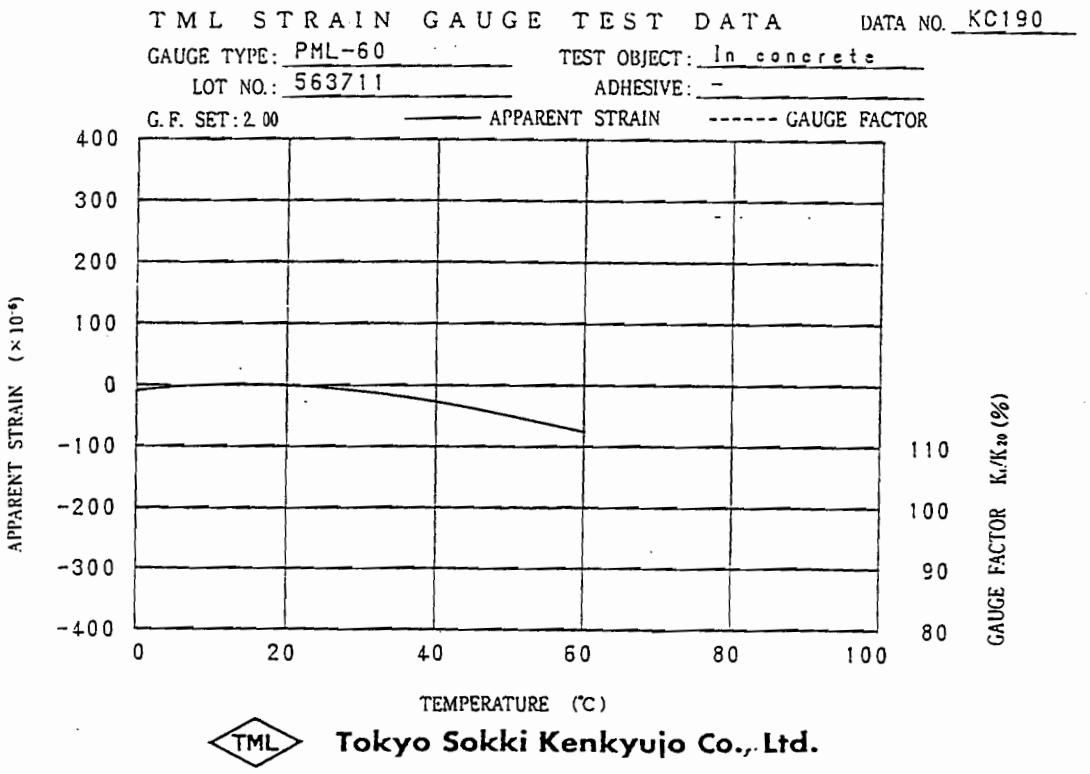

Figure 2.3 Typical temperature sensitivity of a Tokyo Sokki PML 60 gauge

Tokyo Sokki PML 120 Gauges

Made by: Tokyo Sokki Kenkyujo Co., Ltd.
Dist. by: Texas Measurements
P. O. Box 2618
College Station, TX 77841
Tel. (409) 764-0422
Contact: Susan Harris
Temp. Sensitivity: NA

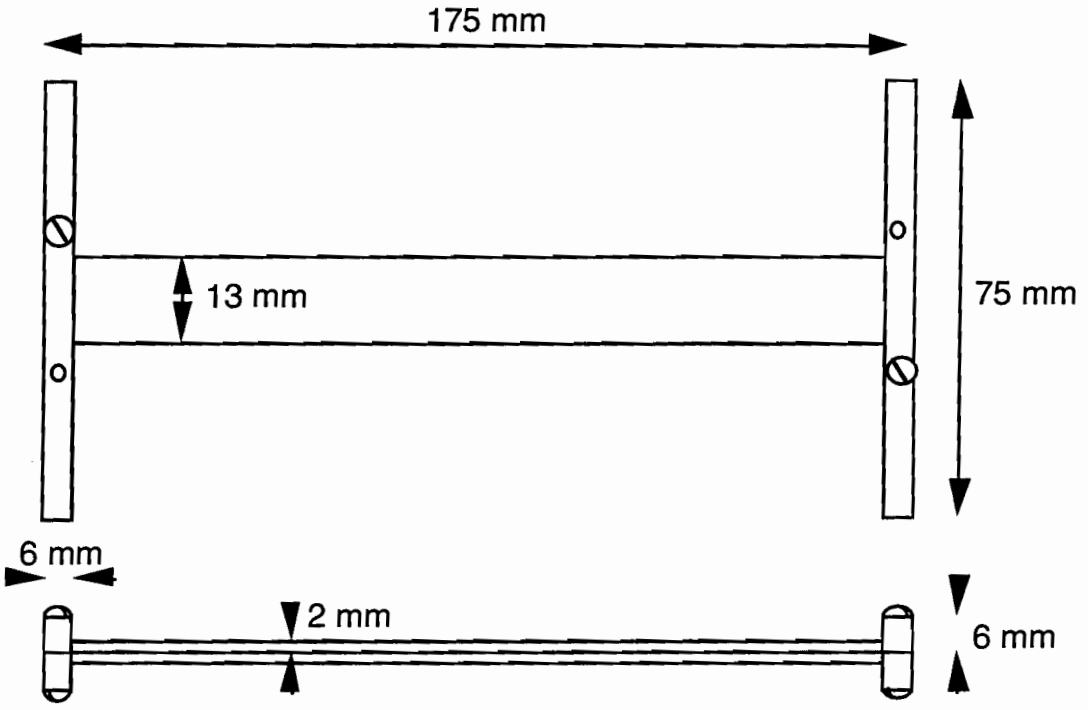

Figure 2.4 Dimensions of Tokyo Sokki PML 120 gauges

Tokyo Sokki PMR 60 Gauges

Made by:	Tokyo Sokki Kenkyujo Co., Ltd.
Dist. by:	Texas Measurements
	P. O. Box 2618
	College Station, TX 77841
	Tel. (409) 764-0422
Contact:	Susan Harris
Temp. Sensitivity:	NA

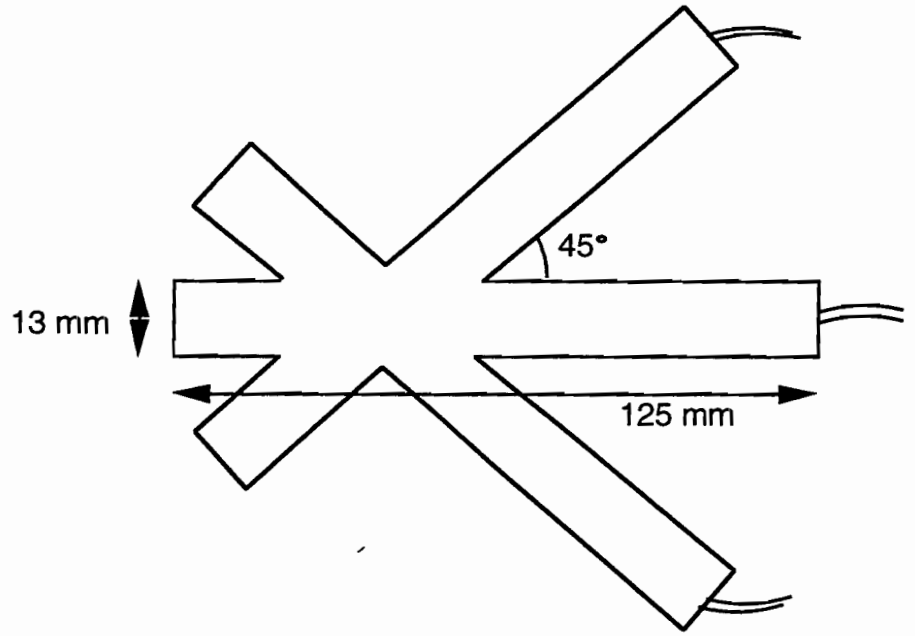

Figure 2.5 Dimensions of Tokyo Sokki PMR 60 gauge

Kyowa SKW 1379 Gauges

Made by:	Kyowa Electric Instruments Co., Ltd.
Dist. by:	SOLTEC CORP.
	12977 Arroyo St.
	San Fernando, CA 91340
	Tel. (818) 365-0800
Contact:	Lonnie Lucas
Temp. Sensitivity:	Max. 1.8 microstrain under measured per degree centigrade more or less than 20°C

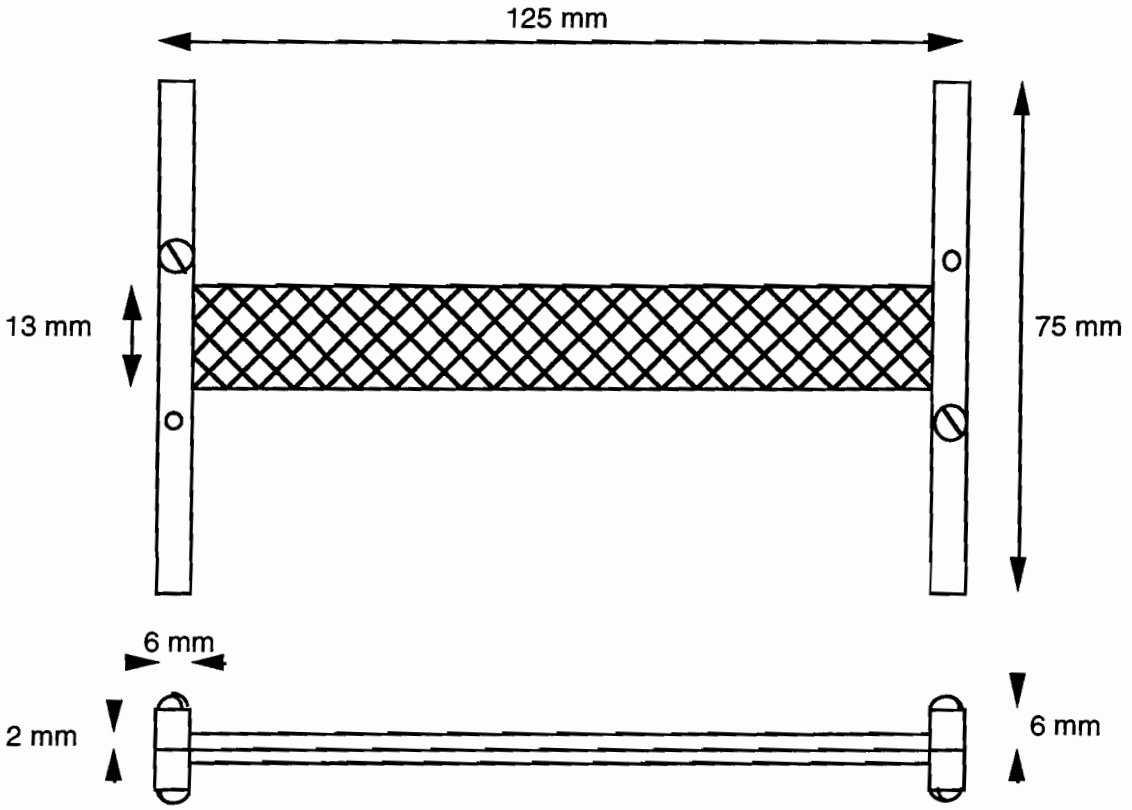

Figure 2.6 Dimensions of Kyowa SKW 1379 gauges

Kyowa PML-120--120-H2 -11 Gauges

Made by: Kyowa Electric Instruments Co., Ltd.
Dist. by: SOLTEC CORP.
12977 Arroyo St.
San Fernando, CA 91340
Tel. (818) 365-0800
Contact: Lonnie Lucas
Temp. Sensitivity: Max. 1.8 microstrain under measured per degree centigrade more or less than 20°C

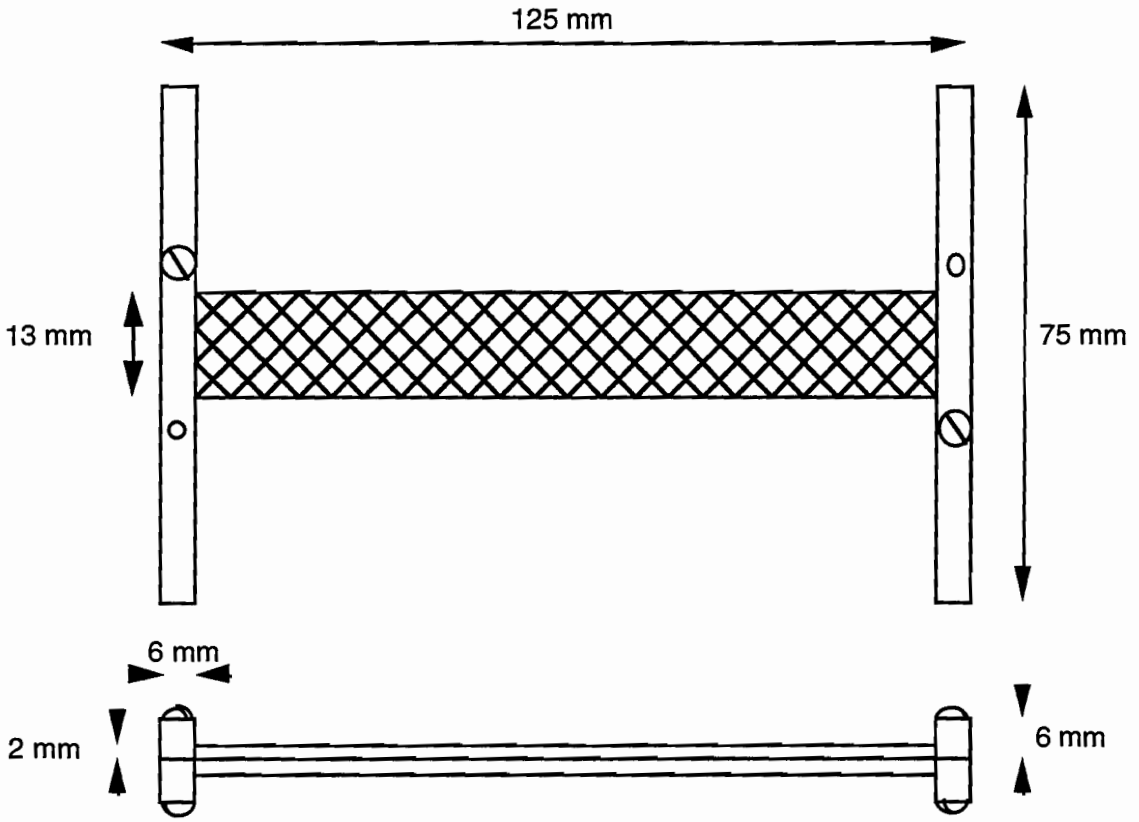

Figure 2.7 Dimensions of Kyowa PML-120 gauges

2.1.2 Pressure Cells

It is generally accepted that accuracies in pressure measurement in soils better than 20 percent are not readily attainable because of the many difficulties in designing and installing these cells [Brown 77]. Nonetheless, some assessment of the stress fields in soil is possible, and this is often a valuable addition to our understanding about the response of pavements under loads.

Of the many different types of pressure cells that exist, most are generally in the form of a circular disk, where either the pressure plate is rigid and the whole disk is compressible or the disk contains a flexible diaphragm. The pressure may be measured in a number of ways, including by hydraulic cells, by LVDT pressure cells, by piezoelectric pressure cells, and by various cells incorporating different strain measuring methods.

The two major problems associated with pressure cells are that they inevitably (1) change the stress state in the soil mass around them and (2) disturb the soil and therefore the material properties around them. The major factors in the gauge affecting the free field stress in the surrounding soil are the ratio of the stiffness of the gauge to the stiffness of the soil, and the aspect ratio, or thickness to diameter ratio, of the gauge. These factors were combined in theoretical analysis by Tory and Sparrow [Brown 77], who also defined a Flexibility Factor.

Aspect Ratio = B/D

Flexibility Factor = $E_s d^3/E_c t^3$

where

B = cell thickness,
D = cell diameter,
E_s = Young's Modulus of soil material,
E_c = Young's Modulus of cell material,
d = diameter of the cell diaphragm, and
t = thickness of the cell diaphragm.

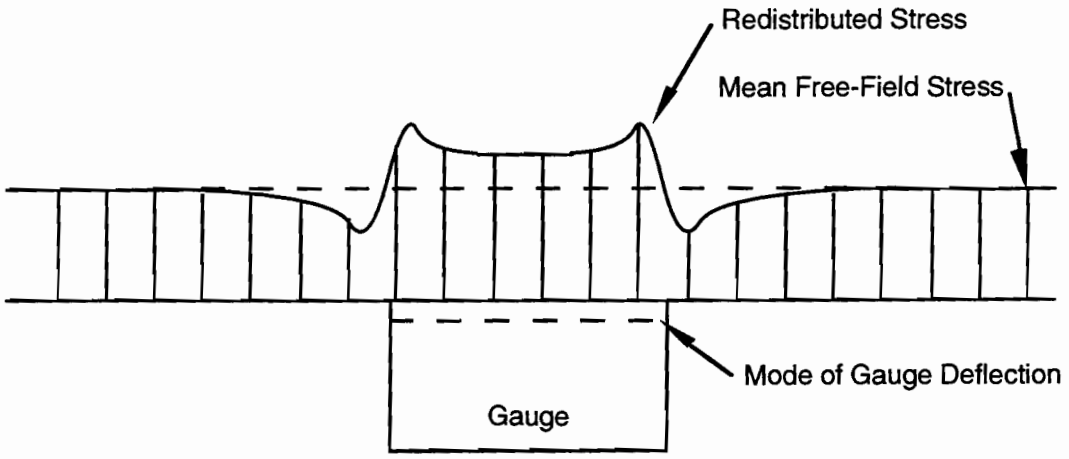

Figure 2.8 Redistribution of stress around pressure cells for gauge more stiff than soil [after Brown 77]

It appears that if the Flexibility Factor and the aspect ratio are kept less than 0.2, relatively good cell readings can be obtained. A further consideration is the size of the diaphragm. Because high pressures develop near the edges of the cell face, as shown in Figure 2.8, this should be relatively large (at least 50 times the diameter of the largest soil particle), but it has been suggested for cells less than about 75mm in diameter, the area of the diaphragm should be less than 45 percent of the total face area.

The two types of pressure cells used in the test pads in Victoria are described below.

Kulite 0234-40-100G Type Pressure Cell

Made by: Kulite Semiconductor Products Inc.
Dist. by: Kulite Semiconductor Products Inc.
One Willow Tree Road
Leonia, New Jersey 07605
Tel. (201) 461-0900
Contact: Paul Thurber/Bill Bayers
Temp. Sensitivity: <1.00% FRO./°F

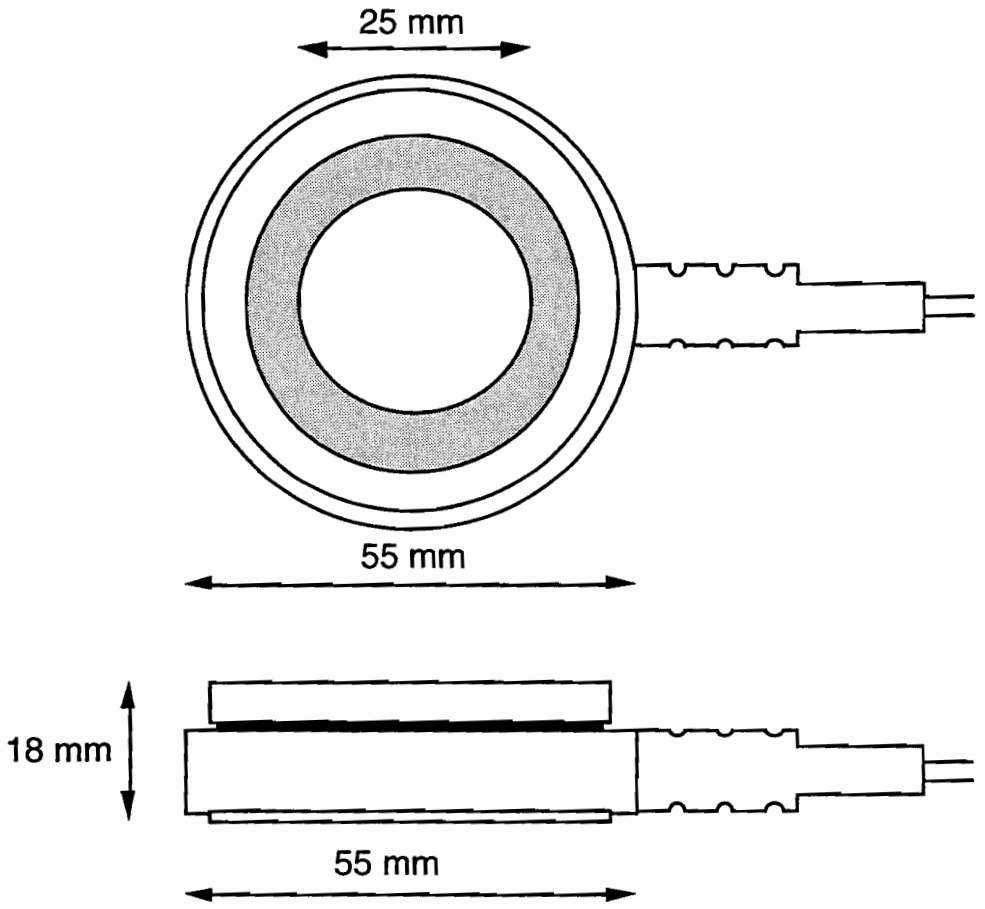

Figure 2.9 Dimensions of Kulite 0234 type pressure cell

Geokon 3500-100/Sensotech LM/2345-02 Type Pressure Cell

Made by:	Geokon
Dist. by:	Geokon
	48 Spencer Street
	Lebanon, NH 03766
	Tel. (603) 448-1562
Contact:	John McRae
Temp. Sensitivity:	NA

This is actually manufactured by Geokon, but incorporates a transducer manufactured by Sensotech.

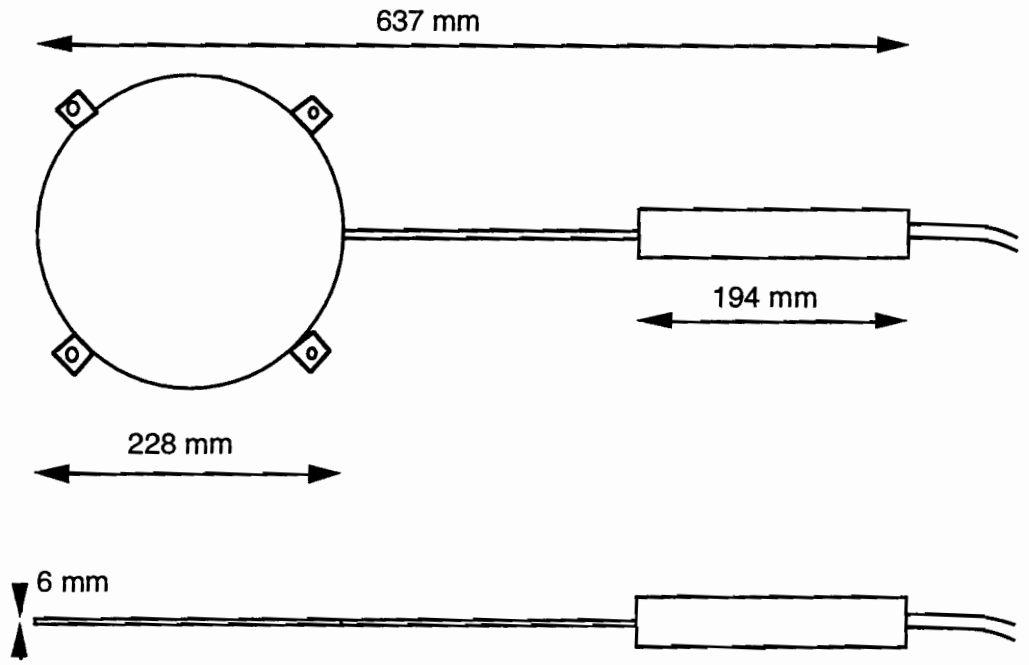

Figure 2.10 Dimensions of Geokon /Sensotech LM/2345-02 type pressure cell

2.1.3 Multidepth Deflectometers

Deflection measurements — both at the surface and within the pavement — have long been of primary interest to researchers. The vast majority of deflection measurement is concerned with vertical deflections, and one of the most common examples of the use of pavement deflections is in the investigation of layer properties using the falling weight

deflectometer (FWD), and Dynaflect. Because pavements behave as multilayer systems with semi-infinite depth, a number of backcalculation procedures exist to assess material properties using various theoretical models which predict what the magnitude and shape of the surface deflection bowl should be. However, because no unique solutions exist and many models do not take into account the dynamic implications of FWD and Dynaflect measurements, it is obviously highly desirable to be able to measure deflections, firstly, at different depths and, secondly, not only maximum deflections, but also their full time history. Different methods of measuring vertical deflections exist and these may be classified into three main groups.

1. Acceleration Measurement
2. Velocity Measurement
3. Direct Deflection Measurement

While it is possible to use accelerometers (acceleration measurement) or geophones (velocity measurement) and integrate the signals to obtain displacement, linear variable differential transformer (LVDT) instruments can be used to construct gauges that measure both static and dynamic deflection directly. In the case of a single depth deflectometer (SLD), a rod is anchored at a chosen depth (normally 2 to 3 m); an LVDT is then placed at the measurement depth with the rod extending into it. In this way the deflection at the LVDT may be measured relative to the anchor position. The SLD can be extended so that deflections can be measured at multiple depths by adding LVDTs at the required points. This is termed a multidepth deflectometer (MDD).

The main reason for the measurement of vertical deflections is to relate these to the material properties and, ultimately, to rutting (the main permanent manifestation of multiple vertical deformation cycles in AC pavements). The use of these in the project was curtailed somewhat because of cost and was also the main subject of a related study. Because of this and the fact that no MDDs were installed in the test pads with the strain and pressure cells, discussion of these instruments and their place in the overall MLS study may be found in more detail in the projects dedicated to these data.

2.1.4. Thermocouples

Although other methods of measuring temperature exist, thermocouples are by far the most commonly used sensor. Thermocouples work on the principle that the voltage generated by the combination of two different metals at their point of contact varies with temperature.

Because many pavement properties, and especially those of asphalt concrete, vary considerably with temperature, it is necessary to keep a record of temperatures in the pavement when measuring other response data. For this purpose, numerous thermocouples were placed in the test pavements in Victoria. These were type T thermocouples (Copper - Constantan) and arranged in "trees." These consisted of specially made tubes with thermocouples protruding at set points. The tubes were then installed vertically with the topmost thermocouple set into the

bottom of the surface AC layer. A diagram of a typical thermocouple tree is shown below in Figure 2.11.

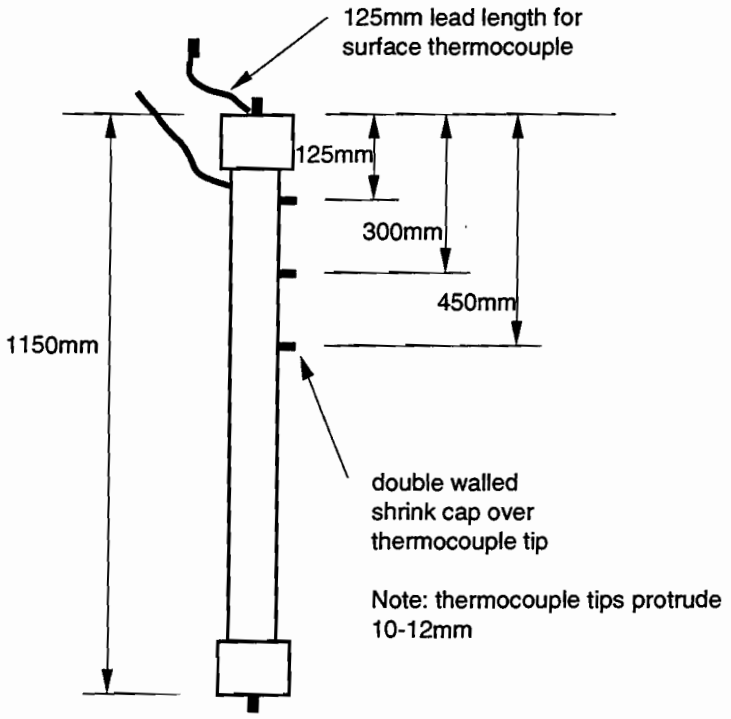

Figure 2.11 Typical arrangement of a thermocouple tree (depths vary)

2.1.5. Moisture Gauges

Pavement performance is also strongly affected by moisture in the soil layers. Indirectly, moisture content is also very important when evaluating potential for frost heave. It is thus important to measure in-situ moisture content when investigating pavement response or behavior. Of the many different methods of measuring soil moisture content, there appear to be two methods which are becoming the most widely used. The first (and older) method is by nuclear probe. The dual tube nuclear moisture and density apparatus has been used for some time and is a tried and tested method. The second method is Time Domain Reflectometry (TDR).

Time Domain Reflectometry (TDR): Since TDR is a relatively new method developed by the agricultural industry for measuring soil moisture content using the soil's dielectric permitivity, some background on this is included here. The basic equipment consists of a waveguide or probe which is embedded in the soil, and a cable tester which is composed of a pulse generator and an oscilloscope for the display of the output. A typical probe may consist of two or three 10mm stainless steel rods, 30cm long and placed 3cm apart.

The generated pulses are generally in the range of 1 MHz to 1 GHz, and the travel time of the pulse through the soil can be measured from the oscilloscope. This is related to the

permitivity of the soil, which is very strongly related to the moisture content. This is because the dialectric constant for water, dry soil, and air are roughly 80, 4, and 1, respectively. Figure 2.12 shows a typical pulse or trace, which generally rises smoothly to a local maximum and then declines smoothly to a local minimum.

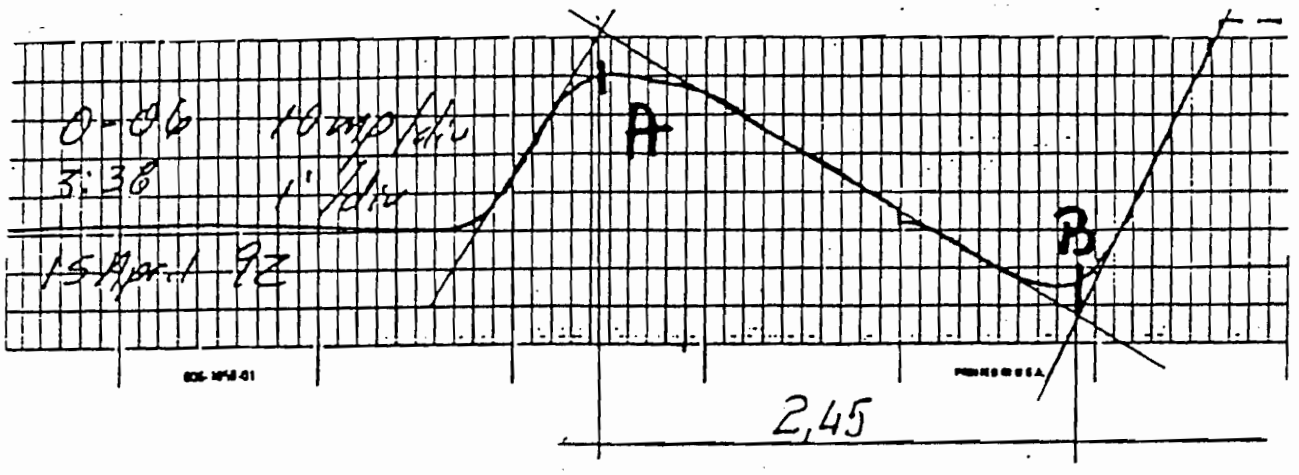

Figure 2.12 A typical TDR trace

The distance between the local maximum and the local minimum is generally termed the trace length and is the main variable in the calculation of the dialectric constant. There are various methods for determining this length, and it appears that although software is available to accomplish this automatically, there are four basic graphical methods which may also be done by hand. These are termed the Method of Peaks, the Method of Diverging Lines, the Method of Tangents and the Alternative Method of Tangents. In a 1994 study for the Strategic Highway Research Program (SHRP), it was concluded that the Method of Diverging Lines and the Alternative Method of Tangents should be the methods of choice when using flat sensors.

In the calculation of soil moisture content, the dialectric constant is first calculated using the formula:

$$Ka = (L/VP)^2$$

where Ka is the dialectric constant, L is the trace length, V is the phase velocity, and P is the probe length.

Considering K(air) is normally 1, K (dry soil) is between 3 and 6 and K(water) is between 79 and 82, the dialectric constant for moist soil is likely to be somewhere between 6 and 82.

Much of the original work in Time Domain Reflectometry has been done by Topp and Davis for use in irrigation; an equation now known as "Topp's Universal Equation" has become a fairly well-documented standard. This is an empirical equation which is applicable to most soils (with the exception of clays, where soil and water interact both chemically and physically). The equation is as follows:

$$X = -0.053 + (0.0292)Ka - (0.00055)Ka^2 + (0.0000043)Ka^3$$

where X is the soil's volumetric moisture content between zero and 1.

In addition to the explicit equation above, there exist at least two other implicit equations for gravel and soil, respectively. These should probably also be investigated when any future data are analyzed.

Finally, the volumetric soil moisture content may be converted to moisture by weight using dry soil densities measured during installation.

TDRs are generally installed using an auger to bore a hole of the relevant size down to the maximum depth required. TDRs may then be placed at a number of depths as the hole is backfilled. While TDRs were on order for the project, none were installed at the time of writing. The reader is referred to the references given for more information [Andrei 94, Campbell 95].

2.2 INSTALLATION OF SENSORS

2.2.1 Pavement Design of Test Sections

Test sections were constructed on the frontage road of LP 175 in Victoria, Texas. The sections included two different designs of flexible pavement: a thin section and a thick section, and a single design of rigid pavement. Only the flexible sections were instrumented. The design of the thin flexible pavement was a 50mm AC type D surfacing over a 300mm flexbase (1.5% lime, river gravel and siliceous fines), with a 150mm lime-treated subgrade (5% lime). The design for the thick section was identical except that an extra 150mm layer of type B ACP was included to make up a total of 200mm AC surfacing. These designs together with the positions of the instrumented test pads are shown in Figure 2.13.

The majority of the strain gauges were installed at the interface between the AC surface layer and the base. Some pressure cells were installed at this depth and some were installed at the base/subbase interface. Thermocouples were installed in trees and spanned a number of depths.

2.2.2 Sensor Layout in Test Sections

The sensors were positioned in the test pads to cover a variety of offsets and were duplicated to alleviate losses from nonsurviving sensors and to provide multiple observations for statistical analysis. Two offsets on either side of the wheel path at 175 and 225mm and the wheel path centerline itself were instrumented. Most of the sensors were installed in one wheel path, though a small selection was also installed in the other for all pads.

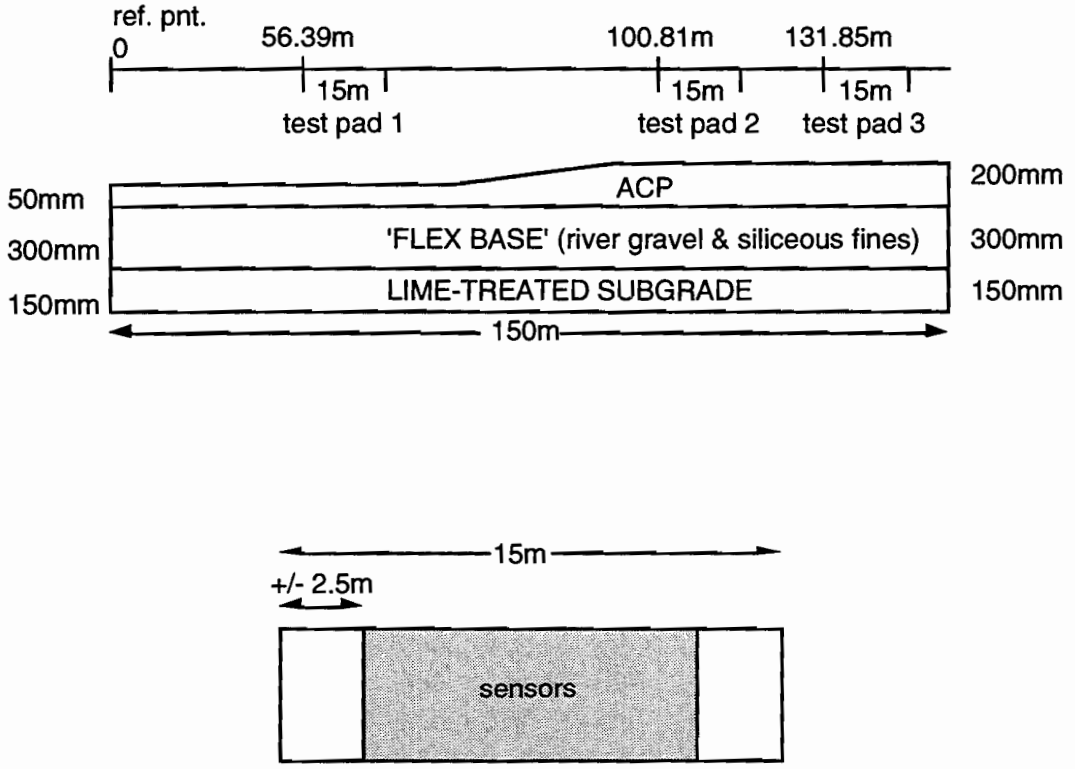

Figure 2.13 Pavement design of flexible test sections in Victoria and positions of instrumented pads

A total of three pads were instrumented in the flexible section: two in the thick section and one in the thin section. No instruments were installed in the rigid test section. The dimensions of the overall layout template used for all three test pads are shown in Figure 2.14. This gives the offset dimensions for all sensors. The longitudinal positions are shown Figures 2.15, 2.17 and 2.19. Finally, the 3-digit identification numbers and types of sensors at each depth are shown in Figures 2.16, 2.18 and 2.20. These identification numbers are the tag descriptions and are used to trace the location of sensors whose tags are quoted in the data output files.

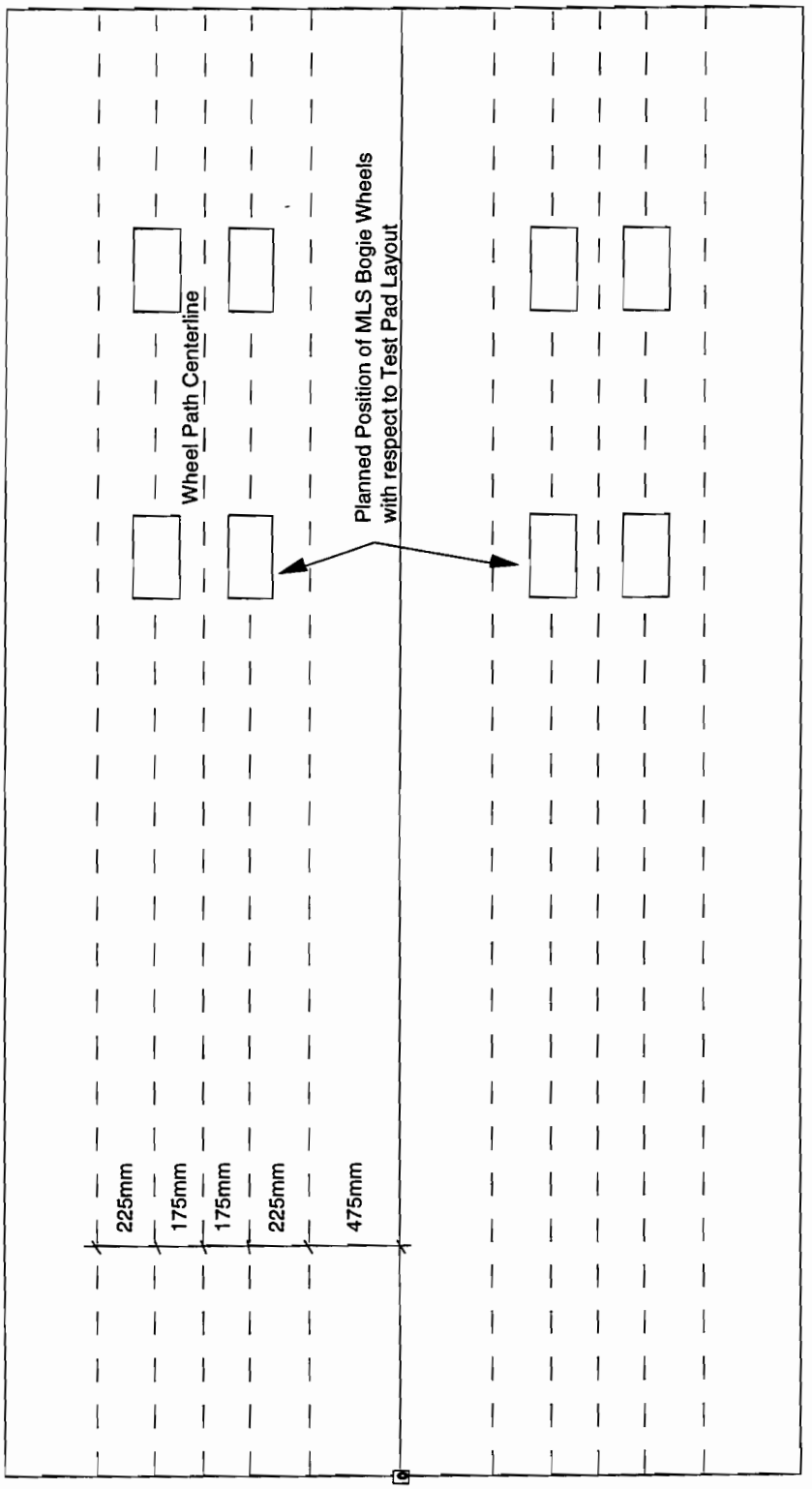

Figure 2.14 General template used for sensor layout in test pads

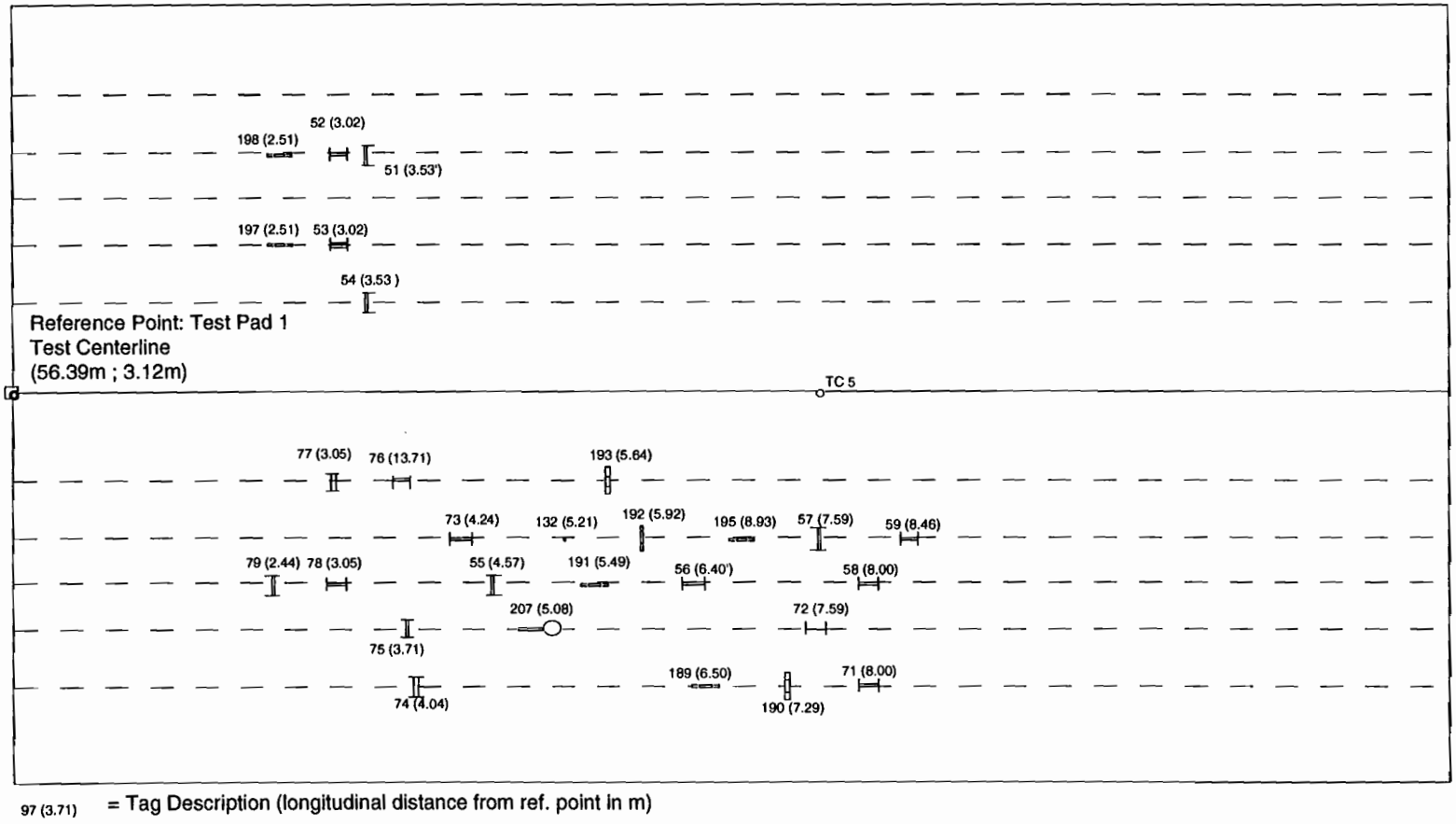

Figure 2.15 Sensor numbers and positions: test pad 1, top of base

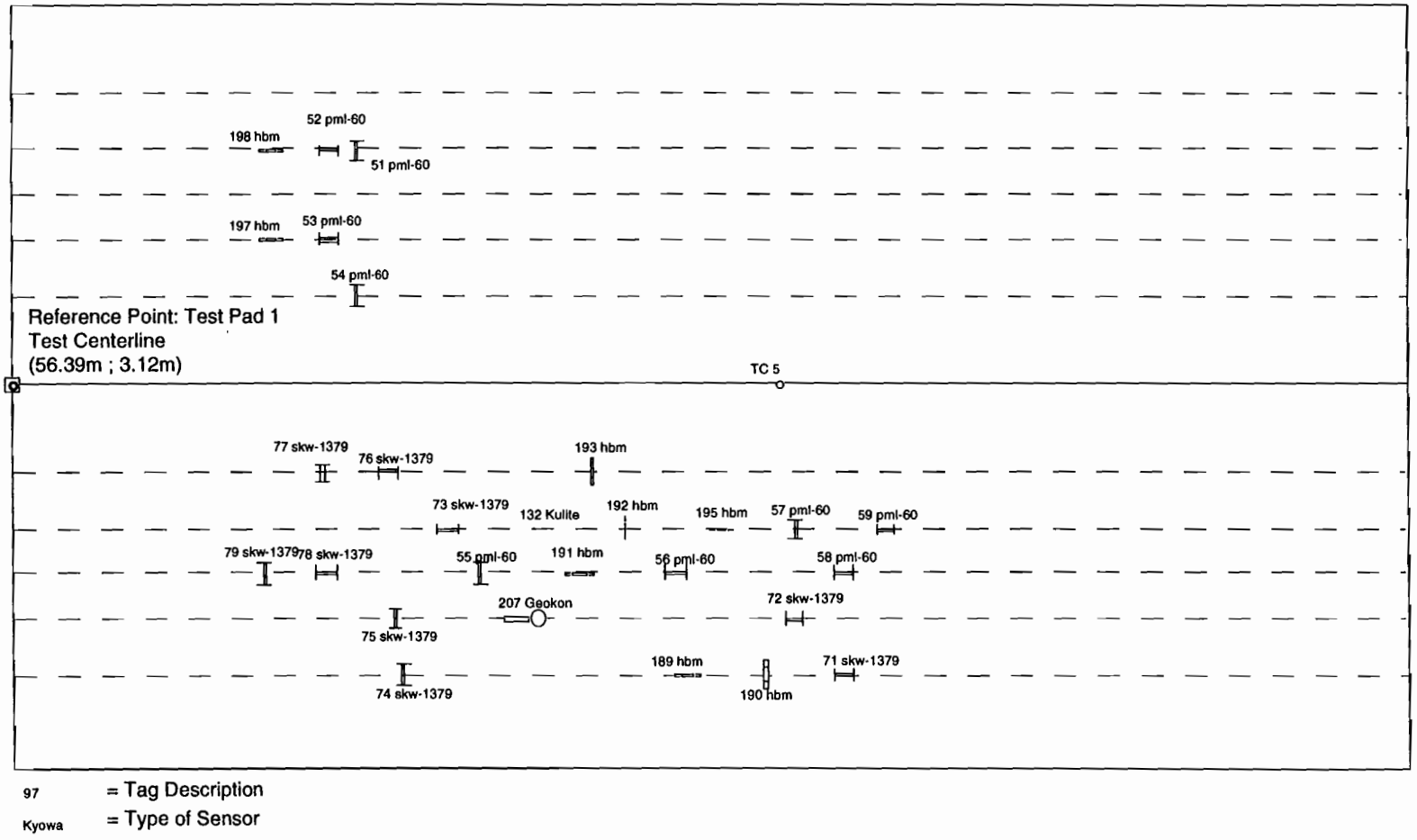

Figure 2.16 Sensor numbers and types: test pad 1, top of base

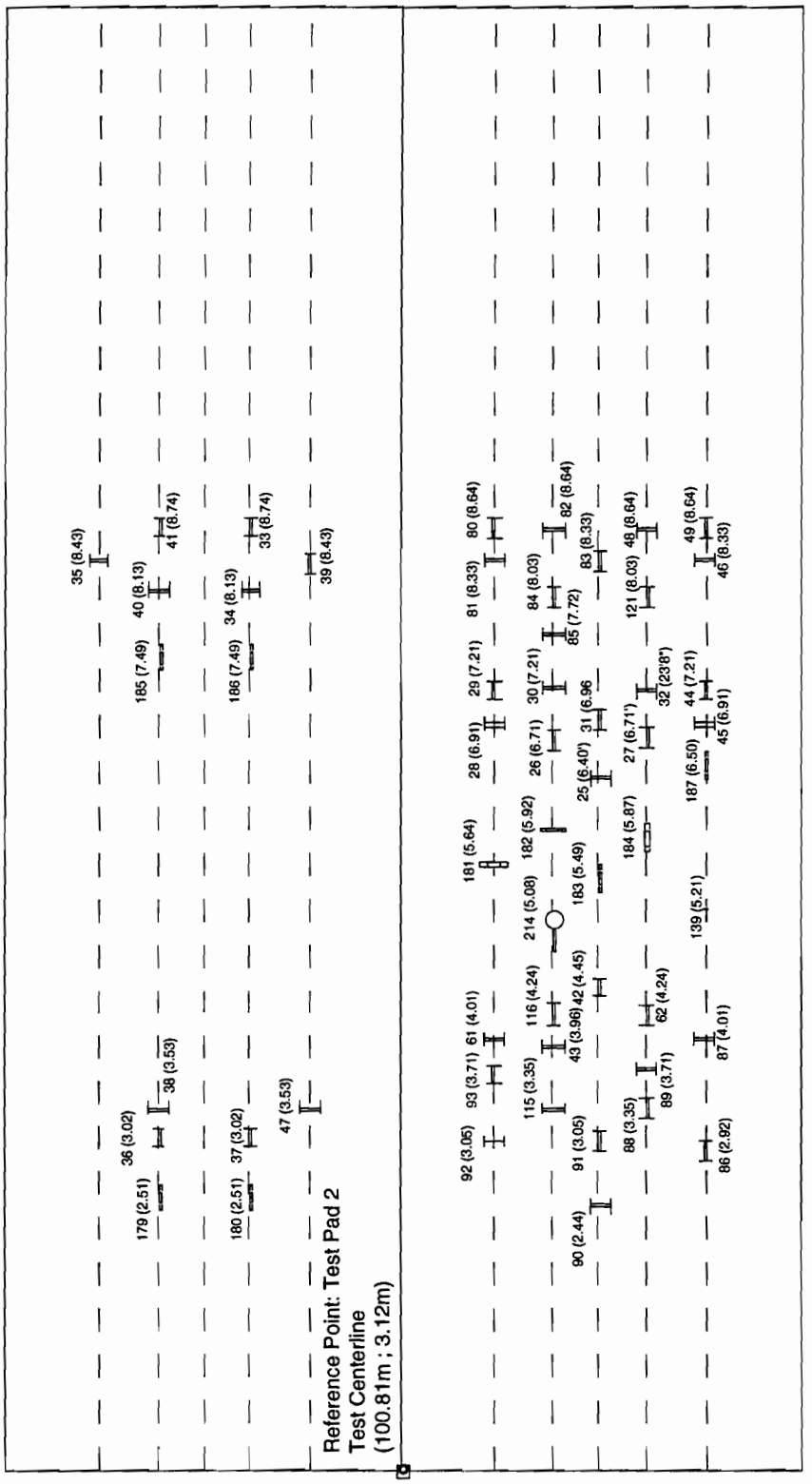

Figure 2.17 Sensor numbers and positions: test pad 2, top of base

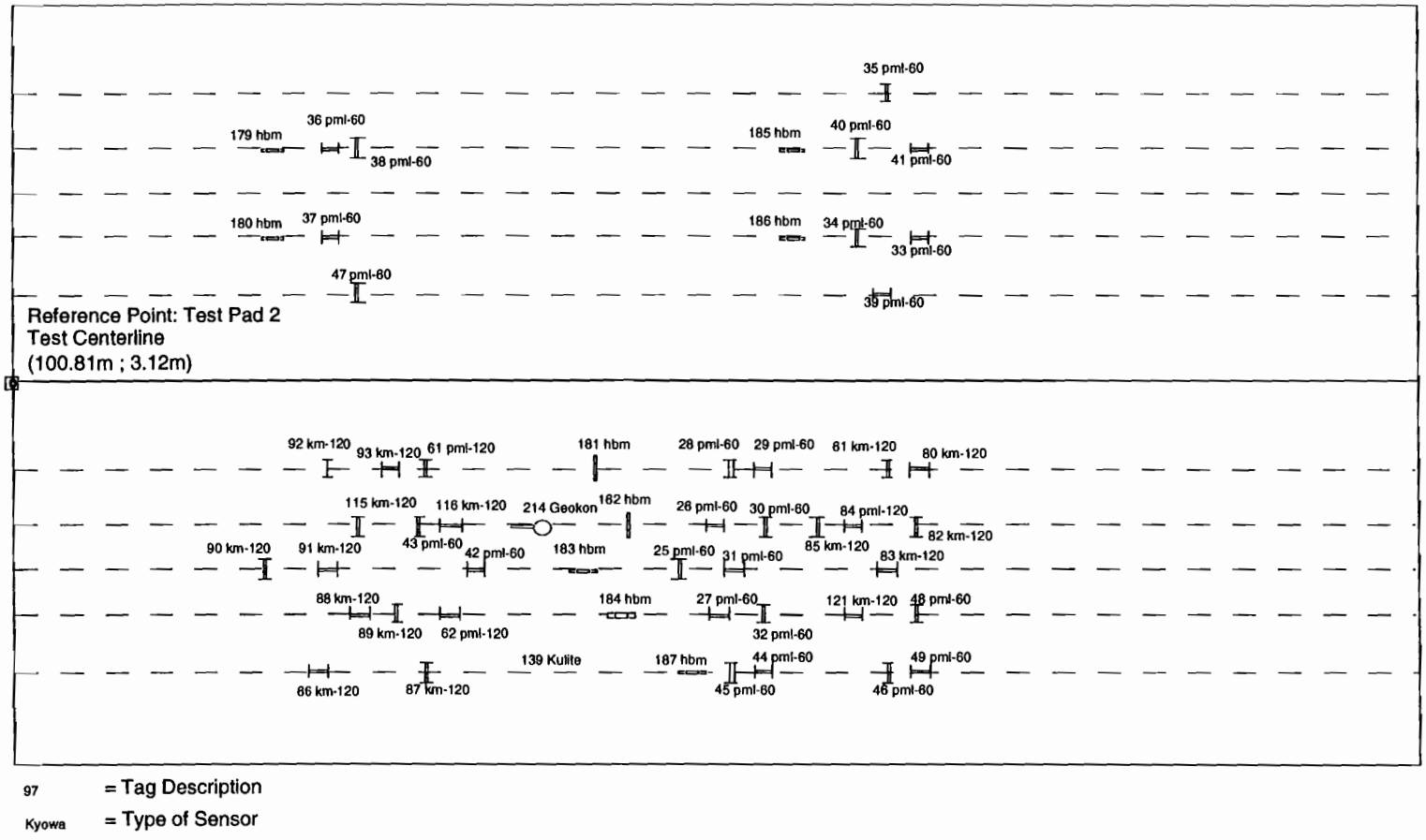

Figure 2.18 Sensor numbers and types: test pad 2, top of base

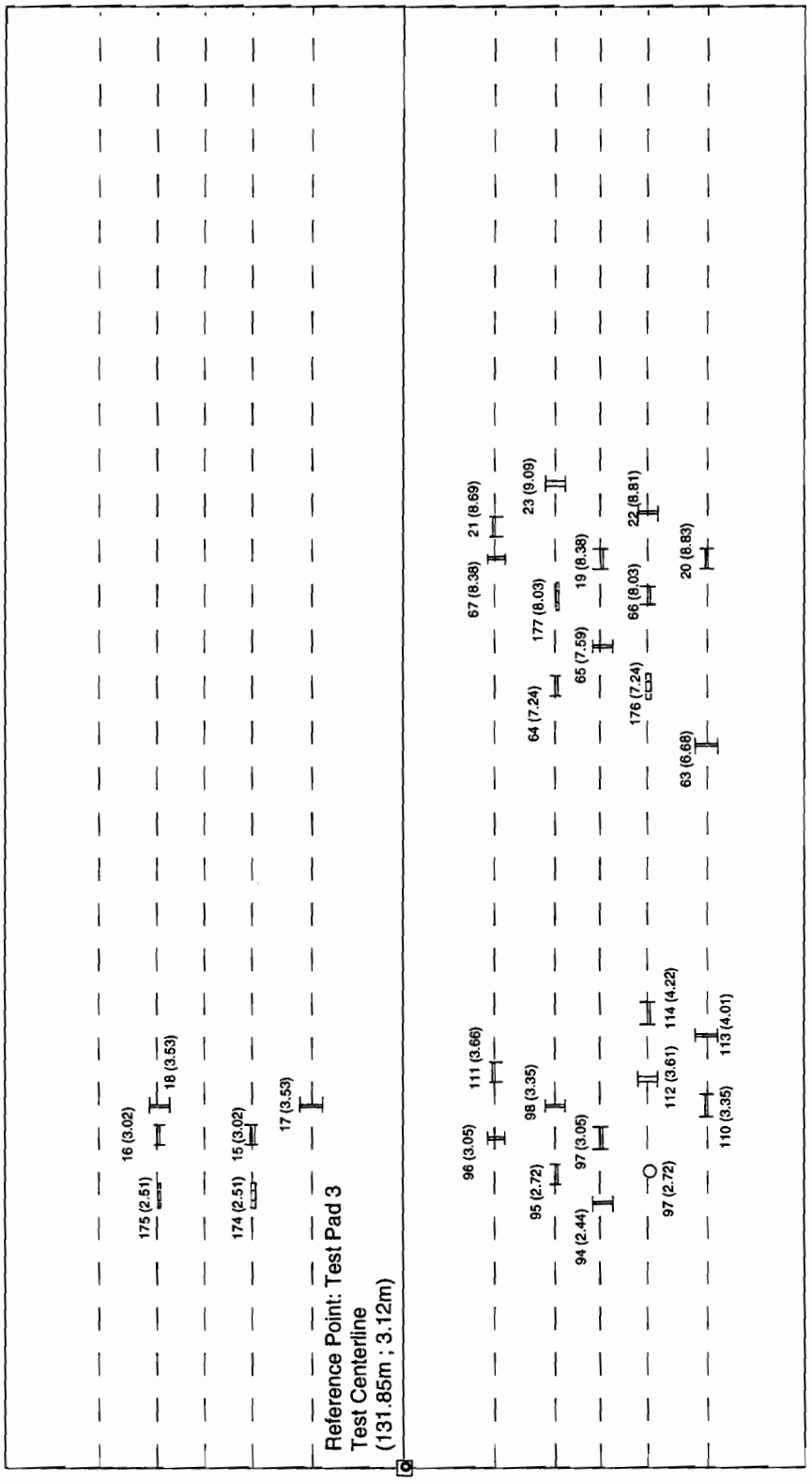

Figure 2.19 Sensor numbers and positions: test pad 3, top of base

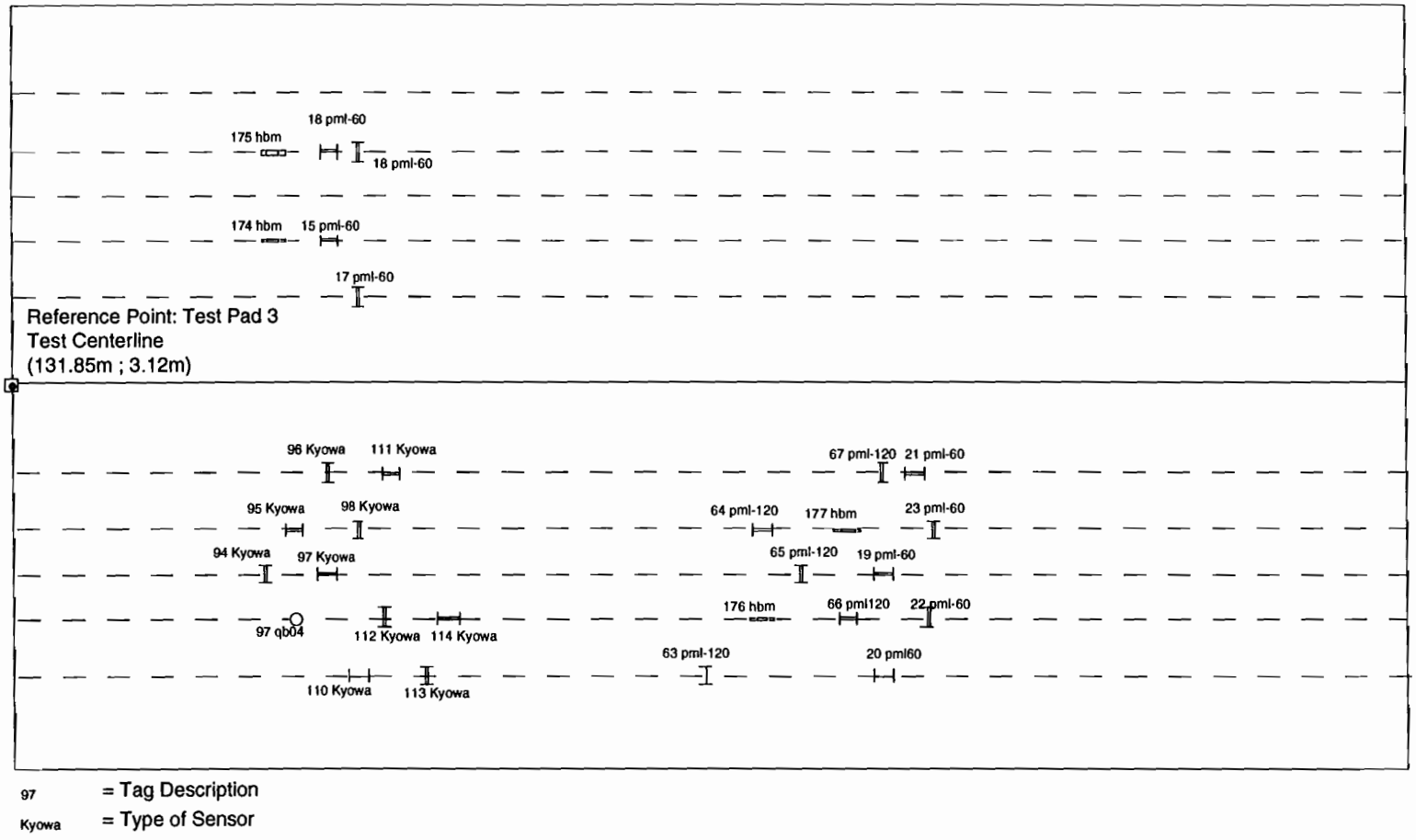

Figure 2.20 Sensor numbers and types: test pad 3, top of base

2.2.3 Sensor Installation in New Pavement

Because the reduction of variability in the final output from the sensors is always important, it is vital that standardized methods of installation for each sensor are documented and adhered to. In this regard, TxDOT has produced a full instrumentation manual for sensors to be used in conjunction with the MLS [MLS 93]. This document aims to:

1. Provide guidance on the acceptance of sensors from the manufacturer.
2. Provide instructions on the assembly of specified sensors.
3. Provide instructions on installing the sensors in the pavement.
4. Provide methods for testing the sensors after being installed in the pavement.
5. Provide guidelines on miscellaneous items, such as splicing lead wire, trouble shooting, etc.

For ease of reference and completeness, however, an overview of the installation methods for the strain, pressure and thermocouple sensors is repeated here. The sensors were installed in the test pads using these methods.

Strain Gauges: Strain gauges are generally installed according to the following basic steps summarized from the instrumentation manual [MLS 93]:

1. Survey and locate the gauge positions according to the installation layout plan.
2. Dig shallow square trench matching the outer dimensions of the gauge. Trench should be flat and horizontal. (Ensure that no sharp stones will be in contact with the gauge when it is in position.)
3. Place hot mix in trench.
4. Immerse gauge in hot mix, ensuring there are no air voids. Verify that the gauge is straight and horizontal.
5. Place and slightly compact more hot mix on top of gauge ensuring that the gauge is completely covered. The mound of hot mix should not protrude from the base by more than 0.25 to 0.5 inches.
6. Dig trench for lead wires and compact.
7. As paving train approaches, take some of the material from the hopper. Using a No. 10 sieve, process some material for use immediately around gauge. Hand work, making sure there are no voids or gaps beneath or around gauge (patty-cake).
8. Using regular material, mound around gauge, making sure there are no voids.

Because the HBM gauges are only a couple of millimeters thick, the above process is used for these; the digging of the shallow trench in the base, however, is not necessary.

Pressure Cells: The basic process for interface layer installation of pressure cells is also summarized below from the TxDOT instrumentation manual [MLS 93]:

1. Place the cell on the surface in the direction indicated by the plans. Trace an outline of the cell and transducer housing.

2. Dig a shallow hole in the shape of the outline deep enough so that the plate sits 10-20mm below the surface. The transducer housing should be in contact with the soil but should not cause the plate to be skewed.
3. Remove from the bottom and sides of the hole any rocks greater than 6mm in diameter.
4. Smooth the bottom of the hole with a hand tamper.
5. Place a thin layer of fine sand (100% passing No. 10 sieve) on the bottom of the hole. Compact the sand with the tamper.
6. Place the pressure cell in the hole and ensure there is good contact between the plate and the sand.
7. Using a bulls-eye level, ensure that the cell is positioned flat. Use small amounts of sand to level the cell.
8. Place some sand over the cell and around the transducer housing and compact by hand.
9. Process some of the removed material by removing all rocks greater than 0.25 inches in diameter. Compact around the pressure cell and in the cable trench.

Thermocouples: As with the strain gauges and pressure cells, the basic installation process is summarized below from the TxDOT instrumentation manual [MLS 93]:

1. Drill hole to depth as indicated on plans. Place removed material in buckets with lids and process. While drilling, notes should be kept on the type and depth of material being removed. When a new layer of material is reached, it should be placed in different buckets and processed separately.
2. Ensure the thermocouple tree has the correct probe locations.
3. Gently press the protruding thermocouple probes into the side of the hole.
4. Refill and recompact using the processed material from the hole, maintaining the same material levels as noted during removal of the original material.

2.2.4 Retrofitted Sensors

Although all the sensors in the instrumented test pads in Victoria were installed as the pavement was constructed, the research team was asked by TxDOT to investigate the retrofitting of strain gauges. This is justified, since in all existing pavements, and particularly in Lufkin which will be the next focus for MLS testing, the only option is retrofitting. Nonetheless, it should be remembered that past experience and a wealth of data gathered through retrofitted gauges have shown retrofitting to result in generally poorer data than those obtained through built-in gauges [Sebaaly 92, p59-60] [Scazziga 87, p587]. In addition, there is also the potential for creating weak spots or stress concentrations in the pavements, which ultimately results in the pavement failing artificially. The basic problem may be summed up by the observation that, especially when retrofitting, the action of taking measurements affects the measurements themselves.

As a result of the above it is very important to carefully examine, firstly, whether the collection of response data (such as strain) is truly desired, which implies having a definite plan and purpose for the data; and, secondly, whether the test section can be instrumented at the construction stage, so as to obviate retrofitting.

In spite of generally poorer results and problems with generating weak spots in the pavement, a considerable amount of work has been done on retrofitting gauges. And while the process is by no means simple, with experience it should be possible to obtain meaningful results from retrofitted sensors. There appear to be two ways to retrofit strain gauges:

1. Glue gauge to specially prepared laboratory specimen and glue into specially made hole in pavement.
2. Take a core from the pavement, glue gauge to core and reinsert core into hole. The cutting space is then filled with epoxy.

The two methods obviously differ considerably in the amount of work and skill level required. As the initial emphasis was on the built-in sensors, we decided to stick with the simpler, second method for pilot trials. In fact, results from the Nardo Road Test [Scazziga 87] showed that the two teams using the second method obtained better results than three out of four teams using the first method. In addition to the method, it was necessary to choose at least one type of sensor to use in the initial tests. From the pilot tests conducted on the built-in sensors in the test pads, it was found that the HBM sensors were by far the most sensitive and noise free. It was in fact found at the Nardo Road Test [Scazziga 87] that the Italian team using the HBM gauges obtained consistently low results. Nonetheless, all the methods used by this team showed low results and no satisfactory explanation was found, except possibly that there was a constantly lower temperature at this site. Based on the results of our study, the HBM gauges were the obvious choice (see section on data analysis).

For the collection of response data, it should also be noted that multidepth deflectometers are somewhat of an exception to the above in that they provide apparently excellent data at numerous depths, are designed only to be retrofitted, and cause considerably less damage to the pavement.

Description of proposed methods for initial testing: All the methods and variations proposed are according to the second of the two retrofit methods described above, where a core is taken from the pavement, the sensor is attached, and the core is then replaced. It should be noted, however, that it is relatively simple to change the basic methods described below to the first of the above methods, and to take a core from a parallel position of a slightly bigger size so that the gap needing to be filled with epoxy is considerably smaller. This would simply entail the procuring of the right core bit size and would require no fundamental change in whatever basic installation method was being used.

The first and simplest method basically involves attaching the gauge to the bottom of a core and replacing the core. This method, however, fails to take into account the fact that the

bottom of the core is rarely flat and, therefore, it is inevitable that a relatively large volume immediately surrounding the gauge is filler material (i.e., epoxy or bitumen).

Because of this and the fact that the chosen HBM gauge is very thin, it was suggested that, at least for thick AC layers, it would be highly beneficial to slice the core horizontally as close to the bottom as possible and to install the gauge in between the two core sections, thereby reducing to a minimum the volume of foreign material. This method was tested for practicality in Victoria and was found to have good potential for further testing. Unfortunately, a 300mm core is still required. These methods were designated Type A methods.

Another proposed method — Type B — is an attempt to reduce the core size and may have the advantage of being able to anchor the ends of the strain gauge to the sides (and thus in undisturbed material) of the core hole.

The method basically involves the drilling of a reduced size core of 150 or 200mm and then cutting into the sides of the hole at two opposite locations so that the ends of the HBM may be inserted into these. In addition, if the core was cut, the gauge could again be installed at any depth as in the previous method. The problems that would occur would probably be associated with getting the epoxy uniformly into the side holes without creating air voids. Depending on the thickness of the saw blade used, the volume of foreign material immediately surrounding the gauge would again be increased over the second method. If the gauge was not installed at the bottom of the core and the core were cut, problems would also be experienced in ensuring the side holes and the cut were exactly in line. Nonetheless, the method has potential advantages and merits at least a "practicality test." The method is illustrated in Figure 2.21.

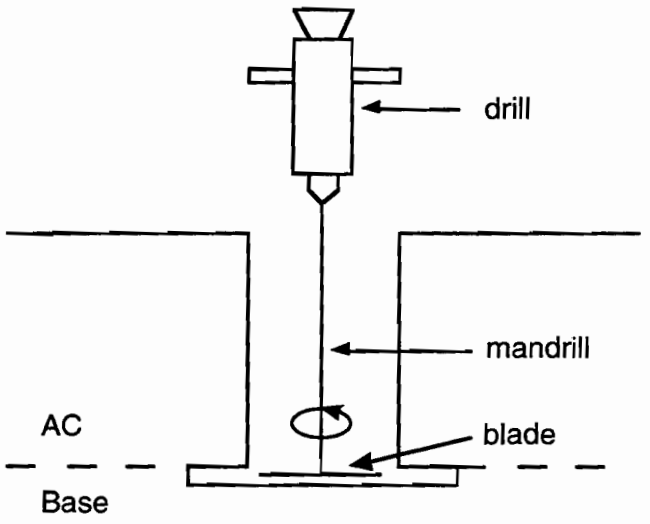

Figure 2.21 Retrofitting method illustration

Equipment needed for proposed retrofit Method B: The first problem that needs to be addressed is getting a suitable saw blade down into the hole for a horizontal saw cut as much as 200mm below the surface. The most obvious way of doing this appears to be by using a fairly large commercial drill with a saw blade attached to a mandrill. Secondly, the sawing could conceivably be performed holding the drill by hand, but in order to reduce unwanted variability in the measured strains created by installation variability, and to ensure that the side cuts are neat, horizontal and at the required depth, it is suggested that some form of apparatus be used to hold the drill vertical (while being able to move it horizontally).

While there are various possibilities, this might take the form of a small trolley onto which the drill would be mounted. Adjustment should be possible up and down so that the depth of the drill cut could be finely controlled. In addition, some adjustment to ensure the blade was horizontal would have to be allowed for, but both of these could be relatively easily accommodated by the conceptual design shown in Figure 2.22.

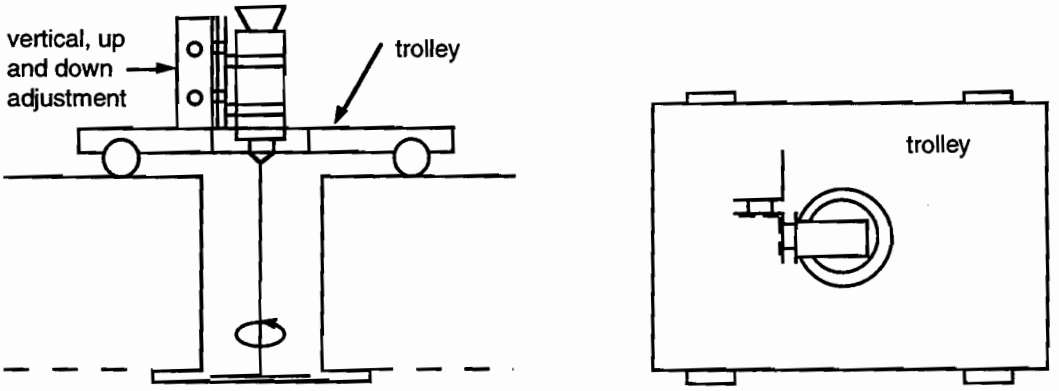

Figure 2.22 Conceptual design of control apparatus for side sawing in retrofit method B

Test installation for retrofit Method B: As the sensor is 250mm long, a 200mm core would allow for the sensor to be recessed 25mm into each side. If a 150mm core could be used however, this would allow for a 50mm recess on each side, which would be ideal. Although the HBM gauge has been tested to ensure that the entire gauge doesn't physically snap for a 150mm hole, the strain gauge might be irreparably damaged by such bending (basically into a quarter circle, radius 150mm). Unfortunately, in this case another consideration takes precedence. In order to insert the gauge, it is necessary to saw a hole in at least one side that is twice the length of the final recessed amount. For a 200mm core, this is no problem. A 150mm core, resulting in a 50mm recess would, however, require a 100mm cut on one side. Given that the maximum radius of the saw can only be 75mm (to be able to fit in the hole), the cutting of a 100mm recess in one side is impossible. The size would therefore have to be a 200mm core.

Finally, it was suggested that this method be given a trial test installation similar to that done for the second method, in order to iron out any practical problems before a pilot experiment

is conducted. This has not in fact been accomplished to date, but is still recommended for the future. The retrofit methods likely to be used in the future for the MLS, and which are recommended for pilot testing, are summarized below.

Summary of retrofit methods: The reason for conducting a pilot test would be to compare a number of different practical methods for the retrofitting of strain gauges. While there are a number of methods used worldwide [Scązziga 87], it is felt that many are too labor intensive and require too high a level of skill to install. The feeling is, thus, that while a simple method may suffer from fundamental problems, owing to excess epoxy grouting, etc., by being relatively simple it may be easier to control and might still give more precise results in the long run. How true this philosophy is can only be tested in the field. It is therefore recommended that the methods tested in an initial pilot test should be limited to the following:

A1. Remove full-size core (300mm) and install gauge at bottom.

A2. Remove full-size core, cut at desired depth, and install between separated pieces.

B1. Remove reduced size core, cut horizontally into sides of hole directly under the AC layer, and install at bottom of core.

B2. Remove reduced-size core (200mm), cut horizontally into sides of hole, and install gauge so that ends are positioned in side cuts at desired depth. (Core will also have to be cut at desired depth.)

These are shown in Figure 2.23 below.

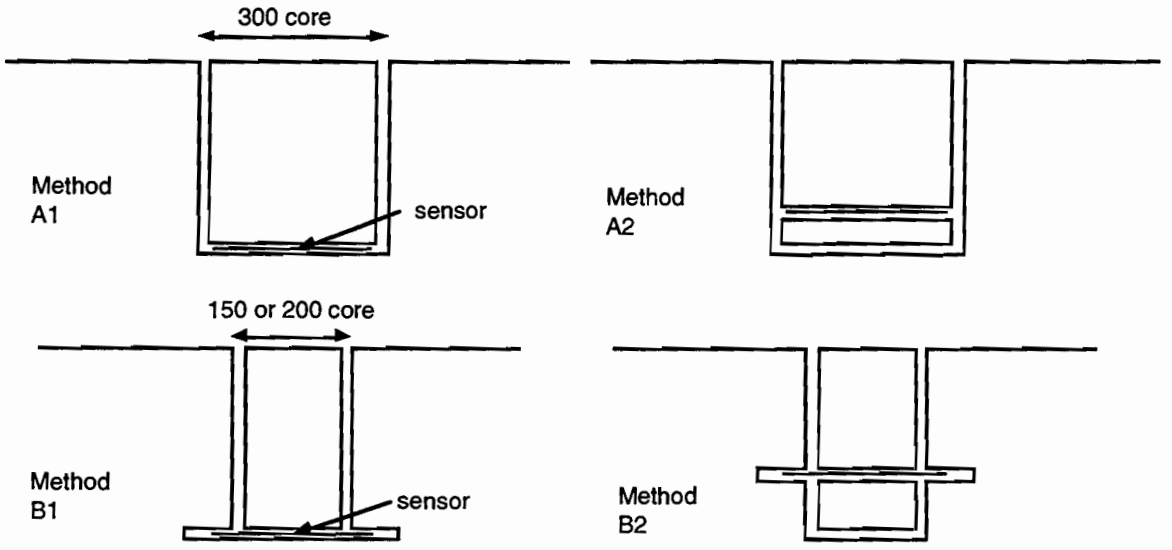

Figure 2.23 Different methods of retrofitting to be tested

CHAPTER 3. DATA COLLECTION

3.1 DATA SAMPLING RATE

3.1.1 Background

We performed a simple pilot test on August 2, 1994, on test pad 1 in Victoria using a crane (gross weight: 224kN; steer axle: 77kN; 1st rear: 73kN; 2nd rear: 73kN). Data were obtained from 10 different sensors in the pavement using a 10kHz sampling rate. As a result of the high sample rate, the physical quantity of data was considerable. The sampling was continuous for approximately 30 seconds, during which time a crane was driven over the sensors at about 16km/h. The main objectives of this initial perusal of sample data were: (1) to see which sensors were still working; (2) to check which sampling rate was statistically acceptable; and (3) to use this knowledge to design a pilot experiment to begin assessing the statistical parameters of the sensor readings.

Data from all the sensors were characterized by digitization and noise at the highest frequency (10kHz). The amplitude of this varied, but was generally not more than 0.5 microstrain for sensors 1-3, roughly 5 microstrain for sensors 4-6, and about 2 microstrain for sensors 7 and 8. In addition, there was a fairly distinct noise source in the 60kHz range that could have come from a number of sources. The amplitude of this was approximately 0.5 microstrain in the HBM sensors (1-3).

In the sensors tested, various waveforms reflected the actual passage of the front and two rear axles over the sensor. The most common waveform, however, shows a negative strain developing over the first 0.1 seconds, followed by a positive peak that develops and drops back over about 0.06 seconds, after which the strain returns to normal levels over a further 0.1 seconds (and apparently including some creep). From the literature it can be concluded that this waveform is typical of the longitudinal strain in the wheel path.

The approximate noise/error amplitude, peak amplitudes, percentage errors, and waveforms are summarized for all the sensors in Table 3.1, where it can be seen that response varied with sensor 2 and sensor 3, showing the highest amplitudes and therefore the least percentage error. The smaller response for sensor 1 can probably be explained by the fact that it was relatively far from the load.

Table 3.1 Summary data from initial roll over test

No.	Position	Offset (mm)	Sensor Type	noise amp.	max. comp.	% error	max. tens.	% error
1	189	400	HBM	0.5	12	4.2	3	17
2	192	175	HBM (transv.)	0.5	200	0.3	0	
3	195	175	HBM	0.5	160	0.3	410	0.1
4	73	175	Kyowa	5	45	11	130	3.8
5	75	175	Kyowa (transv.)	5	40	13	0	
6	78	0	Kyowa	5	25	20	65	7.7
7	57	175	pml-60 (transv.)	2	12	17	21	9.5
8	59	175	pml-60	2	5	40	18	11

With regard to the first objective, therefore, it would seem that none of the gauges can really be said to be inoperative, since placement may account for some of the low responses.

3.1.2 Spectral Density

Although there is a considerable amount of signal processing theory that may be applied to the data, we considered it preferable at this stage to simplify the problem and choose a single sampling rate for the initial pilot experiment. Since the original rate of 10kHz produced an excessive amount of data, this needed to be considerably reduced. In order to assess the worst case in more detail, one of the data sets from the HBM gauges (which give the highest strain) was used to analyze spectral density.

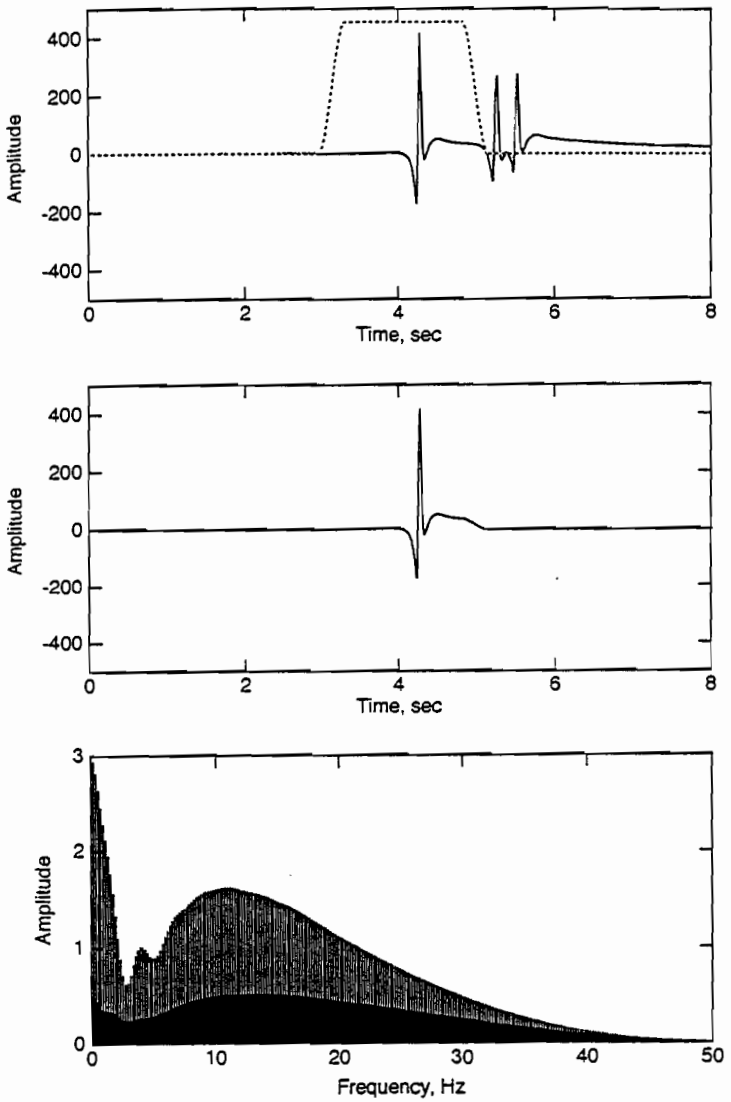

Figure 3.1 Example spectrograph for 100Hz sensor 3 (HBM) data

For the choice of a single sample rate, therefore, the example spectrograph for 100Hz sensor 3 data in Figure 3.1 shows that the majority of energy in the waveform appears to be accounted for below 50Hz. It should, of course, be remembered that frequencies higher than this (if there are any) will still be reflected in the spectrograph, though it is unlikely that this will affect it appreciably.

If the assumption does prove correct, the Nyquist frequency can be set at about 100Hz (or double the frequency above which no energy is evident in the spectrograph). Although sampling at the Nyquist frequency theoretically preserves enough information about the waveform, it is generally recommended that a rate of 3 to 5 times this frequency be used to allow for higher speeds, different waveforms, and to preserve more of the wave shape in the raw data.

3.1.3 Geometric Analysis

It can be assumed from a purely geometric point of view that the greatest inaccuracies will occur at points of greatest radius of curvature on the waveform. Using the tensile peak from a longitudinal HBM sensor in the wheel path, with a peak strain of 450 microstrain and a load speed of 16 km/h, a general equation that ought to be able to be widely applied was developed as follows.

If the shape of the peak is approximated by a sine waveform, then, using the dimensions from the 10 kHz HBM waveform, it was determined that the maximum error that would result from a sample rate of only 100 Hz would be approximately 16/400, or 4%. This implies that 1/100th of a second should correspond to a certain angle on the sine wave that would produce a 0.04 error from the sine wave.

$$\cos(\Delta) = (1 - e) \tag{1}$$

where

Δ = angle corresponding to e, and

e = fractional drop below peak (or under measurement error).

This is illustrated in Figure 3.2.

From Eq. 1, and solving for the actual dimensions of the strain peak of 400 μstrain for 16 km/h, it can be seen that if $\Delta = 0.04$, this corresponds to 16° on the sine wave, and so:

$$e = 1 - \cos(4piv/16) \tag{2}$$

where

e = under measurement error,

p = peak in μstrain,

i = time interval between observations (reciprocal of sample rate in Hz), and

v = speed of load in km/h.

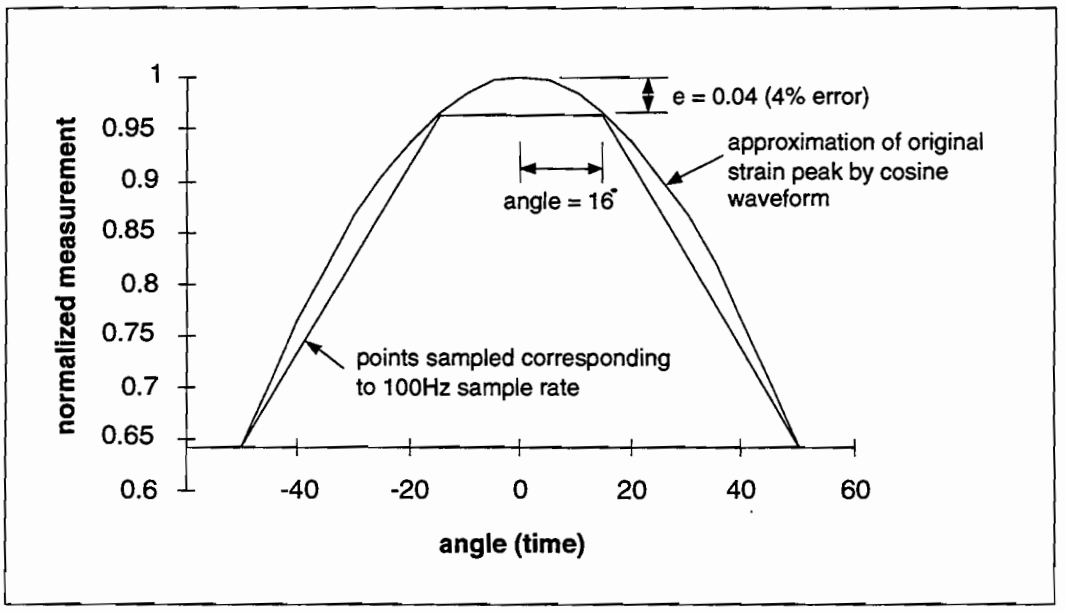

Figure 3.2 Illustration of the approximation of the tensile strain peak by cosine waveform

Conversely, if we wish to calculate the sample rate necessary to ensure a particular minimum under-reading error, the above equation (2) may simply be rearranged as follows:

$$i = \cos^{-1}(1-e) \cdot 16/(4pv) \qquad (3)$$

Given the previous discussion concerning spectral density, it is then also noteworthy that the error for the peak readings owing to sampling at 100Hz for HBM03 (which has the highest amplitude and therefore the greatest radius of curvature, assuming the length is fixed) is still less than 5%. Five times this frequency, or 500Hz, was therefore considered to be a reasonable sampling rate for the pilot test. For general future tests using the MLS, however, a rate of 300Hz should be ample. For illustration, this represents a measurement every 20mm at 21.6 km/h. The minimum rate at this speed, from both the spectral analysis and geometric point of view, would be 100Hz.

3.2 PILOT EXPERIMENT ON TEST SECTION 3

3.2.1 Experiment Design and Factorial Matrix

In order to statistically assess the variability of data, the variables giving rise to that variability first need to be identified. In this case, there are, of course, a great many variables, ranging from the quantifiable data (e.g., temperature) to minute orientation and depth differences in the placement of the sensors, which could conceivably affect the measurements but which cannot be detected. Because a full factorial experiment involving detailed ranges of numerous variables could result in thousands of passes, it is beneficial to perform an initial pilot test to assess the sensitivity of some of the variables. This can be done by choosing what are considered the main (or most sensitive) variables, and then determining that these do indeed account for the main variability. If this is not the case, then the measurements are obviously being affected by some other unmeasured variable that will have to be identified and included before a full experiment is conducted. If one of the chosen variables proves to produce a linear response, then less of its range needs to be sampled in the full experiment. In this case, it was recommended that the following major variables be included in the simple pilot factorial experiment: (1) placement (of load over the sensor); (2) load; and (3) speed. The ranges of the variables should be sufficient to cover the majority of the ranges expected in the full MLS experiment. These will be discussed separately below.

Placement: The variation in placement needs to be checked for two reasons. First, it is necessary to find out how sensitive the measurements are to variations in placement, and how the waveforms differ; second, it is also necessary to check the position of the sensor in the ground so as not to be misled by misplaced sensors. It is envisaged that, although five different placements would be preferable, three should suffice for this initial pilot study. It is recommended that the three placements be 15.2cm apart if possible (with the center pass directly over the sensor), and also that the exact positions be recorded. In fact, since the sensors are all at different offsets to the longitudinal base line, the "center" placement will not actually result in the wheel passing directly over the sensor. Nonetheless, three different placements, combined with a range of lateral positions among the sensors, will result in a fairly good range of placements.

Load: The most obvious variable is load. Varying the load should vary the amplitude of the waveform accordingly. If the origin (no load, no strain) is included, two measured loads should suffice to check for linearity; however, it was recommended that three loads be used so that linearity could be checked in the operating range. Again, while the loads should theoretically span the final operating range of the MLS, obviously in this case the choice of the three loads was dictated by practical considerations.

Speed: It has been recognized for some time (e.g., Dempwolff 72) that variations in speed affect strains because of visco-elastic and inertial effects. Variations in speed will also affect the length of the waveform. This variation in length will almost certainly be linear. For this reason, two speeds should suffice for the pilot experiment. It will still be important, however, to try to

have one speed as low as possible, and one as close to the normal operating speed of the MLS as possible.

Factorial Experiment: Figure 3.3, summarizing the simple experiment described above, represents 18 different combinations of placement, load, and speed. We also expected that if the tests ran smoothly, and if we had enough time, we should rerun the tests (in a different order if possible) in order to obtain two sets of each set of data. In this way, we should be able to get some insight into the repeatability of the results.

With regard to the practical aspects of the test, the hardest aspect we foresaw was in measuring the placements. However, an ingenious set up was constructed on site and fairly good placement control was accomplished. We were also able to measure actual placement with fairly good accuracy.

Another practical aspect was the handling of the data itself. We proposed that the tests be given a designated number from 1–18, and that file names include at least this number. In addition, a master form should be compiled on which all information for each test may be recorded (including the computer file name).

SPEED / PLACEMENT / LOAD	min (8 km/h)			max (24 km/h)		
	left	center	right	left	center	right
empty						
half						
full						

Figure 3.3 Factorial for the pilot test on test pad 3

3.2.2 Description of Field Experiment

The test was performed on test pad 3 in Victoria, Texas, on January 17, 1995. The weather was overcast and rainy. The data recording was begun at 11:35 a.m. an ended at 5:07 p.m., with a rough average air temperature of 22°C and an average asphalt surface temperature of 19°C (measured at 2:35 p.m.). The dimensions of the TxDOT dump truck used are given below in Figure 3.4. The three loads used are summarized in Table 3.2. The order of the experiments

was to start with the center placement, with the lowest load and speed (8 km/h). Thereafter, the left and right placements were run. Next, the speed was increased to 24 km/h and the three different placements were run. These cycles were repeated for the next two load levels.

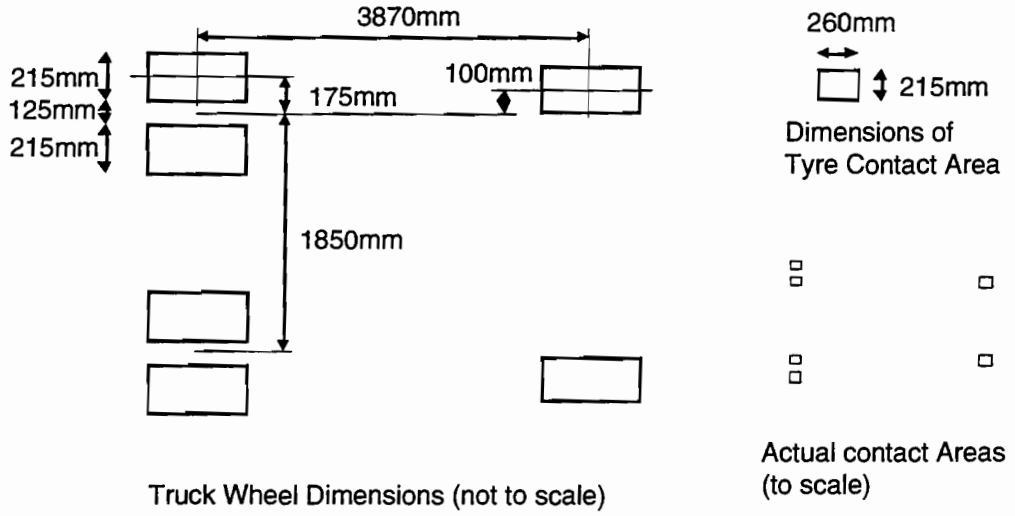

Figure 3.4 Wheel dimensions of test dump truck

Table 3.2 Load levels used in the experiment (kn)

	EMPTY	HALF	FULL
Steer Axle	32	37	43
Drive Axle	36	69	105
Gross Weight	68	106	148

At the beginning of the experiment, a longitudinal base line was painted on the pavement surface corresponding to the future east (highway side) wheel path for the MLS. Since the tests were run in a southerly direction, this corresponded to the driver side of the truck, which was important for placement control. The placements were controlled by attaching a long (about 3m) pole to the front of the truck and bracing this with stays. The position of the tip was adjusted using the stays, so that when it was lined up with the base line (about 150mm above the surface), the center of the gap between the left two tires was also directly over the base line. A number of runs were made in order to fine-tune this before testing began. The resulting configuration of the truck in relation to the test pad is shown in Figure 3.5.

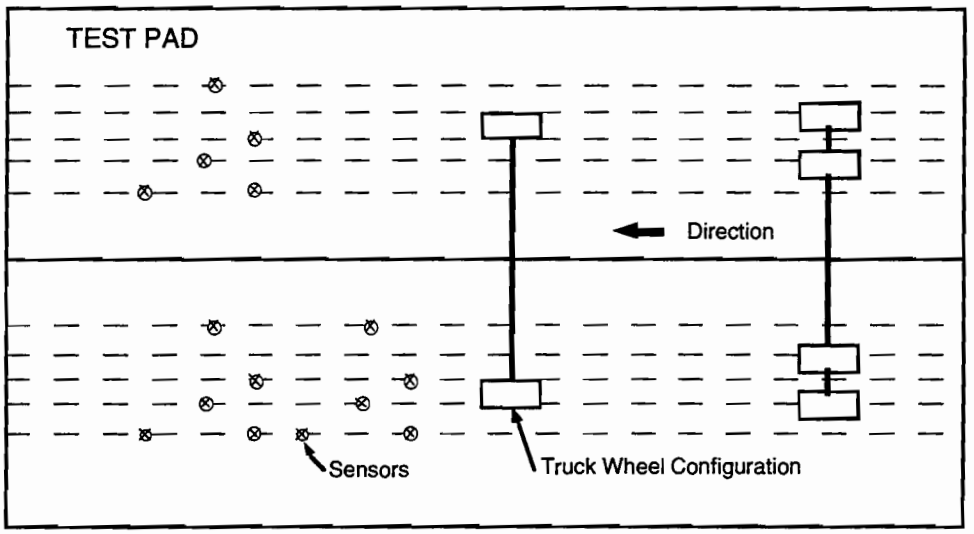

Figure 3.5 Configuration of test truck with respect to pavement for pilot experiment on test pad 3

The exact placements were recorded by stretching a section of paper from a roll across the path of the truck. Because of the relatively wet conditions, the exact placement of the center of the two left tires with respect to the painted base line could be measured from the wet tire tracks left by the truck on the paper. While the lateral placement was measured only at one longitudinal position, the truck was able to travel on a very straight and controlled line because of the pole. The measured placements were estimated to be at least to the nearest 25mm and were in fact considerably more accurate than this.

Unfortunately, time did not allow a full repetition of the experiment in order to obtain replicate values for the factorial cells. In retrospect, it is thought that even if the experiment had been repeated, the differences in conditions (especially temperature) may have resulted in a different set of readings anyway. For similar future experiments, we recommend that any replicates be taken at the same time to ensure conditions are the same.

Based on the conclusions reached previously with regard to sample rate, we decided that a sample rate of 500Hz should be more than adequate for the pilot experiment. Data were recorded for every run made, but only those that were judged close enough to the required placement were saved. Those that were not considered close enough were repeated. The raw data were recorded using the Optim data acquisition system. These data were then saved on tape for transfer to other computers for postprocessing. The raw data are plotted in the appendices of this report.

3.3 PILOT EXPERIMENT ON TEST SECTIONS 1 AND 2

3.3.1 Experiment Design and Factorial Matrix

Because a fairly closely controlled test had already been performed on test pad 3 earlier, we decided that this test should aim for slightly different objectives. The aim here was therefore

to determine the parameters pertinent to the TxMLS data collection. The following objectives were selected initially for further consideration:

1. Check survivability/sensitivity of all sensors using different combinations of load and speed.
2. Check the capacity of the data storage.
3. Check the drift in sensor readings over time.
4. Better understand the roles of creep and viscous behavior in measurement.
5. Check a range of sample rates.

Experiment 1: This would form the major portion of the work. In order to check the survivability of the sensors, the first step would be to perform normal continuity tests on all sensors in the pad. Once the sensors no longer having even continuity had been eliminated, data should be collected from the remainder, which could then be analyzed further.

It was suggested that the placement not be varied as with the original test, and that we should vary only load and speed; two loads and three speeds were to be used.

As with the previous test, a base line would need to be marked and some method of lateral-placement control used. We did not intend, however, to try and record exact placements, as was done previously.

The two loads used would be dependent on the vehicle available, but should probably be "full" and "half-full." The three speeds should range from roughly the normal MLS operating speed of 20 km/h, through a fairly slow speed of about 8 km/h. The lowest speed should be an overlap with the final "creep" experiment, in that it should be as slow as practically possible without stopping. The resulting factorial is shown in Figure 3.6.

TEST PAD / SPEED / LOAD	Test Pad 1			Test Pad 2		
	crawl	8kmh	24kmh	crawl	8kmh	24kmh
half	3			3	3	3
full	3			3	3	3

Figure 3.6 Factorial design for experiment 1 on test pads 1 and 2

In fact, because test pad 1 was so close to the existing MLS set-up position, we could use only the slowest speed here. Although only one value was measured for each cell previously, three measurements should be taken for each factor combination (factorial cell) in this experiment.

Experiment 2: It was suggested that objectives 2 and 3 above be accomplished simultaneously. In order to generate manageable files, we decided to obtain as much data as storage capacity would allow. In order to check for drift, the sensors (probably just HBMs) should be balanced at the start and then not balanced again for the duration of the test. The sample rate should be 50Hz.

Experiment 3: In order to investigate the creep and viscous aspects, a series of incremental static tests were to be performed. These could take the form of rolling over a particular sensor by stopping incrementally at, for instance, 0.5m intervals for a set (long) time of between 5 and 10 seconds. While no exact quantitative measurements of creep compliance or complex shear modulus would result from this, it would nonetheless provide valuable insight into the time-related behavior and may bring to light any drastic limitations of the sensors in this regard. In this experiment, the sample rate should be 50Hz in order to save space.

Experiment 4: The most important contributing variable to the choice of sample rate is the second order derivative of the waveform with respect to time, or, in other words, the radius of curvature. This is likely to be a maximum at the peak tensile and compressive points on the strain waveform. If the maximum expected radius of curvature at these points and their values are known, the sample rate may be calculated by simple geometry to ensure a desired maximum margin of error. In fact, this analysis was performed early on in the study (the investigation into sample rate is described in section 3.1 in this report). In order to check the validity of the previous investigation, it only remained here to check that the shape of the peak of the waveforms could still be approximated as assumed for the initial study. This was to be done on a few of the waveforms obtained from the previous experiments.

3.3.2 Description of Field Experiment

The tests were conducted on test pads 2 (200mm AC and same design as pad 3) and 1 (50mm AC) in Victoria, Texas, on July 5 and 6, 1995. This second set of roll over tests were conducted in a manner similar to the first set. There were, however, notable differences relating to environmental conditions: while the previous set of tests were conducted in winter under mild and fairly wet conditions, these tests were conducted in very hot summer temperatures in the upper 90s on average. This was expected to result in pavement responses different from those in the previous test; this turned out to be the case, with strains of roughly 4 times the magnitude for similar tests on test pad 2. The dimensions of the dump truck, the same as those for the first test, are given in Figure 3.5. The two loads used were also of the same order as those used in the first set; these are summarized below in Table 3.3.

Since it was more practical to complete all experiments on each test pad before moving to the other (owing to the considerable time required to unhook all the sensor wires and reattach them at the other pad), the experiments were split to accommodate this. Initially, with the truck loaded full, we recorded three runs for each speed of 24 km/h, 8 km/h, and as slow as possible.

Once again, the placement was checked to determine if the center of the two left rear tires was close enough to the longitudinal base line. If this was not the case, the run was discarded and not saved. The exact placement was not measured in this less objective experiment. While the placement was controlled fairly carefully, this was not accomplished with the same precision because the previously used sighting pole was not used. The error in the placement was therefore estimated to be generally less than about 50mm.

Table 3.3 Load levels used in the experiment (kn)

	HALF	FULL
Steer Axle	38	42
Drive Axle	75	108
Gross Weight	113	150

Once the factorial experiments had been completed on pad 2, an "incremental static" test was carried out where a mark was placed on the pavement every 0.5m and the truck rolled forward onto each of these marks and stopped long enough for the strain to stabilize (this strain could be monitored in real time in the data collection van). The starting position was generally 1.8m from a target sensor (normally an HBM sensor); one test was performed for each of the front and rear wheels. The time in seconds from the start was recorded every time the vehicle began moving, and then again when it had come to rest. In this way, the final data could be matched to the times when the truck was moving and was stationary.

In order to check the drift characteristics of the sensors, we balanced the sensors and recorded for long periods during which no loads were applied to the test pad.

A slow (creep) speed test was conducted for test pad 1 though no faster runs were performed because of the proximity of the MLS fuel tanker to the end of the pad. Even on the creep speed test, the truck's front tires were over the first few sensors when the truck had backed up as far as was possible prior to commencing the creep run in the forward direction. The incremental static test was conducted in the same way. No drift tests were conducted on test pad 1.

The original study into sample rate concluded that the minimum sample rate should be 100Hz, with the optimum of 3 to 5 times this for speeds of 15 to 25km/h. Since we decided that very slow and even incremental static tests should be included in this test series, the sample rate was generally kept at 300Hz (though it was lowered to 50Hz for the very slow tests).

CHAPTER 4. DATA ANALYSIS

4.1 PILOT EXPERIMENT ON TEST SECTION 3

4.1.1 Survival Rate of Sensors

When a sensor is to be installed in a pavement under construction, it is subjected to the relatively high temperatures of the new asphalt (150-200°C) if it is installed at the top of the base. Even if it is installed at a lower point, it must also withstand considerable stress during compaction. The sensors are further at risk of being dislodged or skewed during pavement construction, which could result in erratic readings later. Finally, during the course of an APT experiment, the sensor will have to withstand a great many load cycles and, conversely, may also be subjected to long periods of purely environmental loading. As a result of this relatively harsh treatment some sensors can be expected to fail. Given that data collection efforts require sensors to be fully operational, it is important to gauge the expected survival rate of sensors. Knowing the expected survival rate then allows researchers to determine the number of sensors to install.

Sensor survival rates may be measured in various ways. At a primary level, it can be said that a sensor is inoperative if it fails a basic continuity test and, therefore, in most cases, gives no signal. Some sensors, however, pass the continuity test but nonetheless provide a completely flat signal or one that consists only of noise, with no visible reaction to a load pass. Finally, some sensors may provide signals that are either weak (and largely obscured by noise) or very erratic; such signals may consequently be insensitive to the primary objects of the experiment (in this case load, speed, and placement). Because weak signals are a matter of degree, such a defect is not included in our assessment of whether a sensor is working, though it is obviously an important indicator of how well the sensors are working.

Thus the survival rates for the sensors on test pad 3 are shown below in Table 4.1, based on the criteria that failed continuity or no sensitivity to main experiment factors constitutes a dead sensor.

Table 4.1 Survival rate of sensors in test pad #3

		TYPE					
		HBM	Kulite	Geokon	PML-60	PML-120	Kyowa
PAD #3	1/17/95	4/5	3/4	2/5	2/5	2/4	8/10
% survivability:		80	75	40	40	40	80

From the table it would appear that the HBM and Kyowa gauges were the best of the strain gauges. The smaller Kulite pressure cells had a considerably higher survival rate than the much

larger Geokon cells. Nonetheless, because it is not sufficient to simply provide a signal, further criteria are needed to analyze the strength of the signal.

4.1.2 Signal-to-Noise Ratio of Sensors

Another criterion for assessing a sensor is its signal-to-noise ratio. If the noise level in a sensor signal is very low relative to the primary signal of interest, the magnitude of the signal can be measured more accurately; additionally, small changes in the shape of the waveform (changes that would otherwise be lost in the noise) can be more easily identified. A relatively high signal-to-noise ratio is therefore important for response sensors.

While noise can be defined in various ways, in this case it is defined as the *standard deviation of the data from the first second of the sensor response history*. This basically captures the noise error in the signal with no load applied. The signal-to-noise ratio (S/N) was then calculated for each sensor for each test (432 data points) as the ratio of the maximum response for the test to the standard deviation of the first second of data in the test.

The plot of the S/N for all sensors for each test against the maximum value is shown in Figure 4.1. At least four distinct linear relationships are immediately evident; in fact, there are five groupings corresponding to the five different types of sensor used in the tests, with the PML and Kyowa strain gauge types showing the highest noise levels. Figure 4.2 shows the same plot for these two gauge types only. The fact that all are roughly linear indicates that the noise level is relatively constant for a particular gauge type and does not depend on the magnitude of the signal. It is also noteworthy that the slope of the linear relationship corresponds to the magnitude of the noise, with the steepest indicating the least noise. Assuming that variation in a maximum reading was due solely to this noise, then, in order to choose a reasonable minimum acceptable S/N, we could further assume that, if we wish a 95 percent population confidence limit for our readings of ±20 percent, roughly twice our noise level (as defined) would be equal to 20 percent of the signal. This yields a minimum S/N ratio of 10. Requiring ±10 percent would yield a minimum S/N of 20. From the plots in Figures 4.1 and 4.2 it is evident that the majority of the readings from the PML and Kyowa gauges would be unacceptable for even ±20 percent accuracy. It can also be seen that the pressure cells provide excellent data from this point of view, with the Kulite cells providing 6 times less noise than the Geokons. The HBM sensors gave S/N ratios comparable to the Geokon pressure cells, though the noise level was more variable. Finally, it should be remembered that the noise levels for the PML and Kyowa gauges are not in fact excessive, and if stronger signals could be obtained this noise would no longer be a problem. The signals for ±10 percent confidence limits would need to be 16 and 50 microstrain, respectively, in this case. It will be seen in the discussion of accuracy that expected strains are generally higher than 100 microstrain (at least in the wheel path). The S/N problem, therefore, has more to do with signal strength than with the inherent noise level.

4.1.3 Analysis of Variance in the Data

For a given experiment in which some major factors are varied — in this case load, speed and placement — general trends would be expected in the measured response, given trends in the

factors. We would for instance expect an increase in maximum strain for an increase in load, or a decrease in strain for an increase in the lateral placement of the sensor with respect to the load. Very importantly, however, changes should occur *only* as a result of changes in the factors. Other variations *not* explainable by changes in load, speed, or placement would be assumed to be caused by various other uncontrolled factors. These may be other, external factors or small differences in the main factors not recorded. In this case, for a single sensor, these are most likely going to be due to slight errors in the recorded values of the main factors — and especially placement. Because of this "error variation," we would then need to take a number of samples in order to establish a mean value with some degree of accuracy.

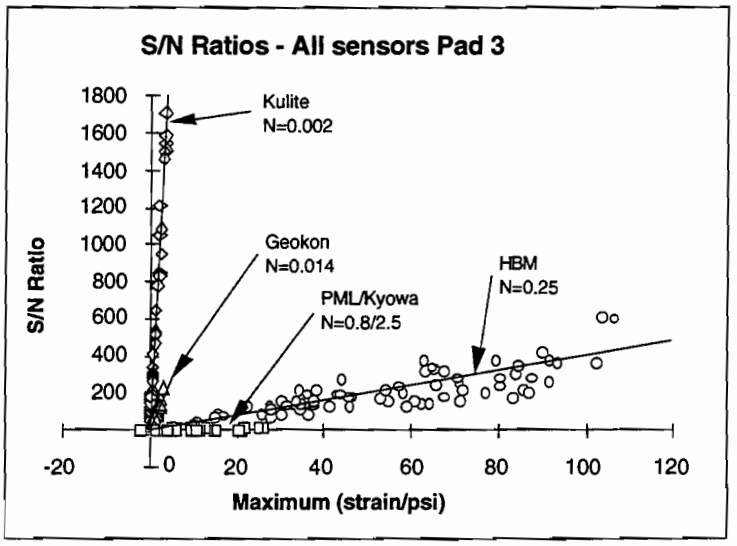

Figure 4.1 Plot of S/N ratio for all sensors for test pad 3 tests

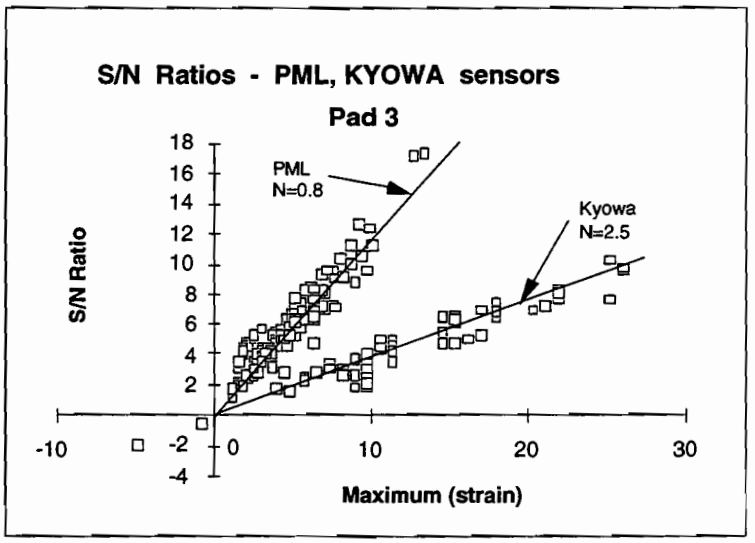

Figure 4.2 Plot of S/N ratio for PML and Kyowa sensors for test pad 3 tests

The most acceptable way of statistically determining if the sensors are sensitive to the main factors as expected is to analyze the variance in the data. An analysis of variance test on the data accomplishes this without attempting to generate a predictive model for the data. Another method is to generate a mathematical model for the data based on the main factors, and then to determine how much of the variance can be accounted for by the model. If both of these tests are done on the data, the total sum of squares given by each will be the same.

It should be remembered that for an entire test section there are different sources of variance. These can probably be divided into four main categories:

1. Variance at a single point in a test pad: This is normally due to the actual load, speed, and placement differing slightly from that recorded but would also include random variation in a single sensor.
2. Spatial variance between points in a test pad: This can be due to such differences as thickness or moduli of pavement layers, slight differences in the main factors, or differences between sensors.
3. Spatial variance between test pad locations on a section: This would be due to similar factor differences as those above and may result in similar or considerably more variance compared to that above.
4. Temporal variance: This may be present in any of the above and would be a result of factors that may be assumed to remain constant over a very short time but can change over the long term (e.g., temperature or moisture).

From the experiment described here on test pad 3, it was possible to get some measure of the first two categories of variance sources by analyzing the data by sensor and then by sensor type. In the first analysis, assessing the category 1 variance would lead to a recommended sample size number of load repetitions to measure. In the second analysis, a measure of the total category 1 and 2 variance would be assessed and, by comparing the results for each sensor type, the inter- and intra-type variance would be separated. The analyses are described in more detail below.

4.1.4 Analysis of Variance by Sensor

Because of the extreme difficulty in controlling the exact lateral placement of the truck over the sensors, we decided to aim for three "levels" of placement, but to record each placement more accurately after the run. While the initial experimental design is balanced, the resulting data are in fact unbalanced, with few, if any, repeats, since each and every recorded placement value is likely to be slightly different. As a result of this difficulty, a general analysis of variance test may not be directly applicable; accordingly, we used a simplified but more specialized procedure that involved modeling the data using a simple quadratic response-surface model estimated by least squares regression. This may be written as:

$$y = \beta_0 + \beta_1 x_1 + \beta_2 x_2 + \beta_3 x_1^2 + \beta_4 x_2^2 + \beta_5 x_1 x_2 + e$$

for combinations of values of two factor variables x_1 and x_2 but which can be generalized to accommodate any number of factors. In this case, the dependent variable, y, has been designated

as the peak tensile strain for the strain gauges and as the peak positive pressure for the pressure cells. While this method is not ideal, it at least allows limited curved surface modeling and provides a good idea of how much each factor contributes to the statistical fit and how much of the total variation can be explained by the model.

Sensitivity to Load: As mentioned previously, the main purpose of analyzing the variance by sensor is basically to assess how well each sensor is working. Since we expect to see some response as the wheel load passes over the sensor, the most fundamental assessment is the sensitivity of the sensor to the load. We have already done this indirectly by looking at the signal-to-noise ratio. In the quadratic surface model, the magnitude of the linear coefficient for load will provide an effective measure of this load sensitivity. Assuming the levels of factors used in the experiment span the long-term operating range, a parameter from coded "normalized" data is estimated in order to directly compare sensitivity to different factors. In addition, it is important to assess whether the parameter is simply a best fit through a random cluster of data or is indeed significant. This may be done using a simple t-test. Table 4.2 shows the actual parameter estimate, its standard error, the value of the t-statistic for the hypothesis that the data could be modeled as well if the parameter was omitted (along with associated probability), and finally the "normalized" parameter estimate discussed above.

In general, we can say that if the normalized parameter estimate is high (and significant as shown by low type I error probability), then the sensor is sensitive to load and performing well. It should be remembered, however, that the dependent variable has totally different units for strain gauges (microstrain) and pressure cells (psi). Thus, while the sensors in each group are therefore comparable, the two groups are not.

Error Variance and Sample Size: If we intentionally change nothing, we would expect to obtain the same answer. Any variance would then be "error variance" or at least "uncontrolled variance" and would require a number of samples to reliably estimate a mean. In the case of our quadratic response-surface model, some of the residual error may be pure random error and some may simply be lack of fit error. Unfortunately, unless a number of replicates are obtained for each factor combination, it is not possible to distinguish between them. Nonetheless, if we assume that a quadratic model *is* adequate, then the total error will be a good estimate of the error variance and the R-Square value will reflect the proportion of total variation explainable by the model (main factors). While this is not ideal, it is certainly not unreasonable. The remaining residual error would be error not quantitatively explainable in the data even though we might speculate that it was because recorded placement or speed was not exact or because bounce in the truck may have caused slight variation in the load. Once we have established that a sensor is sufficiently sensitive to load, we may then judge how consistently it measures by looking at the R-Squared value and at the coefficient of variation (CV).

There are many ways to calculate sample sizes; for our purposes, the method used by Ostle and Malone [Ostle 88] appeared most appropriate. Using their table (Ref 88, page 642), the number of observations for a t-test of the mean is given for various levels of reliability. The sample sizes needed to detect a 10 percent difference (delta mu = 0.10) between two means with an alpha

error of 0.1 and a beta error of 0.2, are shown in Table 4.3 for the sensors with a linear load coefficient greater than 0.5 for strain gauges and 0.05 for pressure cells (arbitrarily chosen and fairly conservative). These sample sizes would correspond to the number of load applications in this analysis by sensor. The R-Square value, CV and the d/s value are also given in the table.

Table 4.2 Quadratic response-surface model linear coefficients for load and other parameters for experiment on test pad 3 by sensor

Sensor	Linear Load Coef. Estimate	Standard Error	t for Ho: Parameter=0	Prob > |t|	Estimate from Coded Data
S1	0.012937	0.002263	5.717	0.0003	24.01
S2	0.011163	0.002116	5.277	0.0005	24.58
S3	0.006303	0.002316	2.721	0.0236	26.14
S4	0.004127	0.002459	1.678	0.1276	20.05
S5	0.00007053	0.00001317	5.357	0.0005	0.220
S6	0.000350	0.00003429	10.205	0.0000	1.022
S7	0.000146	0.00002155	6.774	0.0001	0.209
S8	0.000149	0.00006763	2.198	0.0555	0.811
S9	0.00004680	0.00000969	4.832	0.0009	0.175
S10	0.000289	0.000162	1.779	0.1090	-0.10
S11	0.000607	0.000876	0.693	0.5061	2.09
S12	-0.001100	0.000714	-1.542	0.1575	0.72
S13	-0.000090	0.000786	-0.114	0.9114	0.77
S14	-0.000024	0.000734	-0.0322	0.9750	1.82
S15	-0.000985	0.001547	-0.637	0.5403	0.36
S16	0.000656	0.001118	0.586	0.5721	1.59
S17	0.002879	0.003162	0.910	0.3864	2.99
S18	0.000729	0.001563	0.466	0.6522	-1.33
S19	0.005391	0.002161	2.494	0.0342	6.02
S20	-0.003832	0.002420	-1.584	0.1477	2.41
S21	0.003012	0.003783	0.796	0.4464	3.25
S22	0.002269	0.003745	0.606	0.5595	9.82
S23	0.003880	0.003728	1.041	0.3251	2.52
S24	0.001063	0.002825	0.376	0.7155	0.20

Note: Sensor descriptions are given in Table 4.3

Table 4.3 Quadratic response-surface model r-square values and sample sizes for experiment on test pad 3 by sensor

Sensor	Description	R-Square	CV	d/s	n
S1	HBML	0.988	0.075	1.33	<5
S2	HBML	0.985	0.060	1.67	<5
S3	HBML	0.988	0.068	1.47	<5
S4	HBML	0.978	0.093	1.08	<5
S5	Kulite	0.995	0.050	2.00	<5
S6	Kulite	0.998	0.027	3.70	<5
S7	Kulite	0.991	0.076	1.32	<5
S8	Geokon	0.987	0.076	1.32	<5
S9	Geokon	0.995	0.037	2.70	<5
S10	pml-60	-	-	-	-
S11	pml-60	0.770	0.249	0.40	19
S12	pml-60	0.757	0.273	0.37	24
S13	pml-60	0.581	0.406	0.25	45
S14	pml-120	0.798	0.258	0.39	19
S15	pml-120	-	-	-	-
S16	Kyowa	0.754	0.364	0.27	45
S17	Kyowa	0.693	0.394	0.25	45
S18	Kyowa	-	-	-	-
S19	Kyowa	0.839	0.221	0.45	15
S20	Kyowa	0.637	0.251	0.40	19
S21	Kyowa	0.618	0.450	0.22	70
S22	Kyowa	0.851	0.237	0.42	15
S23	Kyowa	0.660	0.451	0.22	70
S24	Kyowa	-	-	-	-

4.1.5 Analysis of Variance by Type

Having already used the quadratic response-surface model estimated by least squares regression for the individual sensors, it is now appropriate to use exactly the same procedure on all the sensors of a particular type in order to assess the total category 1 and 2 variance; that is, the spatial variance within the test pad as well as the individual sensor variance. Table 4.4 shows the classification of sensors into different types.

Table 4.4 Type classification of sensors in test pad 3

Sensor	Description		Type
S1	HBML	longitudinal	10
S2	HBML	longitudinal	10
S3	HBML	longitudinal	10
S4	HBML	longitudinal	10
S5	Kulite	top of subgrade	20
S6	Kulite	top of subgrade	20
S7	Kulite	top of lime treated subbase	21
S8	Geokon	top of lime treated subbase	30
S9	Geokon	top of lime treated subbase	30
S10	pml-60	longitudinal	40
S11	pml-60	longitudinal	40
S12	pml-60	transverse	41
S13	pml-60	longitudinal	40
S14	pml-120	transverse	50
S15	pml-120	longitudinal	51
S16	Kyowa	longitudinal	60
S17	Kyowa	transverse	61
S18	Kyowa	longitudinal	60
S19	Kyowa	transverse	61
S20	Kyowa	longitudinal	60
S21	Kyowa	longitudinal	60
S22	Kyowa	transverse	61
S23	Kyowa	transverse	61
S24	Kyowa	longitudinal	60

By analyzing the variance by type, we can now check to see what variance is to be expected from a number of different sensors placed in different positions in a particular test pad. Since the variance due to changes in such things as thickness and moduli would be expected to be roughly the same for each type without any knowledge to the contrary, differing variance shown for the different types of sensor would probably be due mainly to inconsistencies between the individual sensors within a type classification. If a particular sensor, an HBM gauge for instance, gives very repeatable and precise results individually, but the measurement from one HBM to another HBM differs markedly, this would lead us to suspect that there was either a lot of spatial variance present in the pavement or that HBM-type gauges were not consistent among themselves. If, on the other hand, Kyowa gauges showed a lot more variability than the HBM gauges, then it would appear that whatever the pavement variation, the HBMs were more consistent than the Kyowas as a group.

Sensitivity to Load by Type: As for the analyses by sensor, it is also important to know the sensitivity to load for the different types of sensor. The quadratic model linear coefficients and

other parameters for load are therefore given for each sensor type in Table 4.5, as was done for the individual sensors previously. Only those types containing more than one sensor were used in the analysis.

Table 4.5 Quadratic response-surface model linear coefficients for load and other parameters for experiment on test pad 3 by type

Type	Linear Load Coef. Estimate	Standard Error	t for HO: Parameter=0	Prob > |t|	Estimate from Coded Data
10	0.008872	0.002233	3.974	0.0002	23.47
20	0.000363	0.000184	1.968	0.0594	0.63
21	-	-	-	-	-
30	0.000215	0.000114	1.892	0.0693	0.49
40	0.00007888	0.000513	0.154	0.8784	1.22
41	-	-	-	-	-
50	-	-	-	-	-
51	-	-	-	-	-
60	0.000236	0.001484	0.159	0.8741	1.67
61	0.004391	0.002559	1.716	0.0912	5.09

Error Variance and Sample Size by Type: Because the analysis of the data by type of sensor includes the variation both spatially within the test pad and between the individual sensors of the group, the same set of t-tests for the detection of differences between means as was used previously may be applied in order to obtain a total sample size for any particular type of sensor. This would include the sample size to account for variation at a single sensor position and therefore the number of sensors requiring to be placed in the test pad could be estimated as the total number given in the previous analysis by type minus the number of load repetitions given in the analysis by sensor. In general we would obviously expect the variation within a type to be considerably more than that for an individual sensor.

The reason for installing more than one sensor should be briefly discussed. While it will often be possible and reasonable to check for trends in the response from a single sensor with accumulating load repetitions during a single MLS experiment, if the data are to be stored in a database, then they should be stored with information on the pavement characteristics to be compared with other similar experiments. If the exact layer thicknesses and moduli are known for each single sensor position, and the sensor at that position is of a type for which sensors are very consistent among themselves, then data from a single sensor may be stored directly. It is more likely, however, that the identification data will pertain to the *mean* pavement layer thicknesses, moduli, etc., and therefore a *mean* response level for the test pad would also be needed. In order to obtain a reliable estimate of the mean for a test pad, it would be imperative to sample different positions depending on the variability.

The total sample sizes, n, for detecting a 10 percent difference in the means with alpha error of 0.1 and beta error of 0.5 are given in Table 4.6. If the previously calculated number of load repetitions was less than five, this would be a good estimate of the number of sensors needed.

Table 4.6 Quadratic response-surface model r-square values and sample sizes for experiment on test pad 3 by type

Type	Description	R-Square	CV	d/s	n
10	HBML	0.909	0.142	0.70	8
20	KuliteTS	0.875	0.346	0.29	32
21	KuliteTLTS	-	-	-	-
30	GeokonTLTS	0.905	0.291	0.34	24
40	pml-60L	0.562	0.412	0.24	45
41	pml-60T	-	-	-	-
50	pml-120L	-	-	-	-
51	pml-120T	-	-	-	-
60	KyowaL	0.230	0.501	0.20	70
61	KyowaT	0.345	0.498	0.20	70

Note: L=longitudinal; T=transverse; TS=top of subgrade; TLTS=top of lime treated subbase

It can be concluded from the above that at least for test pad 3 and associated sensors, the HBM sensors are the most consistent of the strain gauges, with PML-60s requiring more than 5 times as many sensors to obtain comparable precision. The large sample sizes required for the pressure cells are somewhat surprising, considering their individual consistency. The high R-Square values show that this should not be due to lack of fit error from the limitations of the quadratic model and so would seem to indicate either variability from one sensor to another or possibly sensitivity to slight differences in installation (e.g., compaction around the gauge). Because the gauges are not bonded to the bottom of the AC as are the strain gauges, this higher sensor-to-sensor variation for the pressure cells should not be totally unexpected.

4.2 PILOT EXPERIMENT ON TEST PADS 1 AND 2

4.2.1 Survival Rate of Sensors

Table 4.7 shows the survival rate for sensors at the date of the experiment on test pad 2, based on the criteria that failed continuity or no response to load constitutes a "dead" sensor.

Table 4.7 Survival rate of sensors in test pad 2

	DATE	TYPE					
		HBM	Kulite	Geokon	PML-60	PML-120	Kyowa
PAD #2	7/5/95	4/10	7/7	2/7	14/22	1/2	0/3
% survivability:		40	100	29	64	50	0

It is interesting that not as many HBMs survived as in test pad 3, where the rate was 80 percent. As before, the smaller Kulite pressure cells survived better than did the large Geokon cells. Rates for the PML gauges were similar but the rate for Kyowas dropped from 80 percent to zero.

4.2.2 Analysis of Variance by Sensor

Sensitivity to Load: As with the previous experiment on test pad 3, the data were modeled using a simple quadratic response-surface model estimated by least squares regression. This and the reasons for its use are discussed in more detail under the previous test. Once again, in order to assess the sensitivity to load for each sensor, the linear coefficient for load in the model, together with its standard error, t-statistic for the hypothesis that the coefficient is zero (along with associated probability), and the parameter estimate from coded data are all given for each sensor recorded in test pad 2 in Table 4.8.

As for the pad 3 sensors, it can be seen that the HBM gauges (S1-S4) show good sensitivity to load. Because S2 is a transverse sensor offset from the wheel path, it registers only compressive strain (negative in this analysis) and the "maximum" strain data are therefore not meaningful. (This applies to S37 as well, but other transverse sensors appear to have been close enough to the wheel path to register some tensile strain.) The results from the pressure cells (S5-S18) are comparable with the pad 3 figures, although S5 is 1090mm offset from the wheel path, as is S16. S18 has a 630mm offset. S13 and S14 are obviously not working. The pml-60 gauges (S19-S36) show reasonable sensitivity, though S22, S27 and S34-S36 show weak response. S29 is affected by major drifts during the recording time, suggesting that it is not balanced. The Kyowas (S38-S39) showed similar sensitivity to the working pml-60 gauges.

Error Variance and Sample Size: Using the same method as was used for the pad 3 tests, once a grand mean and mean square error have been calculated from the quadratic model, it is possible to estimate a required sample size for each sensor to obtain a certain reliability. This sample size is specific to each sensor and is therefore an estimate of the number of load applications required. As before, the sample sizes given in Table 4.9 below are those that would be required to detect a 10 percent difference between two means with an alpha error of 0.1 and a beta error of 0.2. Only those sensors showing a normalized linear load coefficient greater than 2.5 for strain gauges and 0.05 for pressure cells were analyzed.

4.2.3 Analysis of Variance by Type

As with the tests on pad 3, it is also important to analyze the variance caused by measurements by different sensors at different positions. This may be done by grouping the sensors by type. The classification of the sensors by type is shown in Table 4.10.

Table 4.8 Quadratic response-surface model linear coefficients for load and other parameters for experiment on test pad 2 by sensor

Sensor	Linear Load Coef. Estimate	Standard Error	t for HO: Parameter=0	Prob > |t|	Estimate from Coded Data
S1	0.041151	0.007754	5.307	0.0001	51.24
S2	0.016973	0.002412	7.037	0.0000	18.97
S3	0.094752	0.009131	10.378	0.0000	134.68
S4	0.089677	0.005395	16.735	0.0000	122.89
S5	0.000058946	0.00000820	7.191	0.0000	0.08
S6	0.000155	0.00002801	5.540	0.0001	0.23
S7	0.000359	0.00004659	7.703	0.0000	0.50
S8	0.000018197	0.00000833	2.186	0.0477	0.00
S9	0.001191	0.000110	10.780	0.0000	1.79
S10	0.001140	0.000164	6.964	0.0000	1.66
S11	0.004146	0.000412	10.063	0.0000	6.14
S12	0.000177	0.00001749	10.138	0.0000	0.30
S13	0.000000255	0.00000157	0.162	0.8740	0.0004
S14	0.000001734	0.00000111	1.568	0.1409	0.0026
S15	0.000848	0.000127	6.662	0.0000	1.19
S16	0.000010595	0.00000217	4.889	0.0003	0.02
S17	0.000114	0.00001499	7.598	0.0000	0.17
S18	-0.000122	0.00003062	-3.984	0.0016	-0.09
S19	0.002569	0.000371	6.925	0.0000	3.99
S20	0.001830	0.000370	4.947	0.0003	3.83
S21	0.003136	0.000238	13.174	0.0000	5.74
S22	0.001049	0.000710	1.479	0.1630	-0.07
S23	0.002167	0.000349	6.202	0.0000	3.58
S24	0.003987	0.000220	18.109	0.0000	6.19
S25	0.001015	0.000809	1.255	0.2316	2.60
S26	0.002594	0.000552	4.702	0.0004	3.14
S27	0.000261	0.000431	0.606	0.5551	0.29
S28	0.002048	0.000362	5.662	0.0001	2.73
S29	0.712868	0.120548	5.914	0.0001	561.58
S30	0.003758	0.000344	10.932	0.0000	5.49
S31	0.003297	0.000346	9.541	0.0000	5.62
S32	0.006690	0.000961	6.962	0.0000	8.72
S33	0.002600	0.000366	7.100	0.0000	2.74
S34	0.001013	0.000274	3.696	0.0027	1.00
S35	0.000078202	0.000266	0.294	0.7733	0.02
S36	0.001788	0.000423	4.222	0.0010	2.28
S37	0.002741	0.000245	11.168	0.0000	3.27
S38	0.001728	0.000930	1.857	0.0861	3.02
S39	0.002266	0.000989	2.291	0.0393	5.14

Table 4.9 Quadratic response-surface model r-square values and sample sizes for experiment on test pad 2 by sensor

Sensor	Description	R-Square	CV	d/s	n
S1	HBML	0.89	0.187	0.53	22
S2	HBMT	0.47	-0.564	-	-
S3	HBML	0.98	0.096	1.04	8
S4	HBML	0.98	0.062	1.61	<5
S5	Kulite	0.92	0.128	0.78	12
S6	Kulite	0.82	0.153	0.65	17
S7	Kulite	0.97	0.124	0.81	12
S8	Kulite	-	-	-	-
S9	Kulite	0.83	0.088	1.14	7
S10	Kulite	0.93	0.132	0.76	13
S11	Kulite	0.74	0.105	0.95	9
S12	Geokon	0.01	0.080	1.25	6
S13	Geokon	-	-	-	-
S14	Geokon	-	-	-	-
S15	Geokon	0.91	0.148	0.68	17
S16	Geokon	-	-	-	-
S17	Geokon	0.87	0.102	0.98	9
S18	Geokon	-	-	-	-
S19	pml-60	0.97	0.053	1.89	<5
S20	pml-60	0.91	0.064	1.56	<5
S21	pml-60	0.94	0.048	2.08	<5
S22	pml-60	-	-	-	-
S23	pml-60	0.89	0.078	1.28	6
S24	pml-60	0.98	0.033	3.03	<5
S25	pml-60	0.23	0.275	0.36	52
S26	pml-60	0.69	0.203	0.49	27
S27	pml-60	-	-	-	-
S28	pml-60	0.94	0.069	1.45	<5
S29	pml-60	-	-	-	-
S30	pml-60	0.93	0.050	2.00	<5
S31	pml-60	0.88	0.055	1.82	<5
S32	pml-60	0.89	0.123	0.81	12
S33	pml-60	0.85	0.137	0.73	15
S34	pml-60	-	-	-	-
S35	pml-60	-	-	-	-
S36	pml-60	-	-	-	-
S37	pml-120	-	-	-	-
S38	Kyowa	0.53	0.143	0.70	15
S39	Kyowa	0.51	0.116	0.86	11

Table 4.10 Type classification of sensors in test pad 2

Sensor	Description		Type
S1	HBML	longitudinal	10
S2	HBMT	transverse	11
S3	HBML	longitudinal	10
S4	HBML	longitudinal	10
S5	Kulite	top of subgrade	20
S6	Kulite	top of subgrade	20
S7	Kulite	top of subgrade	20
S8	Kulite	top of lime treated subbase	21
S9	Kulite	top of lime treated subbase	21
S10	Kulite	top of lime treated subbase	21
S11	Kulite	top of base	22
S12	Geokon	top of lime treated subbase	31
S13	Geokon	top of lime treated subbase	31
S14	Geokon	top of lime treated subbase	31
S15	Geokon	top of base	32
S16	Geokon	top of subgrade	30
S17	Geokon	top of subgrade	30
S18	Geokon	top of subgrade	30
S19	pml-60	transverse	41
S20	pml-60	longitudinal	40
S21	pml-60	longitudinal	40
S22	pml-60	transverse	41
S23	pml-60	longitudinal	40
S24	pml-60	longitudinal	40
S25	pml-60	transverse	41
S26	pml-60	transverse	41
S27	pml-60	transverse	41
S28	pml-60	longitudinal	40
S29	pml-60	transverse	41
S30	pml-60	transverse	41
S31	pml-60	longitudinal	40
S32	pml-60	transverse	41
S33	pml-60	longitudinal	40
S34	pml-60	transverse	41
S35	pml-60	transverse	41
S36	pml-60	longitudinal	40
S37	pml-120	transverse	51
S38	Kyowa	longitudinal	60
S39	Kyowa	transverse	61

Sensitivity to Load by Type: Since the fundamental response we are using the sensors to measure is that generated by a wheel load, it is important that the sensors show fairly good sensitivity to load. This is vital for individual sensors, but if we need to sample different positions in a test pad by using a number of sensors of a particular type, it is also important that sensors show this load sensitivity as a group. As before, a measure of this sensitivity is the linear coefficient for load from the quadratic response-surface model generated from the data. This and associated parameters are shown in Table 4.11 for those sensors analyzed individually in the previous section.

Table 4.11 Quadratic response-surface model linear coefficients for load and other parameters for experiment on test pad 2 by type

Sensor	Linear Load Coef. Estimate	Standard Error	t for HO: Parameter=0	Prob > |t|	Estimate from Coded Data
10	0.093282	0.018675	5.000	0.0000	110.97
11	-	-	-	-	-
20	0.000360	0.00002723	13.214	0.0000	0.27
21	0.001165	0.00009140	12.751	0.0000	1.73
22	-	-	-	-	-
30	-	-	-	-	-
31	-	-	-	-	-
32	-	-	-	-	-
40	0.003551	0.000420	8.449	0.0000	4.45
41					
51	-	-	-	-	-
60	-	-	-	-	-
61	-	-	-	-	-

Error Variance and Sample Size by Type: Again, assuming that the variance calculated from the "by-type" quadratic model reflects that resulting from total category 1 and 2 variance, a sample size may be recommended that represents the total number of samples (including the number of load passes calculated previously) for a reliable estimate of the mean response for a test pad. These total sample sizes are given in Table 4.12.

Table 4.12 Quadratic response-surface model r-square values and sample sizes for experiment on test pad 2 by type

Sensor	Description	R-Square	CV	d/s	n
10	HBML	0.68	0.321	0.31	71
11	HBMT	-	-	-	-
20	KuliteTS	0.96	0.153	0.65	17
21	KuliteTLTS	0.91	0.104	0.96	9
22	KuliteTB	-	-	-	-
30	GeokonTS	-	-	-	-
31	GeokonTLTS	-	-	-	-
32	GeokonTB	-	-	-	-
40	pml-60L	0.85	0.149	0.67	17
41	pml-60T	0.70	0.335	0.30	71
51	pml-120T	-	-	-	-
60	KyowaL	-	-	-	-
61	KyowaT	-	-	-	-

Note: L=longitudinal; T=transverse; TS=top of subgrade; TLTS=top of lime treated subbase;TB=top of base

4.2.4 Temperature

All analyses up to this point have related to strain and pressure gauges. Although these measure the chosen dependent response variables, the measurement of the independent factor variables is also important. Up till now, these have generally been accepted to be load, speed, and placement, but it is evident that moduli of layers is also a very important independent factor variable. Because this is dependent on temperature, it will certainly vary with time as temperature varies, unless strict environmental control is available. Unless the moduli are to be measured in some way every time a sample is taken, it is thus vital that at least temperature be recorded. A secondary advantage of recording temperature is that, if sensor measurement itself is temperature sensitive, this can be corrected for, if temperature is known.

While temperature at the surface is not difficult to measure, a thermocouple tree that measures temperature at a number of depths is required to obtain a full temperature gradient through the pavement layers. These have in fact been installed in the test pads; and although temperatures were not recorded for test pad 3 tests, they were recorded from three thermocouple trees in test pads 1 and 2. By referring to the graphs of temperatures in the appendices, it can be seen that while temperatures do not differ much between tests conducted within an hour or so, there are marked differences, for instance, between the tests with a full (pm) and half-full (am) truck on pad 2, with temperatures in the AC ranging from 43-38°C in the former case to 35-36°C in the latter case.

The reliability of the temperature measurements appears to be good in both test pads 2 and 1, with temperatures measured by the three different thermocouples agreeing generally to within

one degree. Temperature measurements at the surface may vary by more (if one happens to be in the shade for instance). The observed differences at deeper depths (±1350mm) are more difficult to explain but may be due to differing subgrade material.

4.2.5 Drift of Sensors

The measurement of strain or pressure from electrical transducers of almost any sort is complicated by the fact that if continuous measurements are made for an extended time, the signal tends to drift regardless of the fact that no load is being applied. This requires that many have to be balanced first in order to ensure that at least at the beginning of the recording the sensor registers zero for zero load. If some point in time during the recording is known for some reason or another to represent zero response, the recorded measurements can be "calibrated" by simple translation at a later date, even if the sensor was not balanced to begin with. If the sensor output signal tends to drift erratically, however, it is very difficult to correct for this later.

If it is assumed that measurements from the sensors will be recorded for at least 5 and possibly as long as 20 seconds for any given sample, it is very important to be satisfied that any measurement is made from the same base line for the entire time or, in other words, that no drift occurred during this time. While no quantitative assessment of drift was undertaken, it is nonetheless worth describing some of the subjective findings.

Using the data acquisition equipment to view the measurements in real time, the signals from a number of sensors in test pads were observed for almost 10 minutes. In general it appeared that drift, if present, tended to be slow and gradual and did not step suddenly up or down (though this did occur on a small scale). The one Kyowa gauge being watched, for instance, wandered erratically by around 7 microstrain at a time. One of the HBM gauges held steady for long periods, but would then suddenly change over about 5 seconds to a new level, while another stayed absolutely steady for the entire time. We suspected that this may have been linked to movement by individuals in and around the test pad and data collection van. A pml-60 gauge wandered slightly, but generally stayed within 3 microstrain of zero. All sensors showed noise in the signal, but, as described in the discussion on signal-to-noise ratio, this was for instance most evident in the Kyowa gauges and least evident in the HBMs. There was no observable noise in the pressure cell signals.

In conclusion, the drift would appear to be small and restricted to certain sensors. No definite difference in drift susceptibility was evident among the different types of sensor. It is possible that such things as the electrical connections to the data acquisition equipment and earthing may play a significant role in limiting drift, and that the sensors themselves have little to do with it. It is definitely an important consideration, however, and should be checked at times.

4.2.6 Incremental Static Tests and Visco-Elastic Creep

In addition to the other tests carried out on test pads 1 and 2, very slow speed and incremental static rollovers were also performed to investigate visco-elastic response in the pavement. As with the other test results, the time histories for the sensors that were recorded are graphed in the appendices. From these time histories, it is evident that the visco-elastic behavior is

present and can be easily detected by the HBM sensors. The general form of the experiment was to incrementally advance the truck by 0.304m (this movement taking 1 or 2 seconds) and then let it remain at each position at least 10 – 30 seconds in order to let the strain increase rate stabilize as required for visco-elastic characterization by creep compliance described below.

Given that visco-elastic properties of pavements are increasingly the subject of practical research, it may be very useful to be able to measure these properties in-situ in the controlled but realistic environment of APT research. Two basic ways to characterize visco-elastic properties of a material are by creep compliance at various times and by complex modulus [Huang 93]. The method more applicable to field experiments is probably the creep compliance method. It is possible to determine the visco-elastic constants (the elastic moduli E for springs and the relaxation times T for the dashpots) of a generalized mechanical model consisting of a Maxwell and a number of Kelvin models from a plot of the time-dependent compliance (defined as the time-dependent strain divided by the constant stress). In order to do this, the curve must be plotted until the slope is constant. Since the compliance is directly proportional to the strain for constant stress, the curves seen in the strain histories for the incremental static tests should have basically the same shape as the creep compliance curves, assuming the stress is constant. Since the load is stationary, this might be expected to be a reasonable assumption. It is interesting, however, that this appears to be more or less the case for the second repetition of the front axle, 19kN, incremental static test on pad 2 but not for the first repetition.

While no actual calculations were performed at this time, it would appear that if it is determined that strain and stress behavior can be measured eventually with some degree of accuracy and precision, and questions regarding how constant the stress is can be resolved, it may well be possible to analyze visco-elastic behavior in the future.

4.3 COMPARISON OF TESTS AND DISCUSSION

4.3.1 Survival Rate of Sensors

It can be seen from Table 4.13 that the overall survivability of the sensors varied considerably. Of the strain sensors, the HBMs and the PML-60s had survival rates of about 60 percent, with the PML-120s and Kyowas showing considerably lower survival rates. Of the pressure cells, it would appear that the Kulites are very robust, with an almost 90 percent survival rate. The Geokons, however, had a survival rate of only 34 percent.

Table 4.13 Overall survival rate of sensors

		TYPE					
		HBM	Kulite	Geokon	PML-60	PML-120	Kyowa
PAD #3	1/17/95	4/5	3/4	2/5	3/5	1/4	4/10
PAD #2	7/5/95	4/10	7/7	2/7	14/22	1/2	0/3
average % survivability:		60	88	34	62	38	20

4.3.2 Repeatability (Precision) of Sensors

From the preceding analyses in this chapter, it is evident that sensors show considerable variation both individually and as a type. A good measure of the repeatability or precision of the sensor readings may be summarized by their coefficients of variation (CV) from the previous quadratic response surface models. Graphs of the coefficients of variation for each sensor individually and as a type for each test pad are shown in Figures 4.3 and 4.4.

The graphs show that, individually, the HBM strain gauges (S1-S4) and both the Kulite and Geokon pressure cells (S5-S9) show high sensitivity and high repeatability. The PML and Kyowa gauges (S10-S24) are in general more variable. As can be expected when the spatial variability is added, repeatability is not as good when sensors are considered together as a type.

One reason for this spatial variability is probably the considerably lower pavement moduli in the areas of the test pads, where pressure cells were installed at the top of the subgrade and at the top of the lime-treated subbase. As mentioned in the section on installation of sensors in Chapter 2, the layerworks were brought up to the top of the base using normal construction and compaction methods. Where the pressure cells were to be installed, however, a rectangular area of the base and subbase were removed, the sensors placed, and the layers replaced and hand compacted. Probably as a result of this hand re-compaction, the deflections from FWD tests have proved to be considerably higher in these areas, indicating that the moduli were lower. If this was the case, the strain gauges then placed subsequently at the top of the base in this area would be expected to show higher strains than their counterparts outside the pressure cell area; this has indeed been found to be so.

Another explanation for spatial variability of measured responses in the test pad is the fact that the thicknesses of the AC layer were found by coring to vary by more than 25mm in some cases. This in itself may not influence measured strains by much, but it is interesting that Scazziga et al. [Scazziga 87] reported that, in the Nardo road tests in 1984, the exact depth at which the sensors were installed had a large impact on the measured strains. They concluded that "the influence is not negligible at all, with strain differences of 10% for as little as 5mm of distance [from the bottom of the AC layer] and up to 30% for 20mm of distance." This is borne out to a certain extent by ELSYM5 calculations. Table 4.14 shows typical calculated strains for a typical 200-mm AC layer.

Table 4.14 Typical calculated strains for a typical 200 mm ac pavement and 54kn load at 21°c

	MICROSTRAIN		
Depth (mm)	0 mm from load	50mm from load	150mm from load
175	74.0	67.6	2.2
187	86.0	78.8	5.6
195	94.2	86.2	7.1
200	100.1	91.7	7.8
205	98.1	90.0	9.4
212	95.1	87.5	11.6

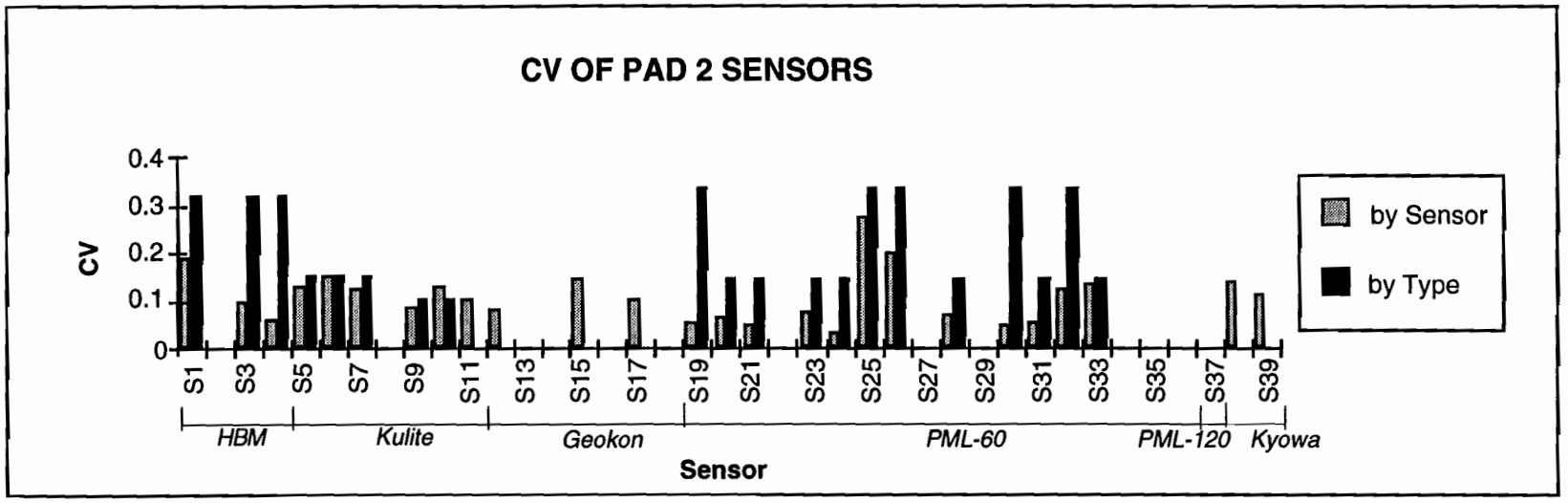

Figure 4.3: Coefficients of Variation for Sensors in Test Pad 2

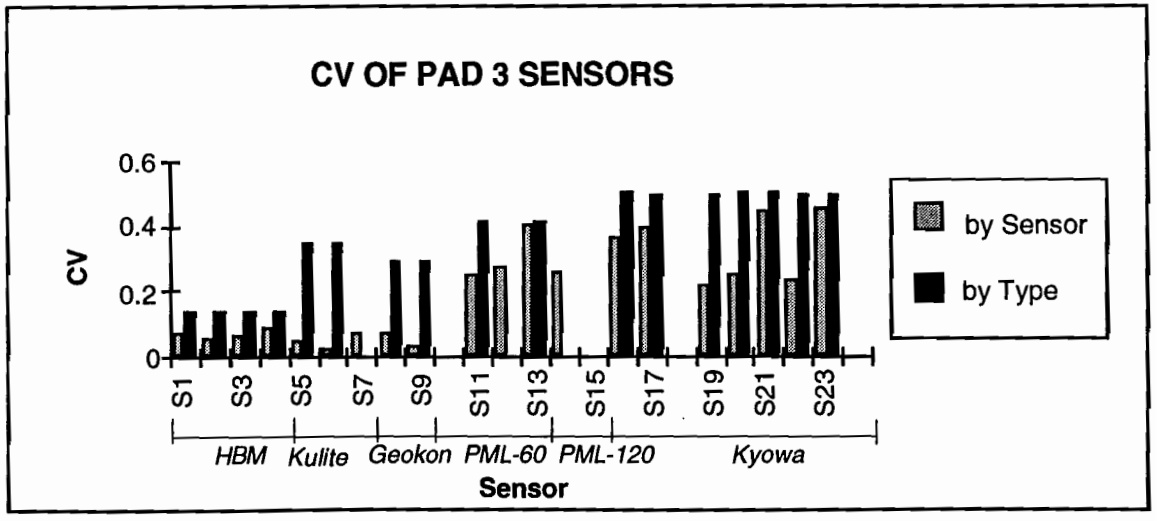

Figure 4.4: Coefficients of Variation for Sensors in Test Pad 3

While these explanations serve to account for some of the spatial variability in the test section, this also emphasizes the fact that, had there been similar variability owing to other unmeasured differences in layer moduli or thickness, it would have been inexcusable to measure only strain at a single point and declare it to be representative of the whole test pad.

What is most evident from the two different sets of experiments, however, is the inter-pad variability. Although pad 2 and pad 3 theoretically have the same pavement design, the two sets of response measurements are totally different. This can be seen in the quadratic response-surface models generated from pad 2 and pad 3 data earlier in the chapter. Examples of the predicted response at different placements for HBM and PML-60 strain gauges are shown in Figures 4.5 and 4.6.

From the models it can immediately be seen that strains as measured by HBM gauges are more than 4 times higher for pad 2 than for pad 3 at zero placement. It is also noteworthy that the two sensors at a placement of 175mm gave very different measurements. This is possibly a result of a difference in the base and subbase stiffnesses created by the installation of pressure gauges as discussed previously. PML-60 gauges showed an increase from around 4 microstrain to 40 microstrain.

While this major inter-test pad variation appeared difficult to explain initially, there may be a number of factors contributing to this difference. The first noteworthy difference falls under the temporal (category 4) type variation discussed earlier. While the temperatures within the pavement were not recorded directly for the experiment on test pad 3, the afternoon pavement surface temperature was recorded as 19°C. The test was performed in January on a rainy day, so this is not surprising. The tests on test pad 2, however, were carried out in July under hot summer conditions, with the temperature of the pavement surface between 38°C and 43°C. It was reported by Scazziga et al. [Scazziga 87] that, in the Nardo road tests, it was easily possible to get a fourfold increase in strains at the bottom of a comparable AC layer for such large increases in temperature, and that "a temperature change of 5°C can lead to a difference of almost 50% in the measured strain." This having been said, however, it should also be remembered that the gauges themselves are also subject to temperature sensitivity. While this has been quoted, for example, as a maximum undermeasurement of 1.8 microstrain per degree centigrade either side of 20°C for the Kyowa KM gauges and less than 3 microstrain for other makes of HBM, in fact no quoted temperature sensitivity for the HBM DA3 used in these tests is available; in addition, the manufacturer strongly suggests that a "compensating gauge" be used in conjunction with the DA3. Since no compensating gauges are used in the test pads, it is therefore difficult to know the extent to which temperature sensitivity of the gauges themselves is responsible for the large difference in strain levels between the two test pads.

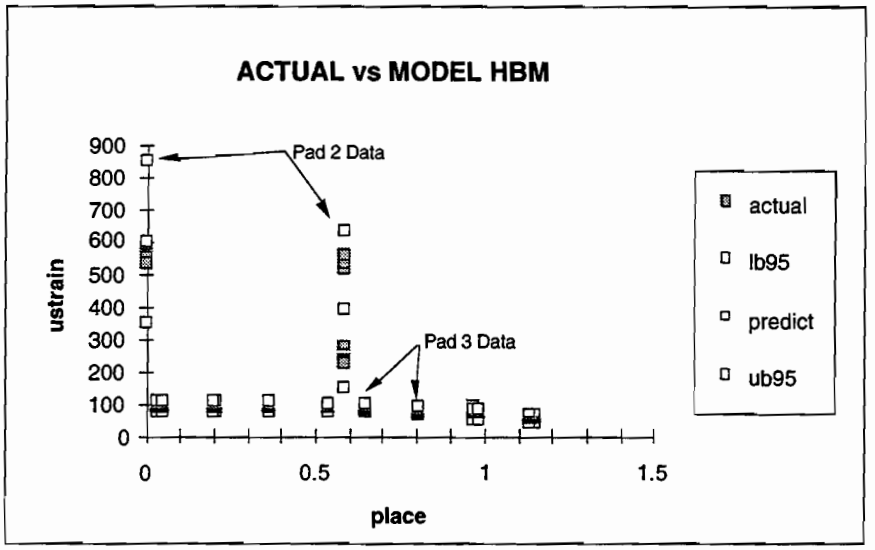

Figure 4.5 Strain vs placement model from pad 2 and pad 3 data for HBM sensors

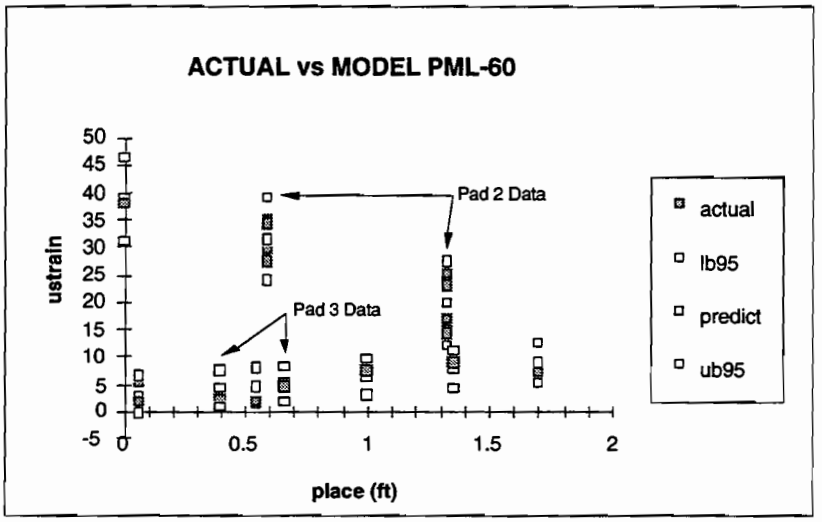

Figure 4.6 Strain vs placement model from pad 2 and pad 3 data for PML-60 sensors

In conclusion, though, even if the sensitivity of the HBM DA3 gauges was an order of magnitude greater than comparable gauges, it is unlikely that the temperature difference in this case would account for more than 40 or 50 microstrain, and it is probable that the majority of the difference was due to the actual temperature-related difference in AC moduli.

4.3.3 Accuracy of Sensors

Accuracy is an indication of how close measurements are to the real or actual values. This implies that we need to know the actual values in order to compare them with our measured ones. In the case of pavement response measurement, it is in fact extremely difficult to say with certainty

exactly what the *actual* values are (as discussed in Chapter 1). Nonetheless, even without being able to measure the accuracy of the sensors quantitatively, it is still important to know whether the measurements are at least in the range of the expected values. There have been two main approaches to this in similar studies [Sebaaly 92; OECD 91]. The first is to compare the measurements of a particular sensor with the mean of all the sensors. While this has its advantages, it really does little more than establish how different a sensor is to the others; and even though the method may be applicable within one particular make of sensor, it is doubtful, especially in this case, that it would be useful in comparing different types of sensors.

The second method of making some assessment of the accuracy is to attempt to predict theoretically what the actual value of the response should be. It should be pointed out that this is by no means perfect either, since the mathematical models used are far from being proven to accurately represent real pavements and, more importantly, because all models rely on accurate input parameters (such as thicknesses and elastic or resilient moduli) that are just as hard to come by. Ultimately, input values may be backcalculated from one response (deflection) and then used to predict other responses (strains and pressures). However, if we assume that deflection bowl measurement is relatively accurate and that the theoretical model is not a major source of error, this approach is not unreasonable. Accordingly, we decided to assess tentatively the accuracy of the sensors by using simple linear elastic layer theory (ELSYM5); that is, to try to match falling weight deflectometer (FWD) deflection measurements and measured strains and possibly pressures. It was felt that if reasonable values of moduli could be found that modeled both measured FWD deflections and strains or pressures, this would indicate that the strain and pressure sensors might be measuring relatively accurately.

It should theoretically be possible to reproduce the entire response history waveform for a rollover load pass. Using ELSYM5 assumes that the pavement is behaving as a homogeneous linear elastic layered system, and also that the response is axisymmetric. Given these assumptions, it follows that the measurement of a response at a single position while moving a load across the surface is analogous to having a fixed load and measuring the response profile along the locus of relative points of the original fixed-position sensor relative to the moving load. The two profiles, including both the response magnitudes and their time/distance scales, may then be directly compared to assess the accuracy of the measurements. If FWD deflection measurements could be matched as well, this would add considerably to the credibility of the results. Nonetheless, even if the shape of the waveform could be reproduced, this would indicate that at least the form of the response is as expected. This is in fact the case; thus, the shapes of the measured and calculated strain profiles for a longitudinal HBM strain gauge in the wheel path are shown in Figures 4.7 and 4.8.

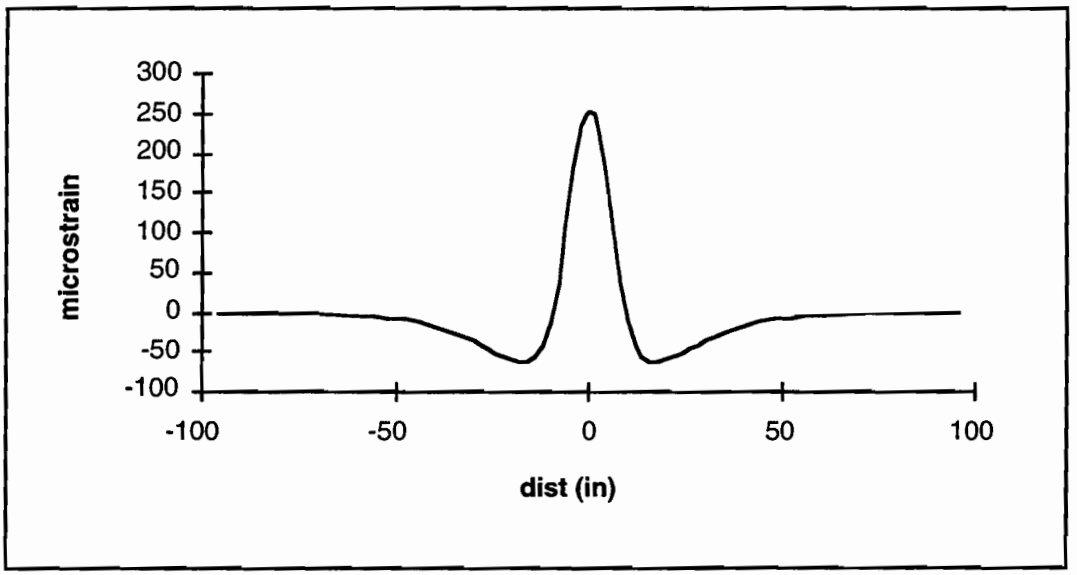

Figure 4.7 Example strain profile calculated using ELSYM5

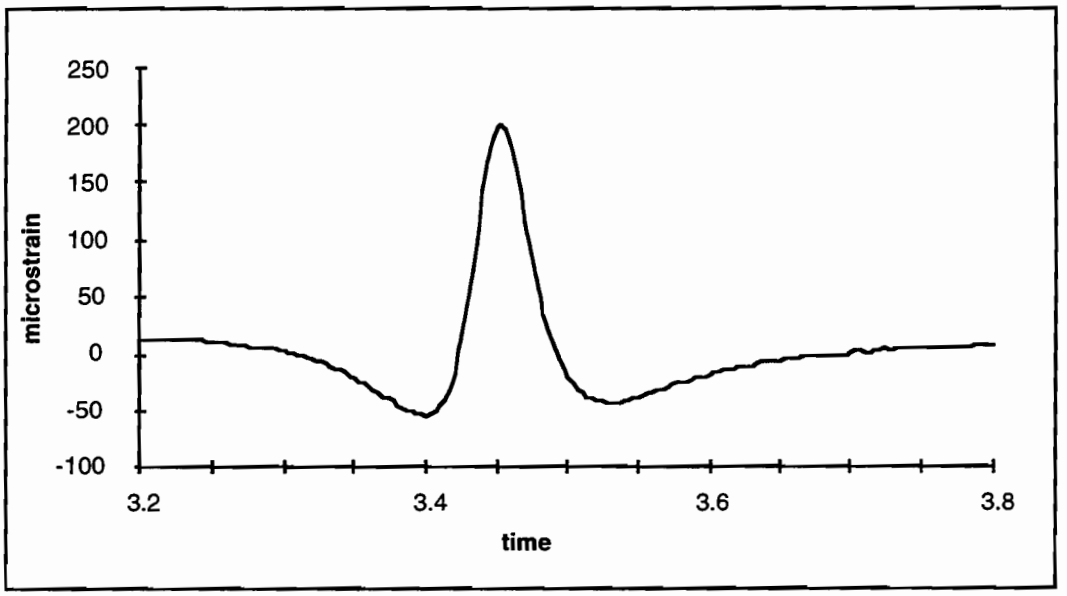

Figure 4.8 Example strain profile measured by HBM sensor

Some mention has already been made, however, regarding the large difference between the strains measured on the supposedly similar test pads 2 and 3. It was noted that various literature sources [Dempwolff 72, Scazziga 87, Kim 95] indicate that temperature is a very important factor (both with regard to the AC modulus and possibly to the temperature sensitivity of the gauge) and that the exact depth of the sensor has a considerable influence on strains. It was also noted that moduli of the base and subbase may have been considerably different within the test pads owing to

the removal of a rectangular area of base and subbase for installation of pressure cells and subsequent backfilling and recompaction of the layers. Finally, it was evident that the levels of strains measured by the different makes or types of sensor also differed markedly with the HBM sensors, recording considerably higher strains than other types of strain sensor.

As a result of the considerable variation evident both within and between test pads, a better method of assessing accuracy of sensor measurements might be to perform the analysis on a "by sensor" basis, and attempt to eliminate as much variability as possible. In addition, it might be questionable to try to compare rollover strains with FWD deflections. For this reason, the best way of assessing accuracy for individual sensors would, in fact, be to perform an FWD drop directly over a particular sensor and record both the maximum deflections measured by the FWD as well as the maximum strain or pressure measured by the sensor. While this is not ideal, it is probably preferable to trying to match rollover strains and pressures with FWD deflections.

Unfortunately, owing to various schedule changes concerning acceptance testing of the MLS, we were unable to include in this report the FWD/sensor data recorded for this purpose. A general discussion of the results and some rough conclusions with regard to accuracy are nonetheless drawn from the considerable data recorded initially.

In order to make a basic theoretical prediction as to what order of tensile strain magnitude we should expect, the first factor that needs to be recognized is that visco-elastic effects at the slow rollover speeds that were used in the tests result in strains considerably above the levels predicted by basic linear elastic layer theory. According to Dempwolff and Sommer [Dempwolff 72], radial strains can increase by 25 to 33% for a decrease in speed from about 30 mph to 8 km/h. Assuming that the FWD pulse (typically 0.033 seconds [Haas 94]) models a relatively high speed where visco-elastic effects are much reduced, the strains measured for 5 mph might be expected to be 0.25 to 0.33 more than ELSYM5 modeled strains using backcalculated moduli from FWD measurements.

The second aspect that should be recognized is that the stiffness of asphalt concrete is obviously a strong function of temperature. An example of this effect is given by Kim et al. [Kim 95] in a recent paper on temperature corrections for backcalculated moduli, where they derive an empirical relationship based on data collected from pavements in North Carolina. This relationship is given as:

$$E_{68} = 10^{0.0153(T-68)} \times E_T$$

where

E_{68} = corrected AC modulus to the reference temperature of 68°F,

E_T = backcalculated modulus from FWD testing at temperature T°F, and

T = the AC mid-depth temperature (°F) at the time of FWD testing.

If it is assumed that base, subbase, and subgrade moduli did not vary much with temperature, then by using the relationship above to determine the approximate AC modulus at different temperatures, the horizontal tensile strains at the bottom of the AC layer may be modeled using ELSYM5 for different temperatures. If it is further assumed that actual measured strains will be perhaps between 25 percent and 33 percent higher than the ELSYM5 strains because of the effects of speed, a likely envelope for expected strains may be generated for different temperatures for a chosen set of nominal layer thicknesses, Poisson's ratios and base, subbase, and subgrade moduli. Although FWD measurements directly correlated with particular sensors were not included, moduli values were backcalculated for other FWD measurements taken during the course of the project. The moduli values from these drops appeared to show distinctly different moduli for base and subbase between the disturbed area where base and subbase were removed for installation of pressure cells and that left undisturbed. Using these backcalculated values for base, subbase, and subgrade, approximate AC moduli from Kim et al. [Kim 95] and Dempwolff and Sommer [Dempwolff 72], generally accepted Poisson's ratios and design nominal thicknesses, the expected ranges of tensile strain for disturbed and undisturbed areas for different temperatures was modeled using ELSYM5. The ELSYM5 input values are given in Table 4.15, and the ranges are plotted with the actual mean measured values from the HBM and PML-60 sensors in Figure 4.9. It is assumed in the figure that the approximate middepth temperature in the asphalt was 41°C for the tests in pad 2 and approximately 21°C in pad 3.

Table 4.15 Assumed input values for ELSYM5 modeling of longitudinal tensile strains on test pads 2 and 3

LAYER	ELASTIC MODULUS 20/46°C	POISSON'S RATIO	THICKNESS (mm)
Undisturbed:	(MPa)		
1	1050/ 5100	0.35	200
2	176	0.35	300
3	61213	0.38	150
4	46	0.45	semi-infinite
Disturbed:			
1	1050/ 5100	0.35	200
2	42	0.35	300
3	20193	0.38	150
4	46	0.45	semi-infinite
Two Loads	350mm apart		
Total Load	26.4 kN		
Load Radius	132mm		

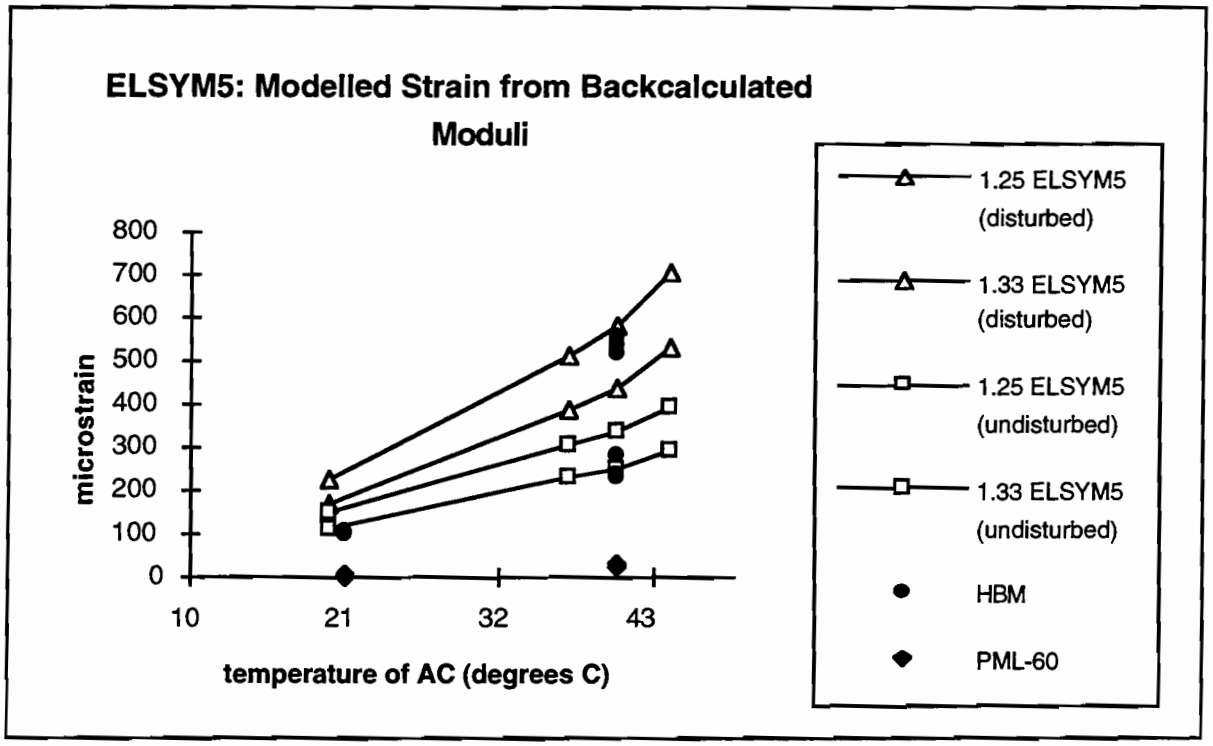

Figure 4.9 Modeled expected longitudinal strain under one wheel for bottom of AC layer at 8km/h and comparable actual mean measured strain from HBM and PML-60 gauges for disturbed and undisturbed areas in test pads 2 and 3 for different temperatures

It can be seen from the figure that the HBM measurements are definitely of the same order of magnitude as the modeled expected strains. The PML-60 measured strains are, however, well below the expected strains.

4.3.4 Recommended Choice of Sensors for Future Use

The choice of sensors for future use should be based on two main aspects of a sensor's measurement. Since it is always theoretically possible to "calibrate" systematic error in a sensor's measurement, the secondary aspect to consider is the accuracy of the sensor, although this should certainly be within some roughly expected range. In order to reduce the sample size and, therefore, ultimately the cost, the primary consideration in judging a sensor is the precision of the measurements. Finally, such things as survivability, drift, ease of installation, availability, and cost are obviously also important.

There are two main contributing factors to the precision of a sensor's measurements. The first is the signal-to-noise ratio (S/N). If this is too low, it can easily be seen that the precision of any local maximum or minimum in the time history waveform will suffer accordingly. It was found that for all the sensors, the noise level was relatively constant and independent of the signal strength. The Kulite and Geokon pressure cells were found to have similar and very low noise levels. The Kulite cells, however, showed much higher signal strengths and, therefore, exhibited

high signal-to-noise ratios of as much as 1800. The Geokons, with their lower sensitivity to load, still showed acceptable S/N ratios of up to 200. Among the strain sensors, only the HBM sensors were found to have reasonable S/N ratios of up to 200; all other strain sensors showed S/N ratios of less than 20. The noise level for HBMs was approximately 0.25 microstrain; the PML and Kyowa gauges gave noise levels of 0.8 and 2.5 microstrain, respectively.

Apart from general noise in the signal, additional random variation can be expected both in the measurements from a single sensor and within the measurements from a group of sensors of the same type. This is the second main contributing factor to the precision of sensors. Assuming that the spatial variation inherent in the test pads would be similar for all sensors, differences in variation (precision) between sensors and sensor types may be used for comparison of sensors.

From the results of the first test in cool conditions on test pad 3, it can be seen from Figure 4.4 and Tables 4.3 and 4.6 that the HBM sensors show a coefficient of variation (CV) of 0.142 and individually have CVs of less than 0.1. Other strain sensors, however, show considerably higher CVs, with PML-60s and Kyowas having CVs of 0.4 and 0.5, respectively. For the pressure cells, the individual CVs are very low, with an average of about 0.05; but as a type, the CVs climb to 0.35 for the Kulites and 0.30 for the Geokons in pad 3. In pad 2, however, the CV of the Kulites fell to 0.1 and 0.15 for top of subbase and top of subgrade, respectively. (Too few Geokons survived for analysis.)

Interestingly, the figures for the second test on pad 2 conducted under hot summer conditions were somewhat different. First, the HBMs performed slightly worse than before, with a type CV of 0.321. The PML-60s, however, improved, showing CVs often around 0.05 individually and 0.149 for the longitudinal group. The explanation for this may well be that the dominant source of variation for the PMLs in the first "cold" test was the signal noise, because the signal itself was so low. In the second test, however, with a stronger signal, the noise became less important and the CV dropped. In the case of the HBMs, there was no signal noise problem, though the problem of having two longitudinal sensors in the area disturbed by pressure cell installation and one in the undisturbed area was certainly a factor. Individually, the CVs probably suffered from the less stringent control on the placement. Strangely, the pressure cells showed higher CVs individually but lower CVs as a type. This indicates that there was possibly less spatial variation in pad 2; perhaps because the pressure magnitude was higher in hot conditions in pad 2, the individual variation increased.

In considering the accuracy of the sensors, a less rigorous method was used. Nonetheless, with reasonable assumptions based on well-documented research from the literature, a rough expected range for strains was deduced through simple linear elastic modeling with ELSYM5 using moduli based on backcalculations from FWD measurements and a correction for visco-elastic effects. From this analysis, it is very evident that the only strain measurements that correspond roughly to those predicted mechanistically are the HBM measurements. From Figure 4.5 it can be seen that the HBM measurements on pad 2 are split into two distinct groups corresponding to the areas disturbed (by the installation of pressure cells) and those undisturbed. Using backcalculated moduli from FWD deflections and corrections for temperature, however, both groups of data seem reasonable. The data from the "cold" tests on pad 3 are also at least of the right order of magnitude.

The measurements from the PML-60s (and other gauges for that matter) can be seen to be considerably below either of the predicted ranges.

Using the preceding summarized information, it would appear that, for future use of strain gauges in MLS-related research, the HBM DA3 gauge should be the gauge of choice. Although this costs considerably more than other types of gauge, and despite questions as to its temperature sensitivity, it has the lowest signal noise of the gauges tested, the best signal-to-noise ratio, good precision, and appears to give a reasonably accurate result. In addition, owing to its flat physical construction, it is the most easily installed (in both initial construction and retrofit situations); also, it does not appear to have any significant problems with drift, has a relatively good survival rate, and, finally, is specifically manufactured for use in pavements and thus requires no modification.

The second choice for a strain gauge type is the PML-60 type gauge. Because of this gauge's higher signal noise level and lower sensitivity, it appears that it is better suited to hot conditions where the response is higher. However, even then it would appear that the strain is grossly undermeasured, with measured strains in the 30- to 40-microstrain range when the expected range is 200 to 600 microstrain. Nonetheless, the precision of the measurements might be comparable to HBM gauges in high-response situations; therefore, it might be possible to use PML-60s in a comparative environment when absolute strain values are immaterial.

With regard to the other strain gauges, not enough data are really available to make firm judgments on PML-120 gauges, but Kyowas appeared to be the least desirable. Unfortunately, most of the data pertaining to these were obtained in the "cold" test on pad 3, and the response magnitude was therefore relatively low. Nonetheless, the gauges had the highest measured noise level and would require responses of at least 50 microstrain to obtain a statistically acceptable signal-to-noise ratio. Since this level was not attained even in the "hot" test on pad 2, the use of these gauges is not recommended.

For the choice between the two pressure cell types tested, it would appear that the smaller Kulite cell is superior to the much larger Geokon. Although research indicates that a lower aspect ratio is preferable for accuracy (indicating that the Geokon might be preferable), the much higher survival rate of the Kulite, the higher sensitivity, and the considerably lower signal noise (and consequently higher signal-to-noise ratio) probably outweigh the disadvantage of a higher aspect ratio in this case. From the initial data gathered from the rollover tests, we therefore recommend that the Kulite pressure cell be used in future work with the MLS.

CHAPTER 5. DESIGN OF FUTURE EXPERIMENTS

5.1 EXPERIMENTAL DESIGN

5.1.1 Possible Areas of Future Experiment

The long-term planning for the MLS is overseen by an Executive Management Committee of TxDOT. The four primary objectives set by this committee will no doubt form the basis for future experiments using the MLS. The primary and secondary objectives are the following:

I. Investigate load damage equivalency
II. Determine remaining life and its impact on rehabilitation guidelines
    1. Investigate remaining-life prediction
    2. Compare viable rehabilitation options
III. Investigate new pavement materials (use the MLS as a validation tool for Superpave)
IV. Truck component-pavement interaction
    1. Determine operational limitations of the MLS
    2. Study pavement response under controlled multiple axles

Truck component — pavement interaction: Considering the role of response measurement in this framework, it is obvious that it should play a major part in the investigation of truck-pavement interaction, as set out in the last primary objective. The dynamics of this pavement-vehicle interaction have become an item of interest to researchers recently. Mamlouk [Mamlouk 95] notes that vehicle characteristics have changed significantly since the AASHO Road Test, and that this has somewhat biased current design methods based on empirical models derived from these original tests. The more mechanistic methods now being sought require a better understanding of pavement and vehicle interactions. Two extensions to the simplifying assumptions of static linear elastic theory used in many models (e.g., ELSYM5 and BISAR) that are being recognized by researchers include the fact that visco-elastic effects can become considerable at lower speeds, and that the inertial characteristics of a pavement system may be important at higher load speeds. These factors, when combined with actual, instantaneous, loading patterns, lead to an extremely complex system. Nonetheless, with the increasing speed and storage capacity of computers, researchers continue to develop models to reproduce this complex system. Unfortunately, one of the major hurdles is the verification of these models by comparison with real traffic and with actual, in-service conditions.

While there are various levels at which the theoretical models can be compared with the real world, the most objective comparisons must be made between actual measured and theoretically predicted pavement response (e.g., strains and deflections). This can be accomplished to a certain

degree by instrumenting in-service pavements. Difficulties arise, however, with the measurement and control of such variables as load, speed, and placement. Yet these are not so significant compared with the major difficulty that arises when the next stage of theoretical modeling is attempted. Even if pavements can be modeled theoretically in the "instantaneous" sense, the ultimate concern for researchers is theoretical modeling of long-term performance and the prediction of such distresses as cracking and rutting. This is the benefit provided by accelerated pavement testing (APT) with the MLS.

Yet accelerated testing, of course, introduces problems of its own. If we are trying to simulate long-term behavior of pavements in the real world, the accelerated simulation should incorporate not only actual moving, loaded, truck tires, but should also recognize the dynamic nature of the pavement-vehicle interactions and the visco-elastic-plastic and inertial characteristics of the pavement. In this regard, understanding the inevitable limitations of APT — and the MLS in particular — is therefore important.

Although the MLS attempts to overcome many of the limitations in simulating actual vehicle-pavement interactions by using actual truck bogies and suspensions, the remaining limitation of the MLS is still that the bogies are not capable of traveling fast enough to realistically simulate average highway truck speeds. As discussed earlier, speed is an important variable in the response of pavements; and while still a considerable improvement over most other APT devices, this limitation will undoubtedly have to be investigated in detail. The major area of investigation should be the extent to which response differs from that at high speeds owing to visco-elastic and inertial considerations. Also to be investigated is the influence of load intervals, and whether realistic rest periods are allowed for visco-elastic effects to dissipate. Once these implications are understood, they can be accounted for and modeled. A second area is the simulation of various "bounce" wavelengths of the different axle/truck components in the loading cycle resulting from roughness in the pavement and the implications for rate of deterioration of the pavement.

A final area of investigation in this regard is the extent to which lateral distribution of loads affects long-term performance of pavements. This may be accomplished by offsetting the bogies of the MLS to simulate typical distributions from real traffic.

The one thing that the MLS is incapable of simulating accurately is time. The major limitation created by almost instantaneous load repetition accumulation is that the environmental loading, which would normally have occurred, is not simulated at all. This is another, albeit fully accepted, limitation which requires methods and calibration in order for it to be accounted for. A possible way of doing this entails loading different sites on a similar pavement to failure at differing times after their initial construction, thus effectively separating the damage caused by loading and that caused by the environment [Hugo 94]. This is summarized below in Figure 5.1, where N1 would represent the total effective number of load applications to failure for a pavement and would be the actual number of loads applied using the APT device on a virgin pavement. If a test site is loaded to failure after some time (and possibly after opening to normal traffic), the environmental load experienced by the pavement during that time, expressed in terms of APT load applications, would be:

$$N_{env} = N1 - N2 - N_{traffic}$$

By plotting a number of such points, it should be possible to determine the accumulated environmental damage over time.

Investigation of load damage equivalency and determination of remaining life and its impact on rehabilitation guidelines: These two primary objectives for MLS research are trend-type studies; and while the main focus would initially be on distress monitoring in order to generate empirical models, the monitoring of pavement response in addition to this could provide valuable knowledge for development and verification of future theoretical models seeking to predict long-term performance, as discussed in the previous section. Response data collection may not be the primary goal in these types of studies initially, but if a systematic and relatively automated data collection and reduction procedure could be employed, with the data stored in a dedicated and well-designed database, the response data would be extremely valuable, both for verifying theoretical models and maybe even for creating empirical prediction models for remaining life similar to those being created in the main studies using distress data.

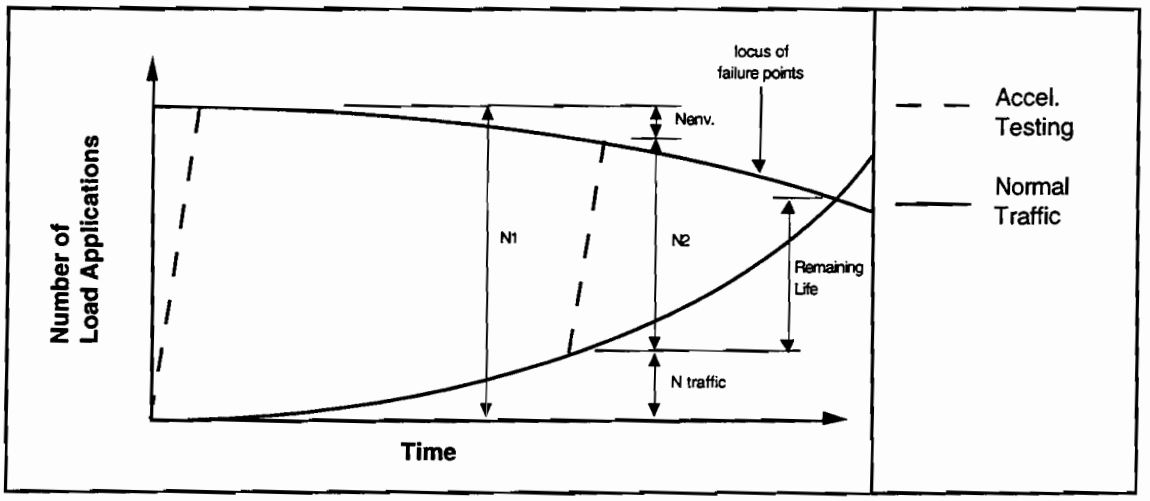

Figure 5.1 Conceptual application of accelerated pavement testing to evaluate environmental effects on pavements [Hugo 91]

Investigation of new pavement materials: The investigation of new materials may or may not utilize response data. It would appear that the main purpose of such studies would be to verify the design life predictions of the new SHRP Superpave design methods, with respect to such distresses as rutting and cracking. As was discussed above, however, the collection of response data simultaneously may be very valuable for improved understanding of long-term trends in response changes resulting from material property changes.

5.1.2 General Requirements for Experiment Design

It has been said that "research implies that the researcher is interested in more than particular results; he is interested in the repeatability of results and in their extension to more and general solutions" [Ostle 88]. The two factors that affect the repeatability of the data measured during an experiment are the variation and the number of sample measurements taken. The design of experiments is therefore concerned with acquiring a certain quantity and quality of information at minimum cost.

In general, the most basic step in the design of an experiment is the selection of independent experimental variables or factors of interest. In our case, the experiment may be designed to include only a few factors (e.g., rut depth and accumulated axle loads) or a number of factors simultaneously. While the choice of these factors will obviously depend on the type of experiment, any factors that may have an influence on the factors of interest and that are expected to change during the experiment must be measured. This includes independent factors that will be changed intentionally, as well as those over which there is no control and which will change regardless. These factors obviously cannot be prechosen for general use in a number of experiments, though it is worth noting that if data from different experiments may be combined at some time in the future (e.g., in a database), the most influential variables should almost always be measured. In this way, even if an influential variable such as load is kept essentially constant during a long-term experiment, by recording that load with the data, it can be compared with data from a different experiment for which a different load may have been used.

Once it has been decided which factors are to be recorded, it is necessary to determine confidence limits required for the measurements. This obviously must be moderated by cost. For narrower confidence limits, either a greater sample size is needed or a greater amount of control needs to be exercised. From this point of view, it may well be that the number of samples is decided on first and the attainable confidence interval calculated afterwards.

To determine exactly how many samples of each measurement need to be taken to attain a required confidence interval, it is necessary to know, or at least have an estimate of, the population variance at a particular level of control. While factors to be measured cannot necessarily be known beforehand for general use, these population variances quite often can. The spatial variance of strain measurements within an average test section, or the variance in readings from a single gauge, for instance, may be used a number of times in a number of different experiments. This process can be summarized as follows:

1. Identify experiment objective(s).
2. Choose which factors to vary and which combinations to measure from (factorial design).
3. Choose confidence limits for measurements.
4. Using these confidence limits and estimated variability in measurements, make choices regarding sample sizes, such as number and position of sites, number and position of sensors per site, and how many axle passes to measure.
5. Set up full and detailed data collection plan.

5.1.3 Specific Requirements for Experiment Design

It would be difficult to provide specific guidelines for MLS experimental design. Nonetheless, it is probably safe to say that the majority of experiments that will be conducted using the MLS will have the following characteristics and requirements:

1. A full experiment may incorporate a number of factors, resulting in the need for a factorial design. Among other things, these may include different pavement designs, different climatic areas, and different loads.
2. The common factor being varied in almost all experiments will be total accumulated axle loads. This is the nature of APT.
3. At least two levels of sampling will therefore be required for response measurement experiments. One will be the sampling required for information in a single cell; the other will be the sampling in the different cells. Response will be measured in windows at chosen stages during the experiment. The windows will be the cell measurements. The number of windows will depend on the factorial design.
4. Varying levels of detail for the information (ranging from peak values to the entire waveform) from individual single load response time histories within a window will be available from each window.
5. A knowledge of the different variabilities will either have to be estimated beforehand or assessed early in the experiment. This might necessitate separate pilot studies before the main data collection plan is finalized.
6. A detailed data collection plan must be the final product of any experimental design.

These characteristics and requirements must be used in conjunction with the experimental design process defined in the previous section to determine the specific requirements for each experiment. The total design of an experiment is mainly concerned with what, where, when, and how many measurements should be taken, so that a detailed data collection plan for the experiment can be drawn up. The different stages of the process are discussed separately below.

Identify experiment objective(s): The objectives for the experiment will presumably be chosen along the lines of the original primary objectives set out by TxDOT's Executive Management Committee. Once the primary objectives for the experiment are chosen, it should be determined if various secondary experiments might be accomplished within the primary experiment framework, or whether other co-primary objectives may be accomplished through small modifications to the original framework. In general, the primary objectives will be to investigate response, distress, or performance aspects dependent on number of accumulated axle loads.

Carry out factorial design: This may be extremely simple or highly involved. In general, however, almost all experiments may be framed as a factorial experiment of some sort. Factorial designs may be thought of as multidimensional tables of cells. The number of dimensions depends on the number of factors chosen, and each dimension will consist of the number of cells corresponding to the number of levels of that factor. Factorial cells represent all the different combinations of all levels of all factors. Obviously, for very extensive factorials not all the cells

will be filled, and various methods for reducing the total number of cells that need to be filled exist in the literature.

The simplest possible objective would be to investigate the number of axles leading to failure by rutting for a number of different pavement designs. As shown in Figure 5.2, it would hardly resemble a factorial at all. A similar experiment may be carried out at the same time to investigate the extent of the rutting at different accumulated axles for two different loads, which would require a factorial like that shown in Figure 5.3. If peak tensile strain was being investigated and a correlation with rut depth sought, the same factorial might be used, though both rut and peak tensile strain would be measured. It can be seen that, for a far-reaching, long-term study, many factors may be investigated simultaneously, with a relatively large factorial possibly required.

It can be seen that factorials may range from the very simple to the fairly complex; and while many experiments need not be formalized in such a framework, the point is that most can, and this provides a sound, standardized step for the overall process of future MLS experimental design.

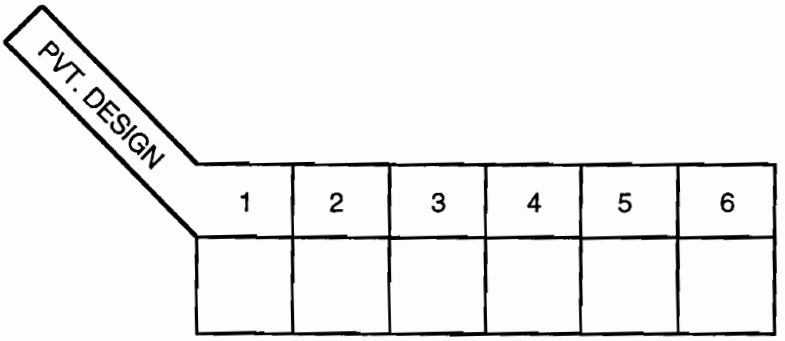

Figure 5.2 Simple factorial for the investigation of number of axle loads to rutting failure for different pavement designs

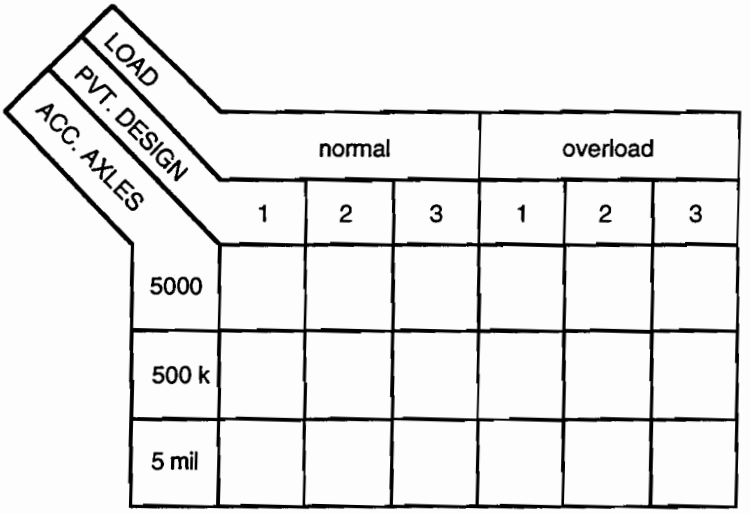

Figure 5.3 Simple factorial for the investigation of rut depth on different pavement designs for different loads at different number of accumulated axles

Choose confidence limits for measurements: When making measurements for each cell in the proposed factorial, some allowance for variation can be made at the time of the measurement, or it can be "discovered" later when the data are analyzed. It is therefore not necessary to calculate exactly how many sensors there should be and where they should be placed. But some prior estimation of variance and a rough calculation of required sample size might often save time by minimizing the collection of excess data or by greatly increasing the quality of the final data by ensuring that enough replicates are taken.

Decide on sample sizes: Using these confidence limits and estimated variability in measurements, the researchers should make choices regarding sample sizes, such as number and position of sites, number and position of sensors per site, and how many axle passes to measure.

Set up full and detailed data collection plan: Because it is often the case that those who develop the experimental design for an experiment are not present on the site continuously when the actual data are being collected, the personnel who actually are on the site need to know exactly what data to collect and when to collect them. At the same time, there is in many cases some justification for incorporating flexibility in the data collection plan; it must always be remembered that very often it is necessary to decide exactly how to proceed with an experiment based on the findings at the beginning. Nonetheless, this should not be an excuse for not setting up a detailed data collection plan. The plan should simply address all the likely alternatives so that the data collection team will know how to proceed within a given scenario.

5.2 STRAIN AND PRESSURE MEASUREMENT FOR FUTURE MLS EXPERIMENTS

5.2.1 Type of Sensor

As indicated in Chapter 4, we recommend that the HBM DA3 gauge be used for strain measurement. The PML-60 gauges may also be considered, though, at least from the data obtained in this study, it appears that they may be less precise, have a higher inherent noise level, and also may grossly undermeasure real strain. For the measure of pressure, we recommend that the smaller Kulite pressure cells be used, primarily because they are smaller and, therefore, more robust (and do apparently have a higher survival rate); they are also easier to install and have less inherent noise and fairly good precision.

5.2.2 Number of Sensors per Test Pad

It should be stressed that the two full factorial tests conducted on the tests pads were performed using a standard dump truck — not the MLS itself. While results for the MLS would be expected to be similar, this has not yet been proven. Greater variability may result owing to the vibration and harmonics of the machine as a whole (variability in nominal load), though the variability may also be reduced through better control of speed and placement.

Furthermore, it must also be remembered that the data were collected only from so-called "built-in" sensors. The results quoted are therefore only applicable to these situations. If sensors are to be retrofitted, it is strongly recommended that a similar study be undertaken to at least assess different retrofit methods and their inherent variability in order to make similar conclusions regarding numbers of sensors needed.

In order to decide on the number of sensors to place in a particular pavement, the method used here has simply sought to distinguish through statistical significance between two means differing by a margin of 10 percent. This not-very-fine resolution indicates that if two mean results for two different speeds for instance were within 10 percent of each other, they are for all intents and purposes the same and cannot be distinguished. In deciding how many sensors to place for future MLS experiments, we believe this would be a good guideline; and using the better results from each test and assuming strains and pressures were required, this would correspond to needing 17 HBM sensors per test pad at the bottom of the AC layer, 17 Kulite pressure cells at the top of the subgrade, and 9 Kulites at the top of the subbase.

Since sample size for a particular statistical significance is theoretically only a function of variance (in fact coefficient of variation, CV, is used here for resolution by percentage), then assuming this total variability between different HBM and Kulite sensors, at different points in the test pad, and owing to small unrecorded variability in load, speed, placement, etc., will be roughly the same for future experiments, these figures should be widely applicable. Nonetheless, if these need to be checked or recalculated for any reason, it is recommended that a factorial experiment, including at least whatever main variables (such as load, speed, placement, layer moduli and thicknesses, temperature, etc.) are expected to vary in the experiment be conducted. Thereafter, the process of constructing a model and analyzing the variance for the sensors as a group outlined in

Chapter 4 will provide the coefficients of variation required to calculate future numbers of sensors required for the desired significant level using the students t-test. It should be remembered that the fewer the variations in the main factors, the smaller the variability is likely to be and therefore the smaller the sample size required.

5.2.3 Placement of Sensors in Test Pad

The position of the sensors within the test pad will depend largely on what data are required from the experiment. If, for instance, a full response model for different x, y, and z positions with respect to load is required (as alluded to in the first chapter for the verification of a full dynamic visco-elastic plastic finite element model), then obviously the positions in all three dimensions must be sampled (assuming the load path is fixed). If, on the other hand, only the critical points of maximum strain were required, researchers might opt for data collection at a single depth at the bottom of the AC layer and only in the wheel path. Whatever the decision, it is vital that a random sampling be taken so that, if only the wheel path measurement at the bottom of the AC layer is required, then sensors should be spaced out along the usable portion of the wheel paths so as to capture as much of the spatial variability as possible.

5.2.4 Window Size for Future MLS Experiment

The so-called "window size" or number of load passes to record at any time is mainly dependent on two things. The first is random variability in the sensor measurement itself; the second is the variability between the load passes (whether this be load, speed, placement, tire pressure, etc.). Because the study was conducted using only a dump truck and not the MLS itself, there is some question as to the latter. From the study data, it appears that for both HBM strain gauges and the Kulite pressure cells, the variation is very small (indicated by individual sample sizes in Chapter 4 of less than 5). If it is assumed that there is likely to be even less variation in speed and placement owing to better control in the MLS, the window size for future experiments theoretically need only be a couple of load passes. Because the load passes will be administered by 12 different axles on 6 different bogies, however, it is recommended that at least one full cycle be collected (12 load passes) per window.

5.2.5 Window Frequency for Future MLS Experiment

The final decision to make in planning an MLS experiment is when to take the various window measurements described above. This, too, would be mostly dependent on the type of experiment being conducted. In general, because it is what accelerated pavement testing (APT) is all about, one of the basic objectives of almost all experiments will be the identification of trends in response owing to accumulating axle loads. If the shape the trend is likely to take is conceivable, then the window intervals may be planned accordingly. In general, one should expect significant changes in response at the beginning of an experiment on a virgin pavement, necessitating more frequent collection early on. On the other hand, rate of response change toward the end of a pavement's life may also indicate more frequent data collection is needed. In-between data may

need only periodic collection. Ultimately, however, this collection plan will be up to the researcher and will be decided on the basis of the expected trend for that particular experiment.

CHAPTER 6. DEVELOPMENT OF SYSTEMATIC DATA COLLECTION AND REDUCTION METHODS

6.1 DATA COLLECTION AND REDUCTION

6.1.1 Available Data

Computers can now summon quantities of data that far exceed the analytical ability of researchers. During this study, we found that a typical file containining 9 seconds of data from 26 sensors at a sample rate of 500 Hz produced an ASCII file of approximately 4 Mb. This resulted in storage requirements of about 16.1 bytes per sensor. Using this figure, we estimated that storing data recorded continuously from a test pad of 26 sensors at 500 Hz for an hour would require 752Mb of computer space.

Quite apart from the storage problems (which in fact are being addressed by more efficient computer storage technologies), these data are virtually unusable to researchers without the aid of totally automatic reduction methods. Assuming that only peak tensile strains were needed for statistical analysis, these would need to somehow be extracted automatically from the data stream, since the only other method would be to go through the data each time and visually extract these peaks. Given that there could be some 7000 peaks per hour, this is clearly unacceptable; the primary information we need to identify is exactly what data are useful.

6.1.2 Data Usefulness

Exactly what data are useful obviously depends on the research objectives of any one particular experiment. If the primary objective is to investigate long-term trends, then data are needed at all points during the accelerated loading. This might easily entail millions of axle loads. If the objective is to analyze in detail the shape of the strain waveform at a particular time in the loading process, the only useful data would be those collected at that time. While it may be reasonable to collect data continuously in this latter case, it is clearly impossible to collect data continuously in the former when investigating a trend over millions of axle loads. The two cases apparently differ on another level as well: In the trend investigation, it might be that only the trend in the maximum responses is of interest, whereas when investigating the waveform shape, enough data to adequately represent the entire time history of the response are required. Unfortunately, even the identification of the maximum requires a reasonably high sample rate, as discussed originally in the previous section dealing with sample rate. Further, the inevitable variation in both the maximums and in the wave shape as a whole must be taken into account; additionally, a number of observations must be made.

It turns out, therefore, that unless automatic sensing and triggering are used to record the maximums in the latter case, in both extremes the data to be collected need to be a continuous "window" of data, incorporating a number of load repetitions that will depend on the level of precision of the measurement required. In the case of trend identification, a number of these

windows would have to be collected so that enough points were identified over the span of the experiment to identify a statistically relevant trend. This would be true for any long-term experiment, such as an investigation into seasonal or even daily cycles.

In conclusion, data are therefore valuable only if they can be used, and only the minimum required to attain a chosen precision for a measurement should be recorded. Collecting any more data is wasteful in terms of collection time, storage, data reduction, and data analysis.

6.1.3 Data Collection

From the discussion above it is evident that, for a majority of experiments with the MLS, it will be necessary to collect windows of data representing a number of replicates that will give a "snapshot" at a particular accumulated axle load value of any particular response. This is illustrated below in Figure 6.1.

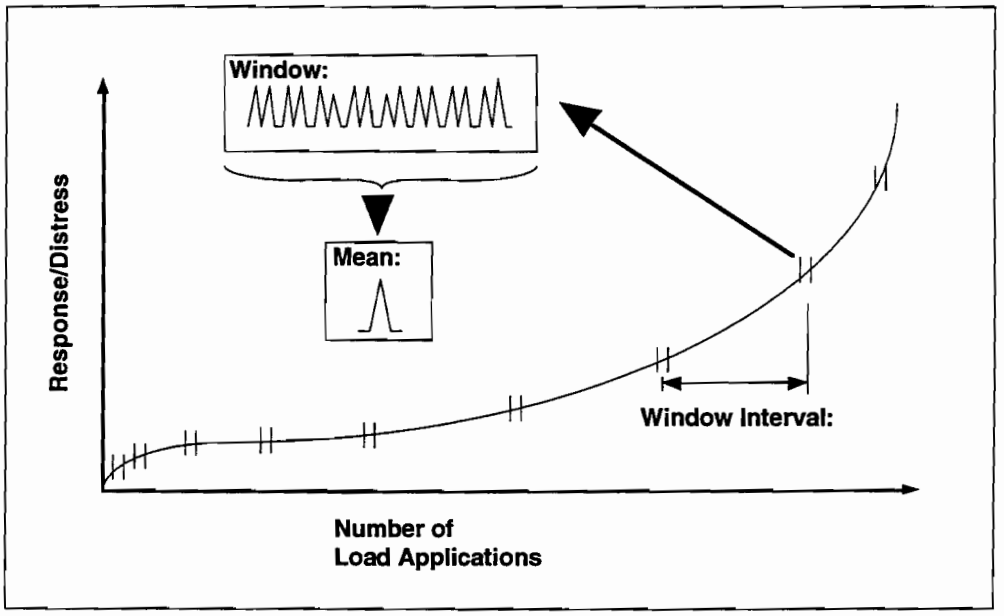

Figure 6.1 Illustration of probable typical data collection for MLS experiments

Assuming that no additions to automate the collection of, for instance, maximum values are made to the hardware or collection software, these windows will be data sets containing continuous readings of response values for times on the order of 10 to 20 seconds taken at sample rates in the range of 50 to 500 Hz. The sets will generally include data from a number of different sensors. This is, in fact, very much how the slow rollover data were collected; a portion of a sample data file appears below in Figure 6.2.

AVICT_2A.001				
+34885.0000				
+000.7127				
+056.0000				
+300.0000				
Time (Secs)	hbm01 ue	hbm02 ue	hbm04 ue	hbm05 ue
+001.9967	+002.8406	+000.3156	+002.3146	+001.0521
+002.0000	+002.8406	-000.2104	+002.5250	+000.6313
+002.0033	+003.3667	+000.1052	+002.7354	+001.0521
+002.0067	+003.5771	+000.5260	+002.7354	+001.6833
+002.0100	+003.1563	+000.5260	+002.7354	+001.8938
+002.0133	+002.7354	+000.0000	+002.3146	+001.2625

Figure 6.2 Sample data collected from response sensors

It can be seen that there are a number of sensors per record, and that the first field in each record is the time. This translates into a full time history for each sensor, such as shown in Figure 6.3.

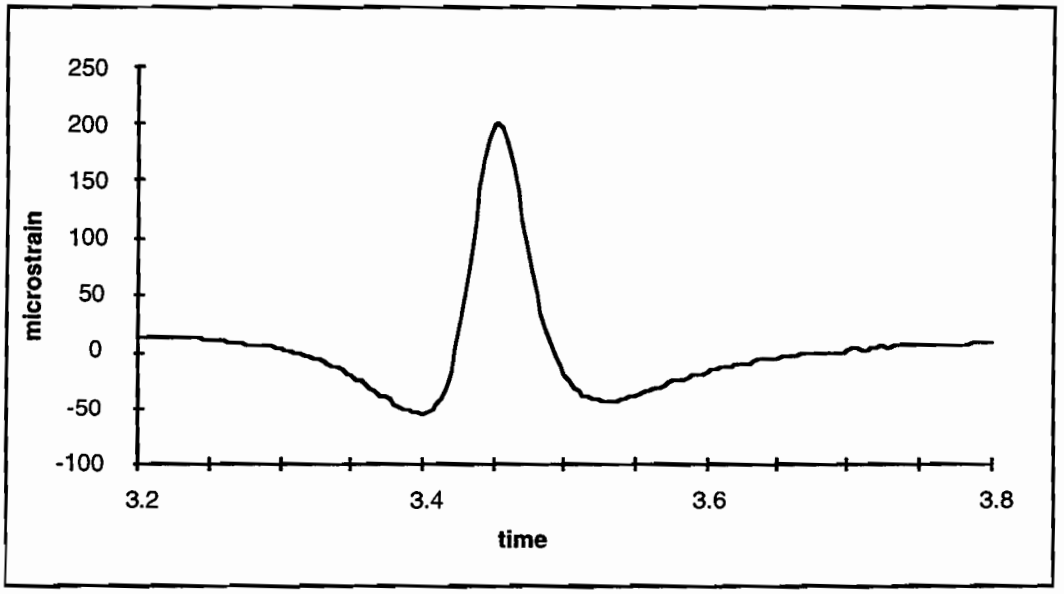

Figure 6.3 Plot for single strain sensor of example data collected from response sensors

Assuming that this form of data collection will be the norm for future MLS experiments relating to pavement response, a full, standard data collection plan will require that the following be understood:

1. Objective of experiment (e.g., trend or shape analysis)
2. Depending on 1, the precision required for the measurements
3. The expected survival rate of the sensors
4. The spatial variability expected in the measurements over an entire road section (if required)
5. The spatial variability expected in the measurements across the MLS test pad
6. The variability expected in the inter-window measurements
7. The variability expected in the intra-window measurements
8. From 4 and 2, the number and position of MLS test sites per road section (if required)
9. From 5, 3 and 2, the number and position of the sensors to be installed per pad
10. From 6 and 2, the number and interval of the windows to be collected
11. From 7 and 2, the size (i.e., the number of axles) of the windows to be collected

6.1.4 Data Processing and Reduction

The reduction of the data to be collected in the standardized form (according to the collection plan described above) may be divided into the following different phases (and corresponding data set formats):

1. Identify and extract from each data set above the characteristics of the waveform required to create a new data set for each window.
2. From the window data sets created in 1, create a new, combined data set containing the mean and standard deviation for each window for each waveform characteristic required, including levels of all relevant variables such as load, speed, placement, accumulated load repetitions, pavement characteristics, temperatures, moisture, etc.
3. Possibly reduce any replicate windows in the combined data set in 2 above to single values of mean and standard deviation.

In the first step, it is necessary to decide if, for instance, only the maximum is required or whether a number of different points on the waveform are to be stored. Taking a strain history as an example, if we take a typical load cycle from the sample strain waveform shown above in Figure 6.3, we might identify five points on the waveform that would adequately categorize its shape for storage in a database. These are shown in Figure 6.4. If we required only the maximum, we would identify and extract only point 3. If we wished to store all five, we would need to extract and store all five, along with their positions in terms of time.

This is not, in fact, unusual. At the OECD full-scale pavement test in Nantes, France, three points were collected [OECD 91]. These were the base strain when the load was 4m away, the first compressive strain maximum, and the tensile strain maximum. These correspond to the first three points in Figure 6.4. The distance between the compressive and tensile strain maxima was also recorded.

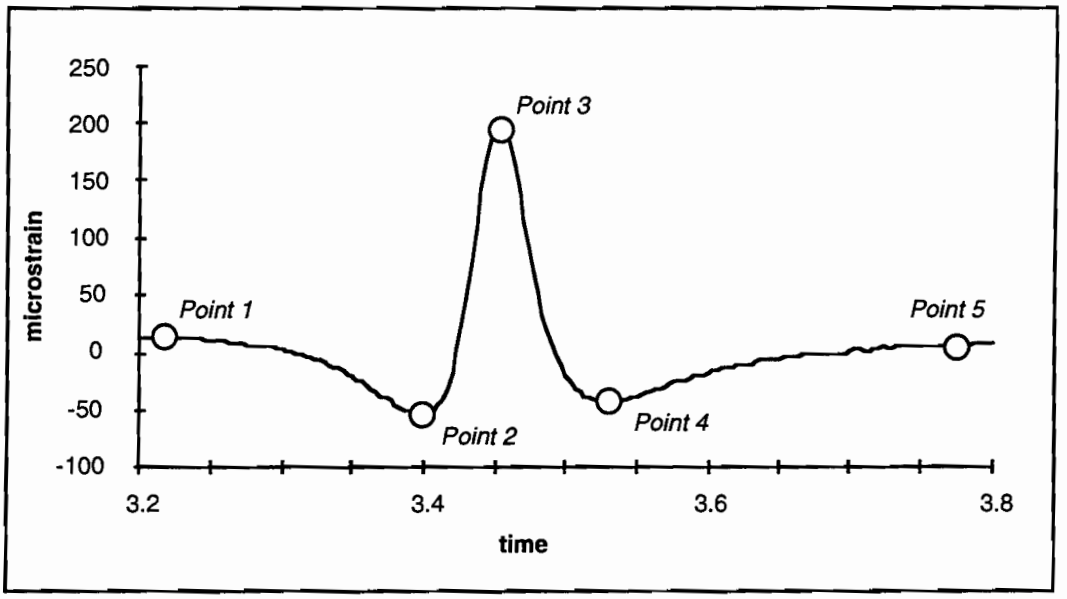

Figure 6.4 Characterization points on a typical moving single load strain history

Whether it is necessary to extract just the maximums or a number of characterizing points from a waveform, it is likely that some form of automatic post-processing method would need to be developed for this for long-term standardized use with the MLS. This is highly recommended. Once a post-processing method has been developed, and depending on how sophisticated it is, the decision about whether to extract one or more points may be immaterial. Even if only the maximums were needed for the immediate experiment, it might require no extra work and only minor extra storage to extract a number (all five perhaps in the case of longitudinal strain). In this way a full and very valuable database could be built for use in future research. This is discussed separately below.

The second stage of the data reduction for general use with MLS response data would entail the statistical reduction of the multiple-axle window data sets from phase 1, to a single mean value with its associated standard deviation. This would create a combined data set containing all cell replicates for the experiment. The combined data set created in the second phase could then possibly be reduced further if required by combining cell replicates; data analysis could also be performed directly on this data set to identify trends or correlations.

Either before or after analysis, this combined data set could be stored in an MLS Response Database for use in ongoing or future research. The conceptual formats for these data sets and the total data reduction process are shown in Figure 6.5.

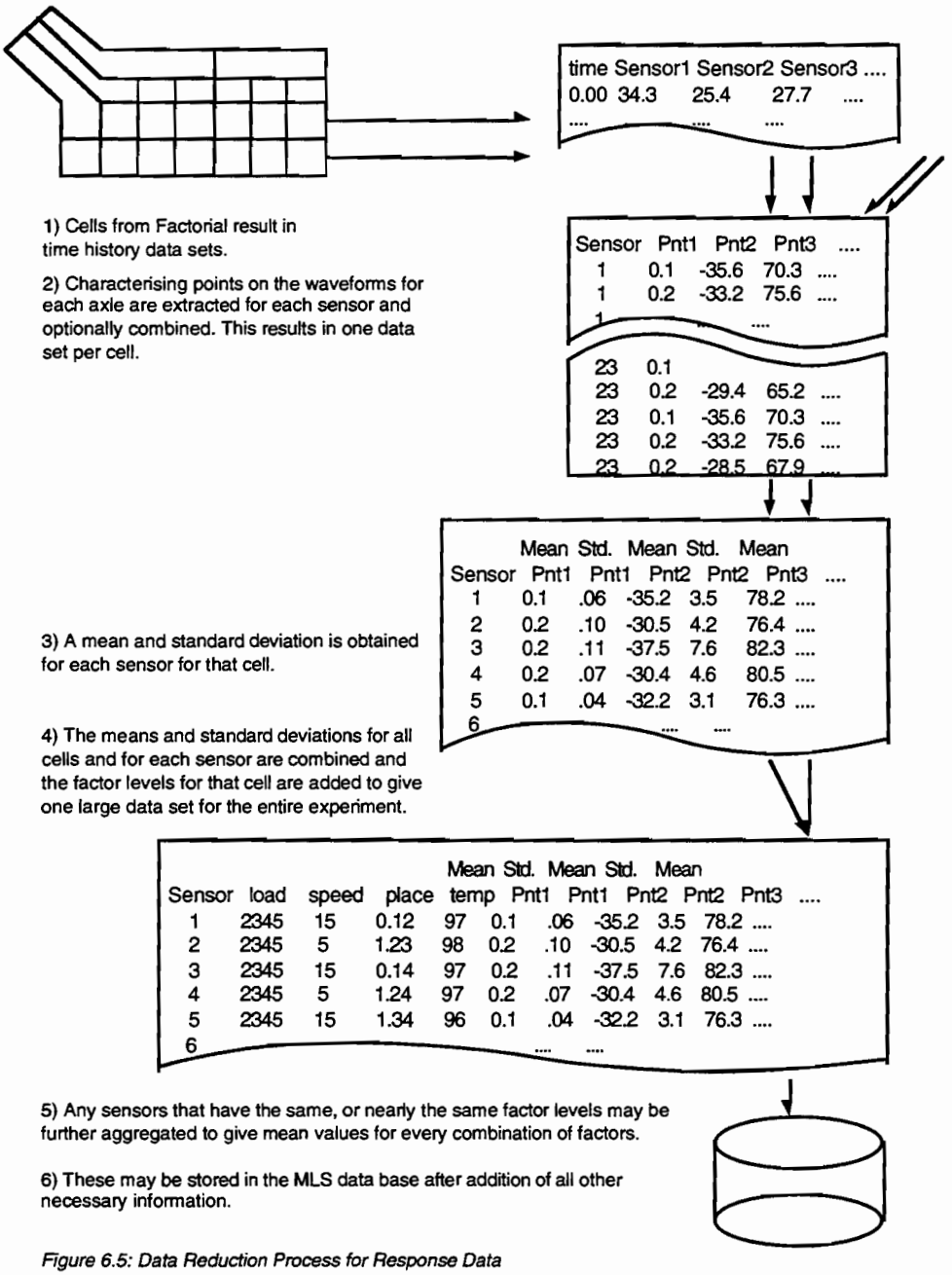

Figure 6.5: Data Reduction Process for Response Data

6.2 DATA STORAGE

6.2.1 Proposed Development of MLS Response Database

Citing our original introductory discussion on the general objectives for instrumenting pavements, it is reasonable to assume that the ultimate purpose of collecting this type of data is to improve our knowledge of pavements in order to increase their efficiency and effectiveness and to

optimize our public investments in them. To make the best use of data gathered in various individual experiments, it should be stored in an organized way so that it can be referenced and reused in future research. The logical way of accomplishing this is to create a database; this process has been followed in many historical and current examples, including the original AASHO road test data, the LTPP database, and the TxDOT PMIS, just to name a few. In fact, a designated database has been in use for some time in South Africa for the HVS. In order to reap the same benefits for the considerable data likely to be produced from the MLS APT experiments, a dedicated database that can nonetheless interact with these other databases should be set up to organize and standardize data collection from the beginning.

For a database to be useful, it is important that it be used to store all variables that might affect the analysis of correlations and interactions. As a result, factors pertaining to inventory data, such as date, location, and pavement characteristics, which would not normally change during a single experiment, would be required. Machine characteristics, such as load, speed, and tire characteristics that might be changed during an experiment, would be required. Climatic variables, such as temperature and moisture, would also be vital. Finally, the response data, as well as possibly distress data, could be stored. Listed below in Tables 6.1 to 6.5 are the data fields that could be stored in a full database.

Table 6.1 Inventory data

Field Name	**Description**
date	
time	
location	
facility type	interstate/primary/secondary etc.
construction date	
pavement surface type	rigid/flex. (though possibly more detail)
pavement surface thickness	
pavement surface moduli	
base type	limestone/siliceous river gravel etc.
base thickness	
base stabilization type	
base modulus	
subbase type	
subbase thickness	
subbase stabilization type	
subbase modulus	
subgrade type	
subgrade thickness	depth to bedrock
subgrade stabilization type	
subgrade modulus	

Table 6.2 Climatic data

Field Name	Description
temperature profile	number of points followed by list of temperature, depth pairs
moisture profile	number of points followed by list of moisture, depth pairs

Table 6.3 Machine characteristics

Field Name	Description
load	nominal load
speed	nominal speed
lateral placement	list of 6 figures giving placement of each bogie
tire type	interstate/primary/secondary etc.
no. of tires	
type of tires	
tire pressure	
tire condition	tread depth
axle configuration	
axle configuration	

Table 6.4 Inventory data

Field Name	Description
inventory data	pointer to inventory data set
climatic data	pointer to climatic data set
machine characterization	pointer to machine characterization data set
type	type of sensor
units	
accumulated normal traffic ESALs accumulated MLS axle loads	if in service pavement
sensor identification	if applicable
installation method	built in/ retrofit method etc.
vertical orientation	vertical/horizontal
horizontal orientation	longitudinal/transverse
depth	
time history waveform	no. of points followed by list of magnitude (mean, std. dev.), position triplets

Table 6.5 Distress (possible)

Field Name	Description
alligator cracking	extent
longitudinal cracking	extent, width
transverse cracking	extent, width
rut depth	
etc.	other distresses may be included

6.2.2 Maintenance of Database

Once such a database is set up, it will be highly beneficial that all future MLS experiments be designed initially with the idea that enough basic data should be collected for the results to be acceptable for inclusion in the database. In this way, all future experimental data can be stored for comparative analysis with past and future data in the database.

Initially, it can be expected that most experiments will be self-contained, with the main objectives accomplished without reference to other data. As the database grows, however, more and more experiments may be designed to explicitly include data from the database. Eventually, a large and organized database will allow experiments to be designed around analysis of existing data, with no additional MLS data required. In the long run, this will enable a sound and extremely valuable understanding of a wide variety of aspects of the MLS.

CHAPTER 7. CONCLUSIONS AND RECOMMENDATIONS

7.1 CONCLUSIONS

1. From the study it is evident that, while general accuracy is important for the rating of sensors, the precision of sensor measurements is equally, if not more, important in obtaining statistically useful data.
2. It appears that a sample rate of 100Hz is adequate for the collection of strain and pressure time histories; such a rate will produce a theoretical undermeasurement error at the peak of around 5 percent for strains up to 400 microstrain and speeds around 16 km/h.
3. Noise in the time history waveforms from all sensors tested was found to be relatively constant and independent of signal strength.
4. HBM strain gauges and Kulite and Geokon pressure cells showed acceptable signal-to-noise ratios; other gauges gave unsatisfactory ratios for the data analyzed. The poor ratios were caused by low signal strength and by noise levels, which, while higher than those of the gauges mentioned, were not excessive.
5. From statistical analysis of variance in the data from the two main tests, varying degrees of sensitivity to load were found among individual sensors. This provides an effective method for screening out defective sensors for further analysis.
6. The factors of speed, load, and placement used in the factorial experiments were all found to be statistically significant for the measurement of strain and pressure.
7. In addition, we concluded that temperature difference in the asphalt layer was largely responsible for the considerable difference in measurements between the two tests on pads 2 and 3.
8. The unexpected increase in variation for HBM sensors in pad 2 we concluded to be the result of spatial variation in the base and subbase layer moduli due to these layers being disturbed and recompacted by hand during the installation of pressure cells.
9. The precision of strain sensors as measured by coefficient of variation (CV) showed that HBM sensors were the most precise in test pad 3, with a CV of 0.14 (PML-60s: CV=0.41), and that PML-60s were most precise in pad 2, with a CV of 0.15 (HBM: CV=0.31 assumed to be artificially high due to conclusion 8).
10. The precision of pressure cells was good for individual cells ($CV<0.15$) but considerably higher ($0.25<CV<0.35$) when grouped by type in pad 3. In pad 2, however, the Kulites showed good precision as a group ($CV<0.15$). Too few Geokons survived in pad 2 for analysis.
11. The results from the precision analysis indicate that around 17 strain gauges (bottom of AC layer) and 9 and 17 pressure cells for top of subbase and subgrade, respectively, would be needed to obtain mean measurements to within a 10 percent confidence interval in any experiment factorial cell.
12. Taking into account the considerations mentioned above for spatial variation in moduli and temporal variation in temperature, HBM sensors showed reasonable accuracy (to the extent this could be defined); PML-60 gauges and other strain gauges tested appeared to grossly undermeasure strains.

13. Including considerations of survivability and drift, it appears that, for future use of strain gauges in MLS-related research, the HBM DA3 gauge should be the gauge of choice. Although this costs considerably more than other types of gauge, and though there are some questions as to its temperature sensitivity, it has the lowest signal noise of the gauges tested, the best signal-to-noise ratio, good precision, and appears to give a reasonably accurate result. In addition, it is the most easily installed owing to its flat physical construction, both in initial construction and retrofit situations. Finally, it does not appear to have any significant problems with drift, has a relatively good survival rate, and is a gauge specifically manufactured for use in pavements and thus requires no modification.
14. The second choice for a strain gauge type is the PML-60 type gauge. Because of this gauge's higher signal noise level and lower sensitivity, it appears that it is better suited to hot conditions, where the response is higher. However, even then it would appear that the strain is grossly undermeasured, with measured strains in the 30 to 40 microstrain range (the expected range is 200 to 600 microstrain). Nonetheless, the precision of the measurements might be comparable to HBM gauges in high-response situations and, therefore, it might be possible to use PML-60s in a comparative environment when absolute strain values are immaterial.
15. Of the two pressure cell types tested, it would appear that the smaller Kulite cell is superior to the much larger Geokon. Although research indicates that a lower aspect ratio is preferable for accuracy, indicating that the Geokon might be preferable, the much higher survival rate of the Kulite, the higher sensitivity, and the considerably lower signal noise (and consequently higher signal-to-noise ratio) outweigh the disadvantage of a higher aspect ratio in this case. Based on the initial data gathered from the rollover tests, we recommend that the Kulite pressure cell be used in future work with the MLS.
16. Given the nature of the entire reduction and analysis process, we conclude that, for MLS strain and pressure data to be useful, both for the immediate experimental purpose and for future research and reference, an automatic system incorporating specialized computer software is vital. Without this, the extraction of maxima and minima from the waveform histories for numerous sensors, load passes, and collection windows will become prohibitively time consuming and labor intensive for continual use.

7.2 RECOMMENDATIONS

1. It is highly probable that the results of this study will remain valid for the MLS. However, because we used only a regular dump truck and not the MLS itself, we strongly recommend that the experiments be repeated using the MLS before full-scale testing begins.
2. Since no retrofitted gauges were included in the experiments, and since this may be the only method of strain and pressure data collection in existing pavements, we recommend that similar experiments be carried out for retrofitted gauges in order to at least assess different retrofit methods.
3. Based on the data analyzed in this study, we recommend that HBM DA3 be used for the collection of strain data in the future, that the sample rate be at least 100Hz for normal applications, and that at least 17 gauges be used for any single test pavement.

4. Again, based on the data obtained in this study, we recommend that Kulite pressure cells be used to record pressure (if required) using the sample rate that was used for the strain gauges. For a confidence interval for the mean of 10 percent, it appears from the study that as few as 9 gauges for top of subbase placement — or 17 gauges for top of subgrade — would be needed.
5. It is strongly recommended that installation procedures, both built-in and retrofit, be standardized and controlled so as to avoid excess variation. For built-in gauges, it is recommended that all gauges, at whatever depth, be installed at the time of construction of the layer above. This will prevent problems associated with the semi-retrofit of pressure cells.
6. It is recommended that the systematic data reduction, analysis, and storage process proposed and documented in the report be adopted. If the proposed process is adopted, however, it is further recommended that the process be automated and that software be written to extract maxima and minima from the response history waveforms and stored in a form usable in successive statistical analysis.
7. Finally, we recommend that a suitable database dedicated to MLS data be established in order to both standardize data collection and to store it in an easily accessible form for further future research.

REFERENCES

[Andrei 94] Andrei, R., A. R. Raab, and D. C. Esch, Evaluation of a Time Domain Reflectometry Technique for Seasonal Monitoring of Soil Moisture Content Under Road Pavement Test Sections, SHRP-P-689, Strategic Highway Research Program, Washington, D.C., 1994.

[AASHTO 93] *AASHTO Guide for Design of Pavement Structures*, American Association of State Highway Officials, Washington, D.C., 1993.

[Brown 77] Brown, S. F., *State-of-the-Art Report on Field Instrumentation for Pavement Experiments*, TRR 640, TRB, National Research Council, Washington, D.C., 1977.

[Campbell 95] Campbell Scientific, Inc., *Time Domain Reflectometry for Measurement of Soil Moisture and Electrical Conductivity*, 1995.

[Carey 62] Carey, W., and P. Irick, *The Pavement Serviceability-Performance Concept*, Highway Research Board Special Report 61E, AASHO Road Test, pp 291-306, 1962.

[Dempwolff 72] Dempwolff, R., and P. Sommer, *Comparison between Measured and Calculated Stresses and Strains in Flexible Road Structures*, Third International Conference on the Structural Design of Asphalt Pavements, Volume 1 Proceedings, 1972.

[Delft] Delft Outlook 89.4., *Lintrack: 10 Year's Traffic in a Month.*

[Haas 94] Haas, R., W. R. Hudson, and J. Zaniewski, *Modern Pavement Management,* Krieger Publishing Company, Florida, 1994.

[Huang 93] Huang, Y. H., *Pavement Analysis and Design,* Englewood Cliff, 1993.

[Hugo 91] Hugo F., B. F. McCullough, and B. Van der Walt, *Full-Scale Accelerated Pavement Testing for the Texas State Department of Highways and Public Transportation*, TRR 1293, TRB, National Research Council, Washington, D.C., 1991.

[Kim 95] Kim, R., O. Bradley, and Y. Lee, *Temperature Corrections of Deflections and Backcalculated Moduli,* TRB 74th Annual Meeting, Washington, D.C., 1995.

[Lu 91] Lu, J., C. Bertrand, and W. R. Hudson, *Evaluation and Implementation of the Automatic Road Analyzer (ARAN),* Research Report 1223-2F, Center for Transportation Research, The University of Texas, Austin Texas, July 1991.

[Mamlouk 95] Mamlouk, M. S., *An Overview of Pavement and Vehicle Dynamics*, TRB 74th Annual Meeting, Washington, D.C., 1995.

[McDaniel 94] McDaniel, M., and F. Hugo, *Use of the MMLS to Investigate Fatigue of Asphalt Pavements at Low Temperatures*, Research Report 1934-3F, Center for Transportation Research, The University of Texas, Austin, Texas, unpublished draft of January 1994.

[McNerney 94] McNerney, M. T., F. Hugo, and B. F. McCullough, *The Development of an Accelerated Pavement Test Facility for Florida Department of Transportation*, Research Report 997-3F, Center for Transportation Research, The University of Texas, Austin, Texas, May 1994.

[MLS 93] *Texas Mobile Load Simulator Project: Instrumentation Manual*, unpublished draft, June 1993.

[Mohammad 94] Mohammad, L. N., A. J. Puppala, and S. Kathavate, *Design and Reliability Assessment of Data Acquisition System for Louisiana Accelerated Loading Device*, TRR 1435, TRB, National Research Council, Washington, D.C., 1994.

[OECD 91] Organisation for Economic Co-Operation and Development, *OECD full-scale pavement test*, OECD, Paris, 1991.

[Omega 92] *The Pressure, Strain, and Force Handbook*, Vol. 28, Omega Engineering, Inc., Stamford, Connecticut, 1992.

[Ostle 88] Ostle, B., and L. Malone, *Statistics in Research,* 4th edition, Iowa State University Press, 1988.

[Rauhut 82] Rauhut, J. B., and T. Kennedy, *Characterizing Fatigue Life for Asphalt Concrete Pavements*, Transportation Research Board, Washington, D.C., 1982.

[Romero 92] Romero, R., A. Ruiz, and J. Perez, *First Test on the Centro de Estudios de Carreteras Test Track*, TRB 71st Annual Meeting, Washington, D.C., 1992.

[Rowe 95] Rowe, G. M., S. F. Brown, M. J. Sharrock, and M. G. Bouldin, *Visco-Elastic Analysis of Hot Mix Asphalt Pavement Structures*, TRB 74th Annual Meeting, Washington, D.C., 1995.

[Scazziga 87] Scazziga, I. F., A. G. Dumont, and W. Knobel, *Strain Measurements in Bituminous Layers*, Sixth International Conference, Structural Design of Asphalt Pavements, University of Michigan, July 1987.

[Sebaaly 89] Sebaaly, P., N. Tabatabaee, and T. Scullion, *Instrumentation for Flexible Pavements*, Publication No. FHWA-RD-89-084, Department of Transportation, August 1989.

[Sebaaly 92] Sebaaly, P., N. Tabatabaee, B. Kulakowski, and T. Scullion, *Instrumentation for Flexible Pavements — Field Performance of Selected Sensors*, Volume 1: Final Report, Publication No. FHWA-RD-91-094, Department of Transportation, June 1992.

[Ueber 94] Ueber, Eric J., D. W. Fowler, and R. L. Carrasquillo, *Implementation Manual for the Use of Bonding Materials for Piezoelectric Traffic Monitoring Sensors*, Research Report 2039-2F, Center for Transportation Research, The University of Texas, Austin, Texas, November 1994.

[Ullidtz 79] Ullidtz, P., and C. Busch, *Laboratory Testing of a Full-Scale Pavement: The Danish Road-Testing Machine*, TRR 715, Transportation Research Board, Washington, D.C., 1979.

[Zaffir 94] Zaffir, Z., R. Siddharthan, and P. E. Sebaaly, *Dynamic Pavement Strain Histories from Moving Traffic Load*, Journal of Transportation Engineering, Vol. 120, No. 5, October 1994.

APPENDIX

EXAMPLE RESPONSE HISTORIES FOR SLOW ROLL OVER TESTS

PAD #3: 174 hbm

11570 lbs., 5 mph, −0.69 ft

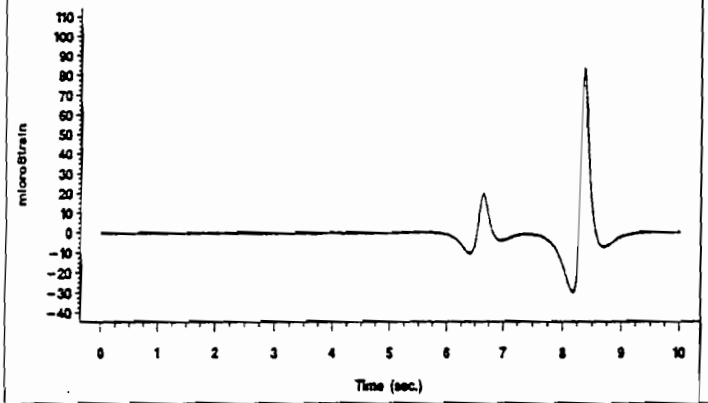

PAD #3: 141 Kulite

11570 lbs., 5 mph, +2.15 ft

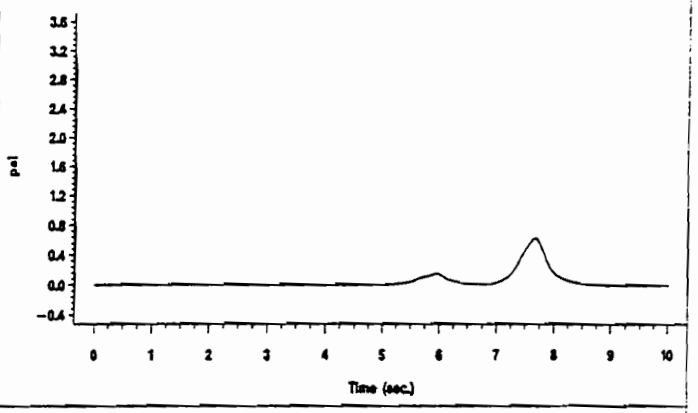

PAD #3: 175 hbm

11570 lbs., 5 mph, +0.47 ft

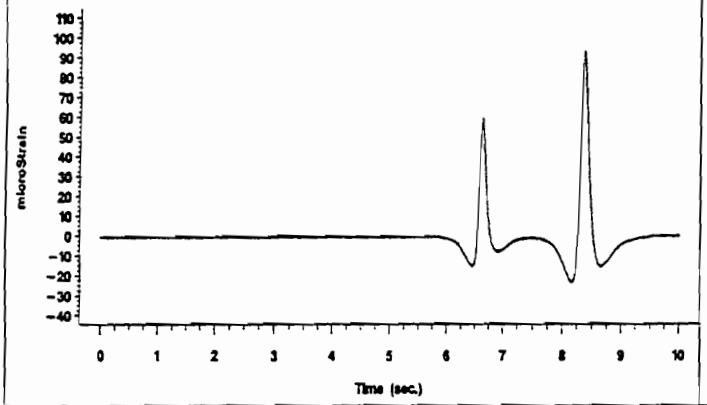

PAD #3: 142 Kulite

11570 lbs., 5 mph, +0.65 ft

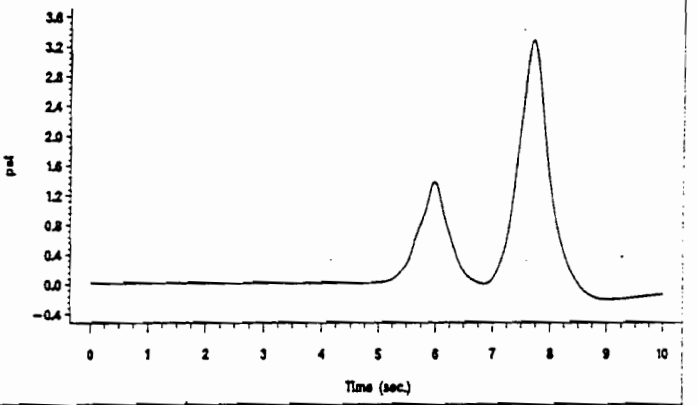

PAD #3: 176 hbm

11570 lbs., 5 mph, −0.53 ft

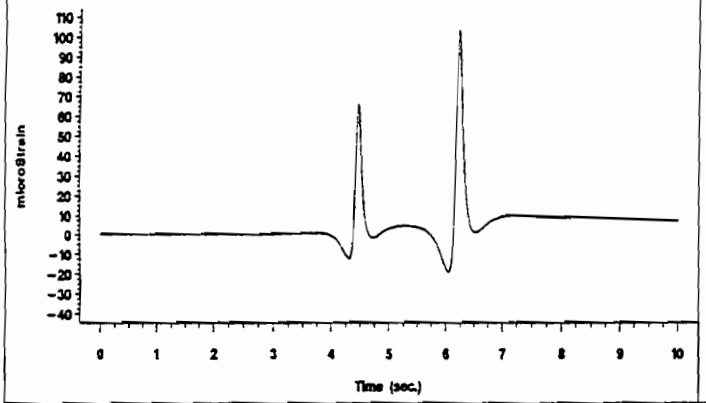

PAD #3: 143 Kulite

11570 lbs., 5 mph, −2.04 ft

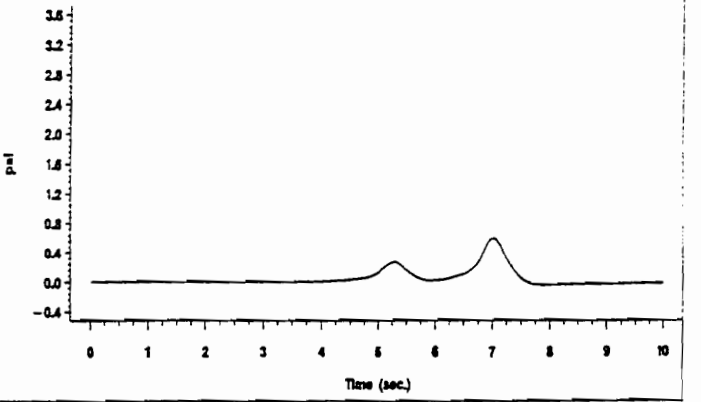

PAD #3: 177 hbm

11570 lbs., 5 mph, +0.64 ft

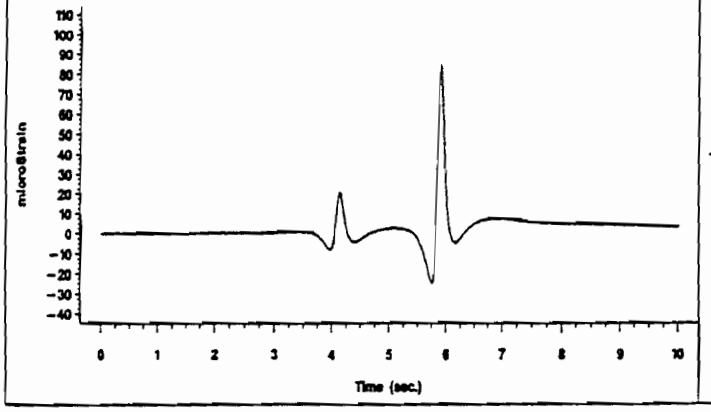

PAD #3: 222 Geokon

11570 lbs., 5 mph, −0.54 ft

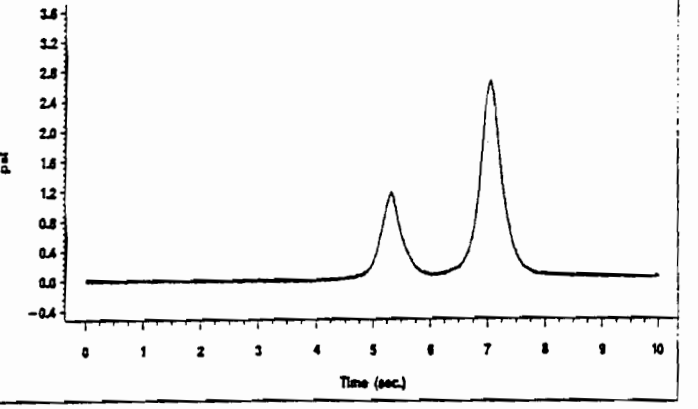

PAD #3: 223 Geokon

11570 lbs., 5 mph, +2.15 ft

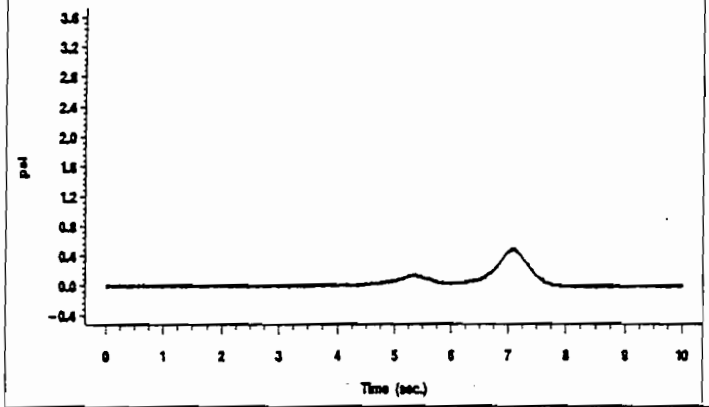

PAD #3: 024 PML-60

11570 lbs., 5 mph, -0.54 ft

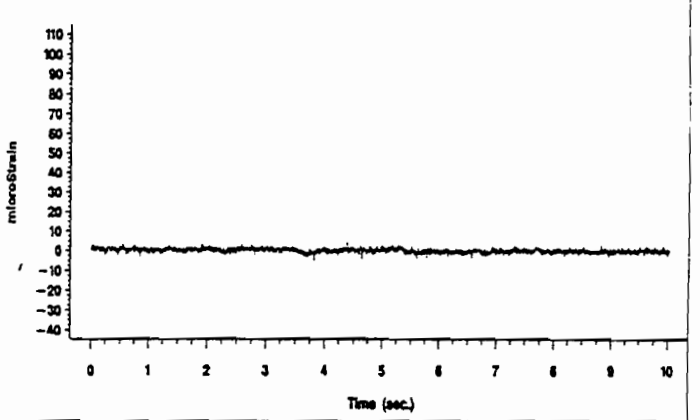

PAD #3: 019 PML-60

11570 lbs., 5 mph, +0.05 ft

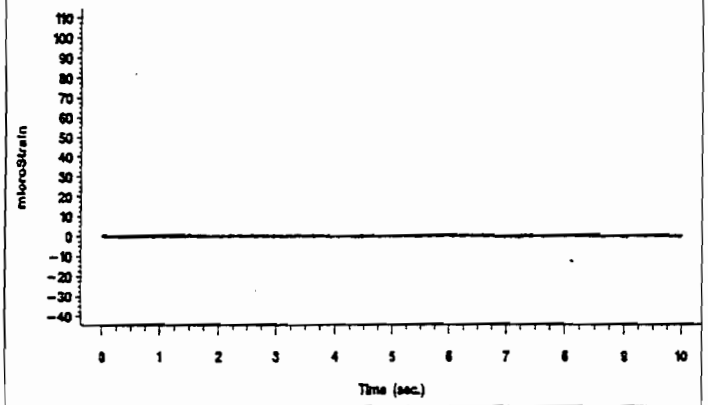

PAD #3: 065 PML-120

11570 lbs., 5 mph, +0.05 ft

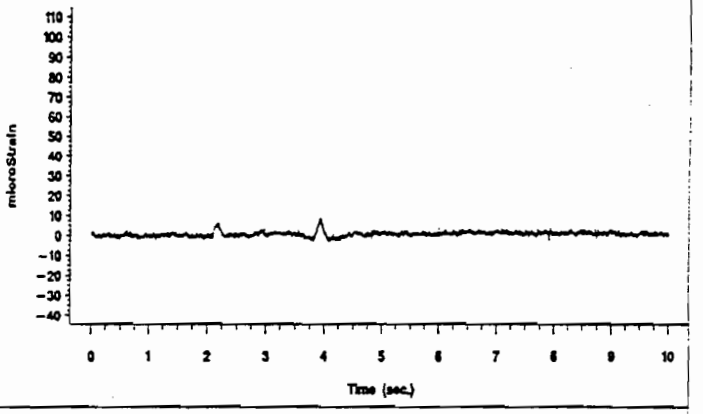

PAD #3: 020 PML-60

11570 lbs., 5 mph, -1.24 ft

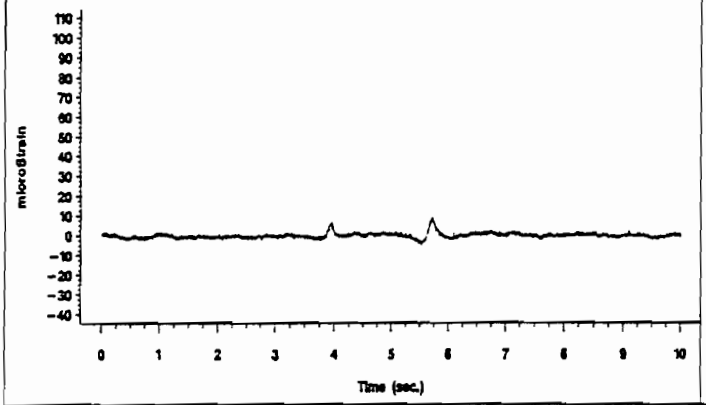

PAD #3: 066 PML-120

11570 lbs., 5 mph, -0.53 ft

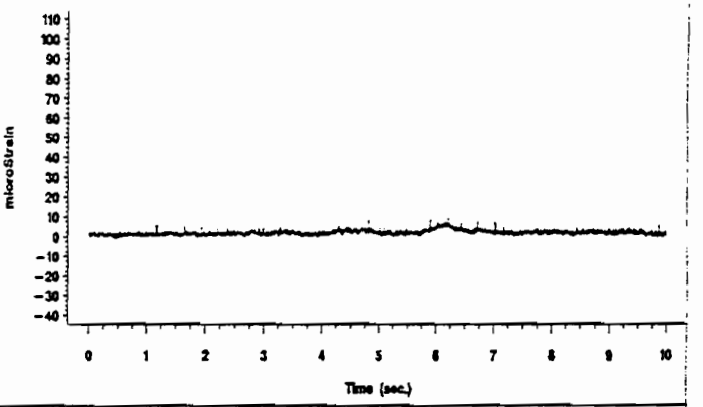

PAD #3: 023 PML-60

11570 lbs., 5 mph, +0.65 ft

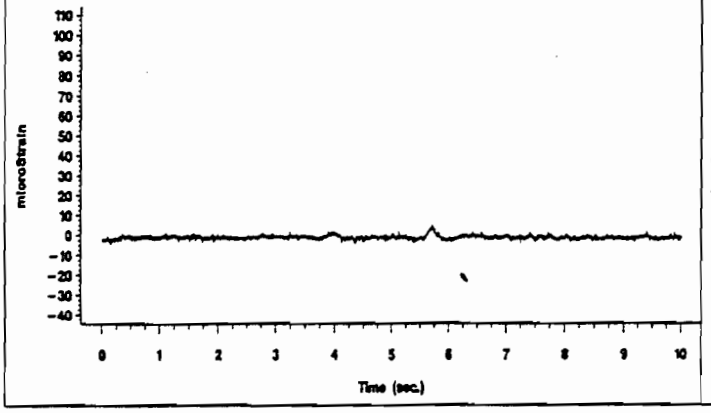

PAD #3: 095 Kyowa

11570 lbs., 5 mph, +0.65 ft

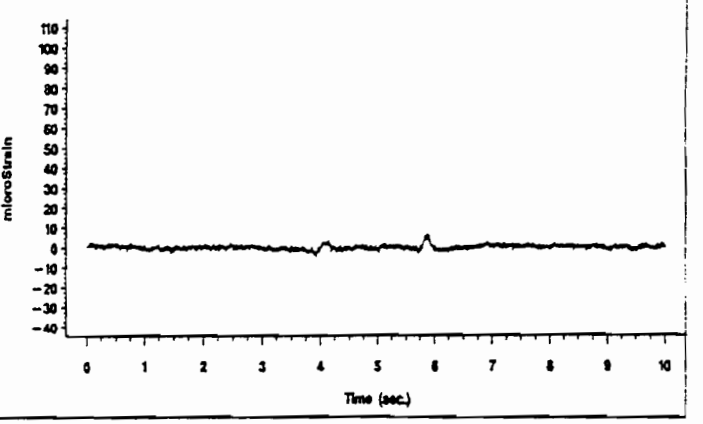

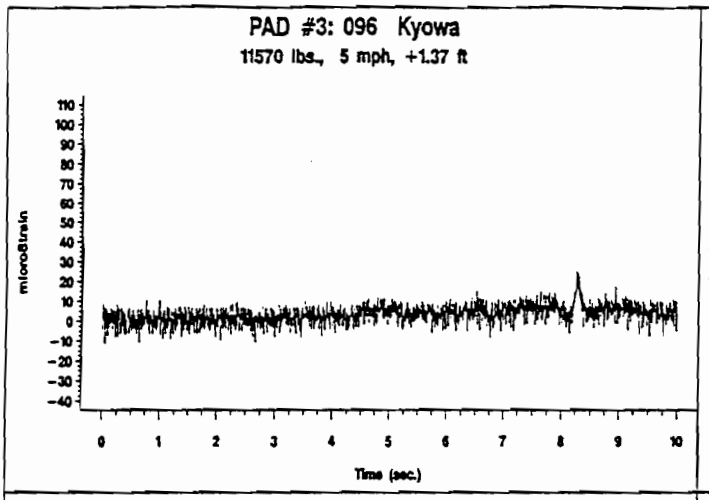
PAD #3: 096 Kyowa
11570 lbs., 5 mph, +1.37 ft
microStrain
Time (sec.)

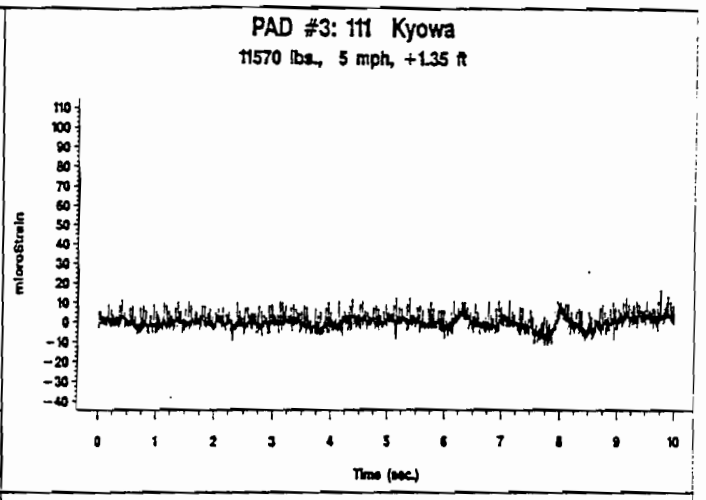
PAD #3: 111 Kyowa
11570 lbs., 5 mph, +1.35 ft
microStrain
Time (sec.)

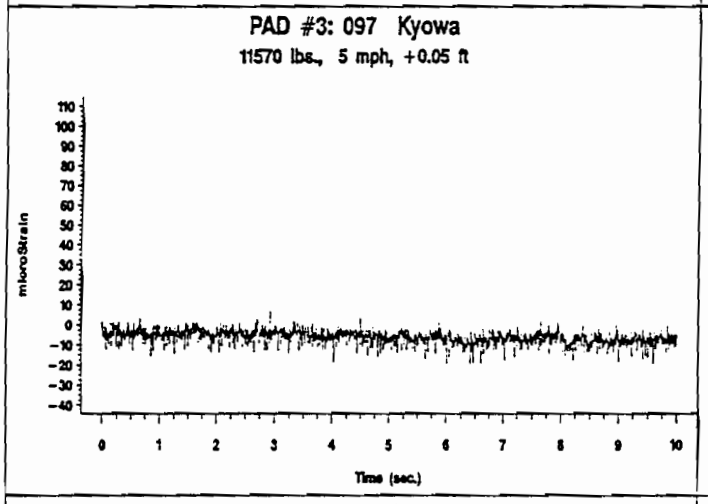
PAD #3: 097 Kyowa
11570 lbs., 5 mph, +0.05 ft
microStrain
Time (sec.)

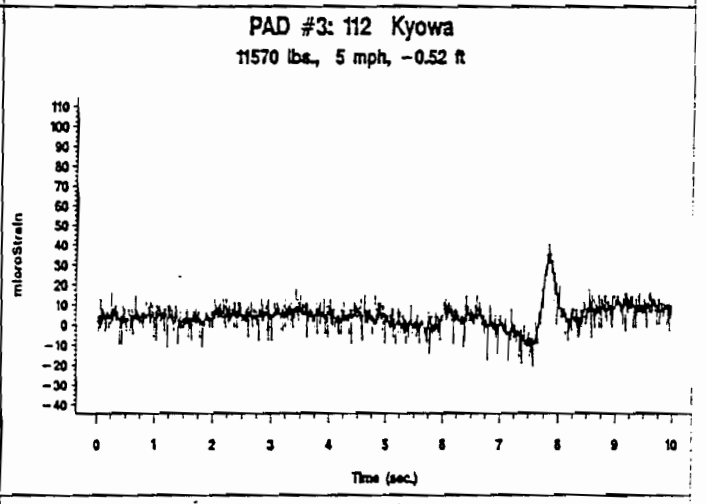
PAD #3: 112 Kyowa
11570 lbs., 5 mph, -0.52 ft
microStrain
Time (sec.)

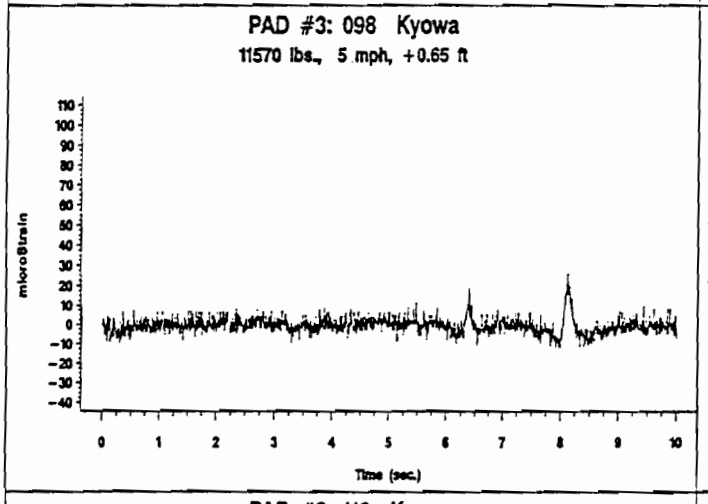
PAD #3: 098 Kyowa
11570 lbs., 5 mph, +0.65 ft
microStrain
Time (sec.)

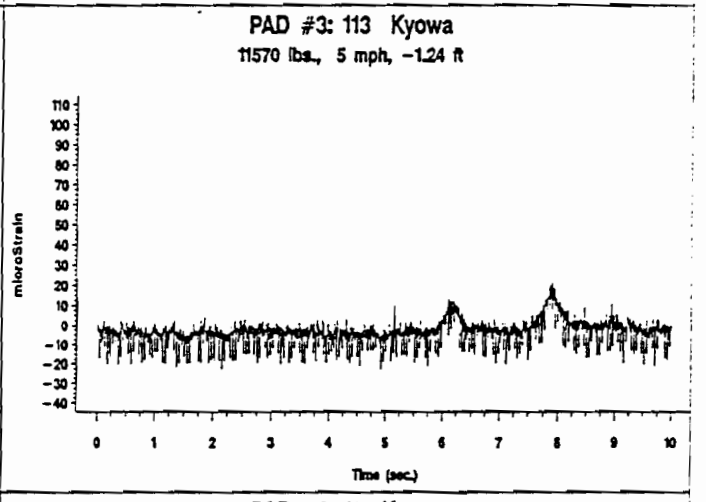
PAD #3: 113 Kyowa
11570 lbs., 5 mph, -1.24 ft
microStrain
Time (sec.)

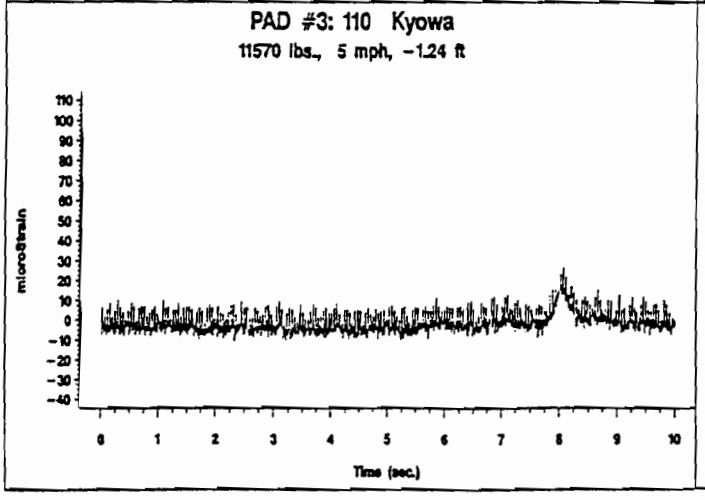
PAD #3: 110 Kyowa
11570 lbs., 5 mph, -1.24 ft
microStrain
Time (sec.)

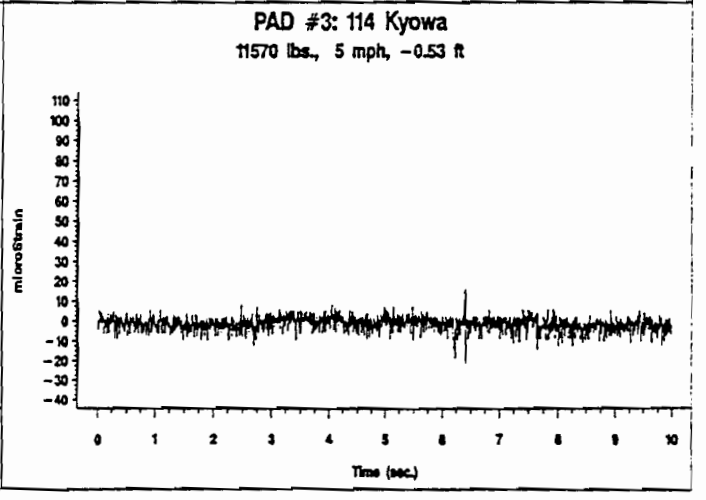
PAD #3: 114 Kyowa
11570 lbs., 5 mph, -0.53 ft
microStrain
Time (sec.)

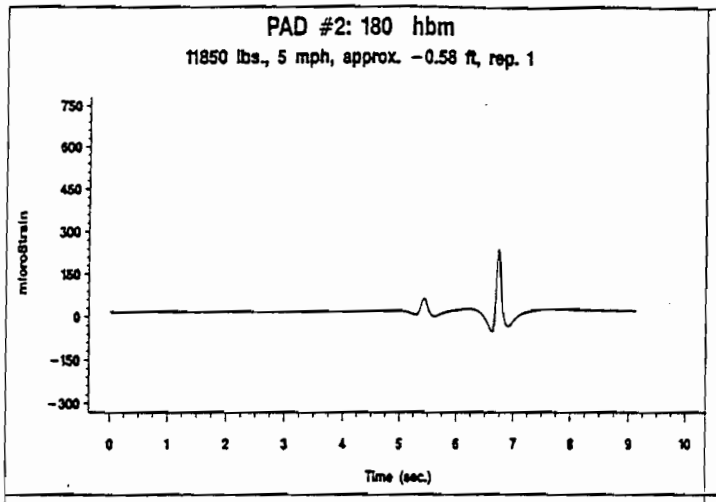
PAD #2: 180 hbm
11850 lbs., 5 mph, approx. −0.58 ft, rep. 1
microStrain
Time (sec.)

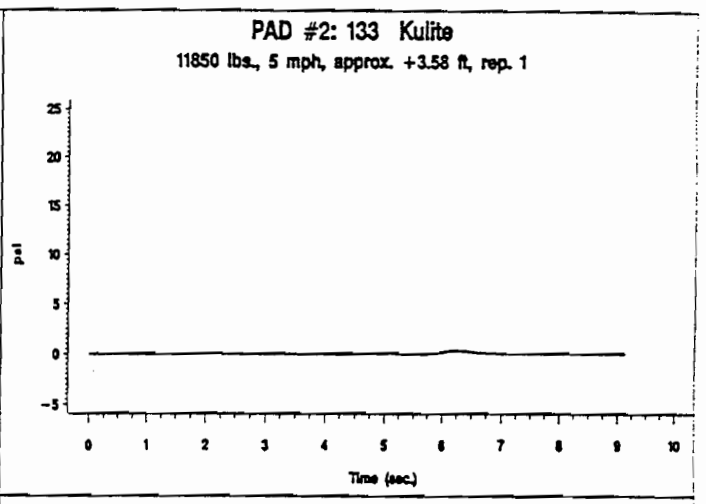
PAD #2: 133 Kulite
11850 lbs., 5 mph, approx. +3.58 ft, rep. 1
psi
Time (sec.)

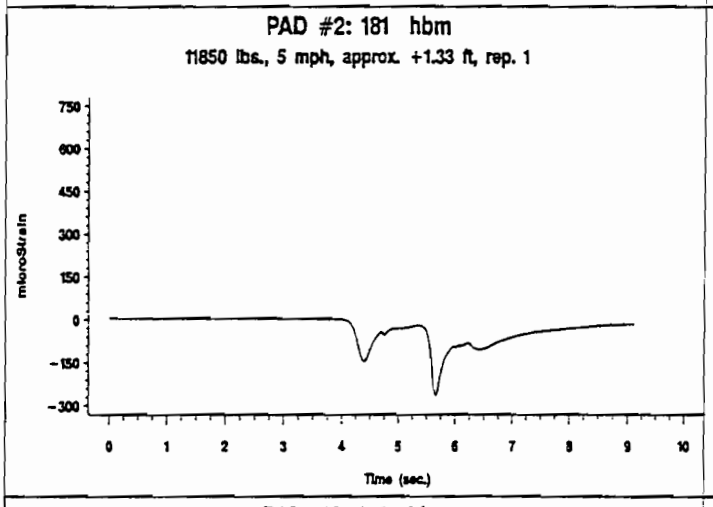
PAD #2: 181 hbm
11850 lbs., 5 mph, approx. +1.33 ft, rep. 1
microStrain
Time (sec.)

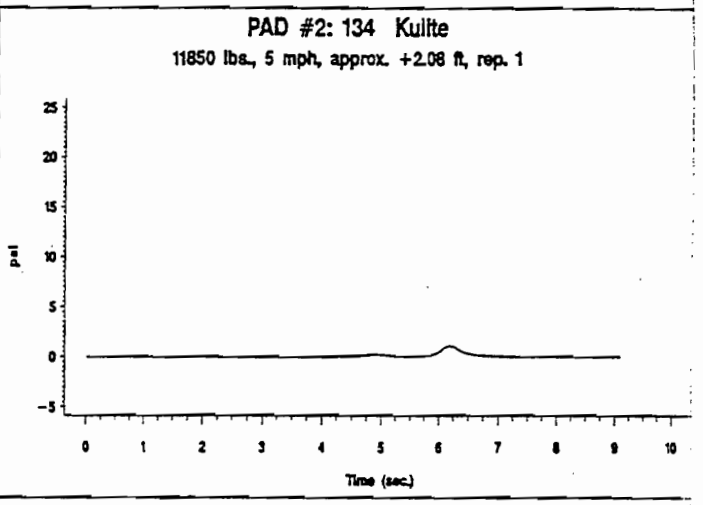
PAD #2: 134 Kulite
11850 lbs., 5 mph, approx. +2.08 ft, rep. 1
psi
Time (sec.)

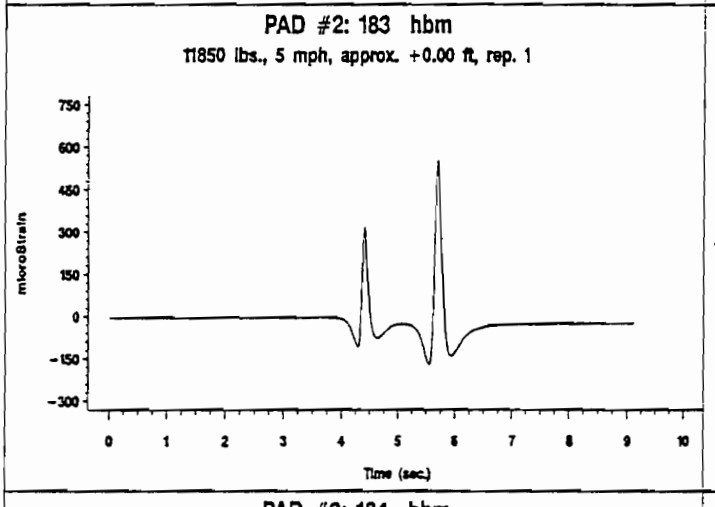
PAD #2: 183 hbm
11850 lbs., 5 mph, approx. +0.00 ft, rep. 1
microStrain
Time (sec.)

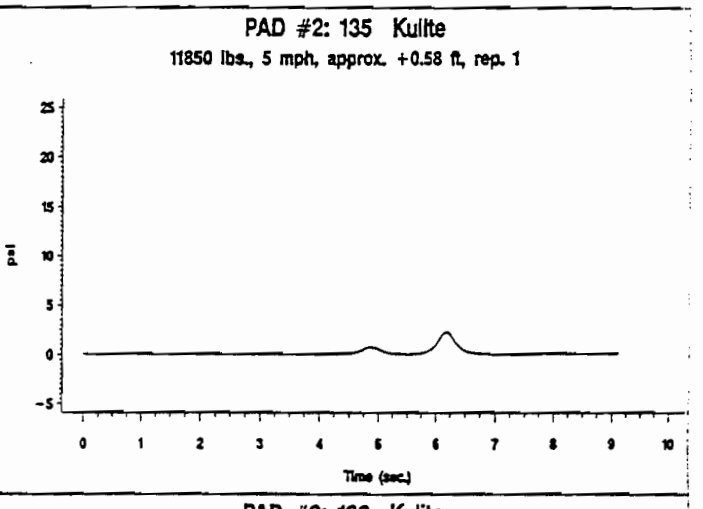
PAD #2: 135 Kulite
11850 lbs., 5 mph, approx. +0.58 ft, rep. 1
psi
Time (sec.)

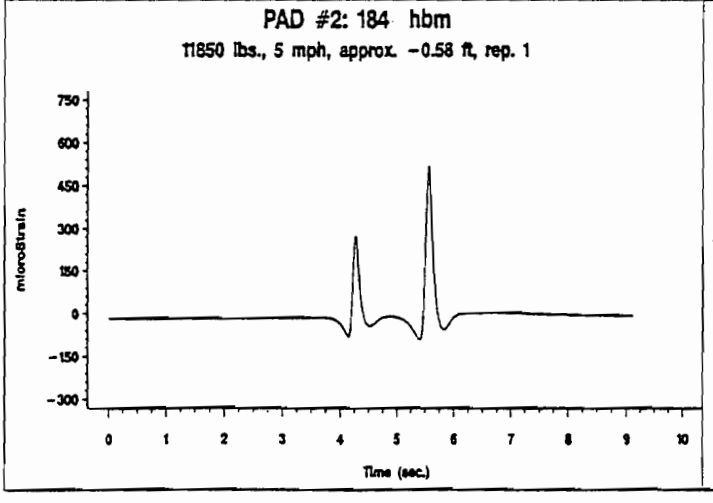
PAD #2: 184 hbm
11850 lbs., 5 mph, approx. −0.58 ft, rep. 1
microStrain
Time (sec.)

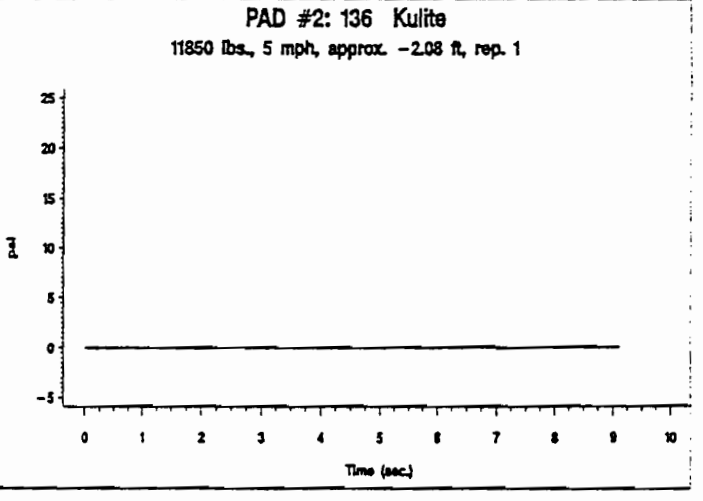
PAD #2: 136 Kulite
11850 lbs., 5 mph, approx. −2.08 ft, rep. 1
psi
Time (sec.)

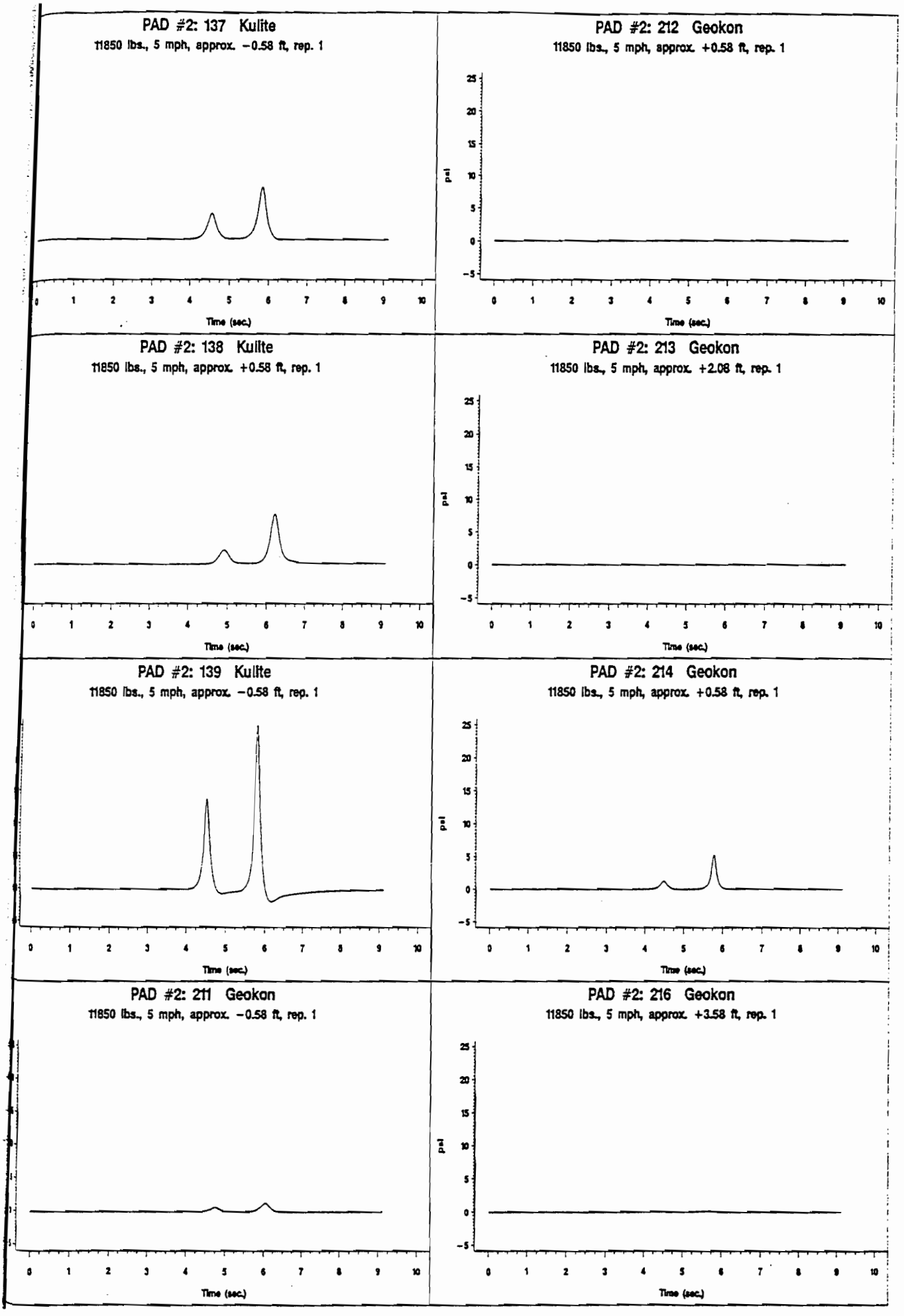
PAD #2: 137 Kulite
11850 lbs., 5 mph, approx. −0.58 ft, rep. 1
PAD #2: 212 Geokon
11850 lbs., 5 mph, approx. +0.58 ft, rep. 1
PAD #2: 138 Kulite
11850 lbs., 5 mph, approx. +0.58 ft, rep. 1
PAD #2: 213 Geokon
11850 lbs., 5 mph, approx. +2.08 ft, rep. 1
PAD #2: 139 Kulite
11850 lbs., 5 mph, approx. −0.58 ft, rep. 1
PAD #2: 214 Geokon
11850 lbs., 5 mph, approx. +0.58 ft, rep. 1
PAD #2: 211 Geokon
11850 lbs., 5 mph, approx. −0.58 ft, rep. 1
PAD #2: 216 Geokon
11850 lbs., 5 mph, approx. +3.58 ft, rep. 1
psi
Time (sec.)

PAD #2: 217 Geokon

11850 lbs., 5 mph, approx. -0.58 ft, rep. 1

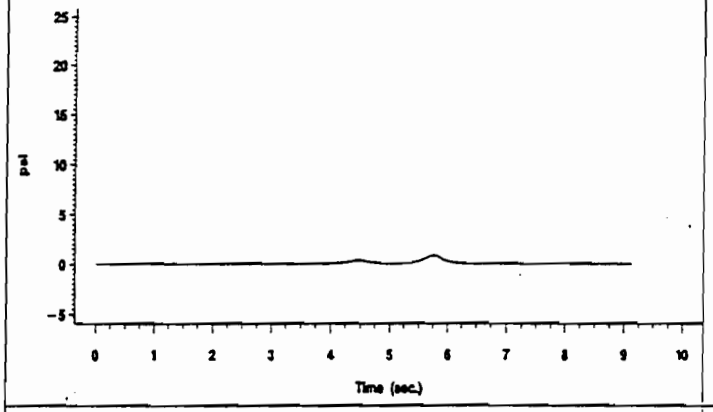

PAD #2: 027 PML-60

11850 lbs., 5 mph, approx. -0.58 ft, rep. 1

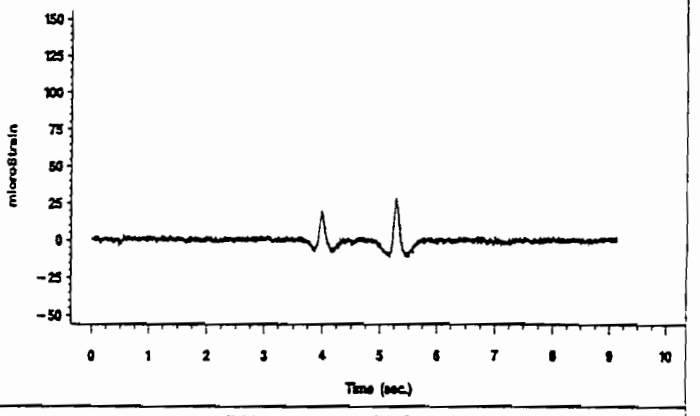

PAD #2: 218 Geokon

11850 lbs., 5 mph, approx. -2.08 ft, rep. 1

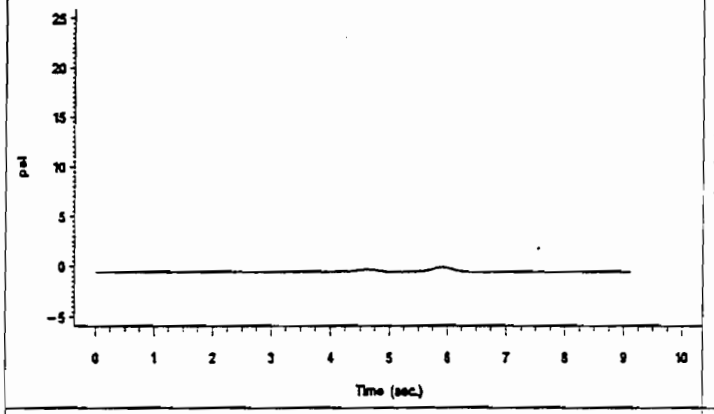

PAD #2: 028 PML-60

11850 lbs., 5 mph, approx. +1.33 ft, rep. 1

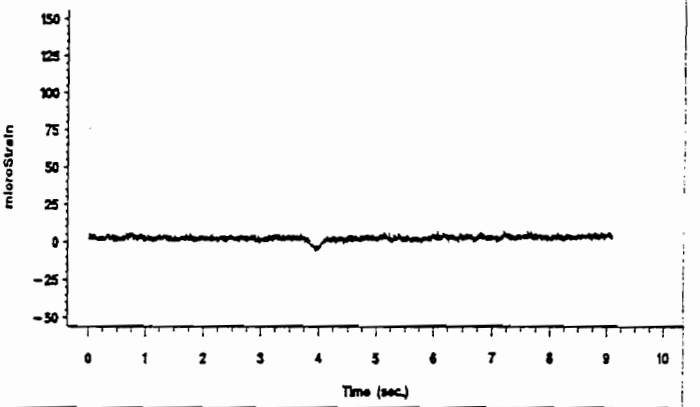

PAD #2: 025 PML-60

11850 lbs., 5 mph, approx. +0.00 ft, rep. 1

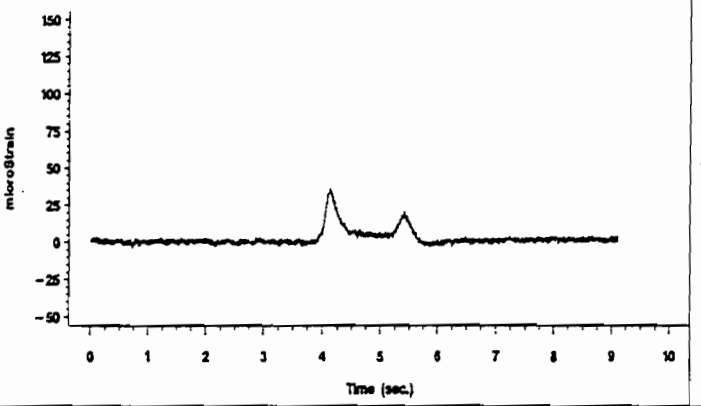

PAD #2: 029 PML-60

11850 lbs., 5 mph, approx. +1.33 ft, rep. 1

PAD #2: 026 PML-60

11850 lbs., 5 mph, approx. +0.58 ft, rep. 1

PAD #2: 031 PML-60

11850 lbs., 5 mph, approx. +0.00 ft, rep. 1

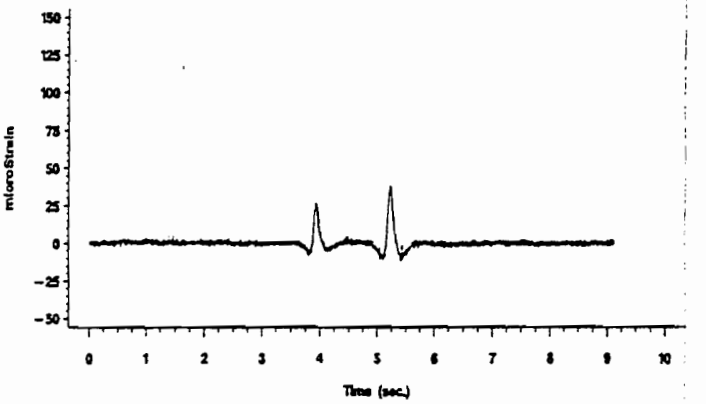

PAD #2: 032 PML-60

11850 lbs., 5 mph, approx. -0.58 ft, rep. 1

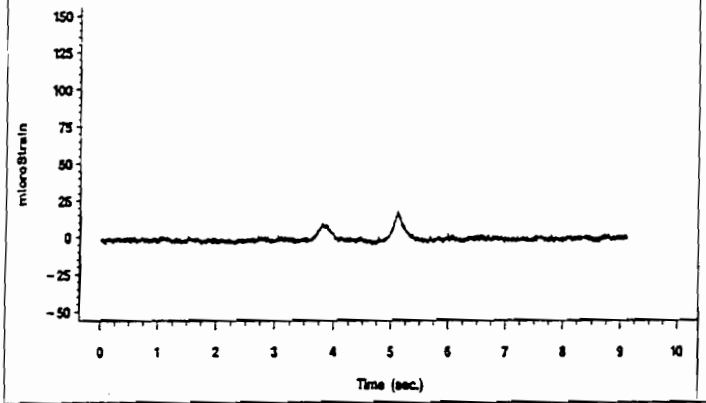

PAD #2: 038 PML-60

11850 lbs., 5 mph, approx. +0.58 ft, rep. 1

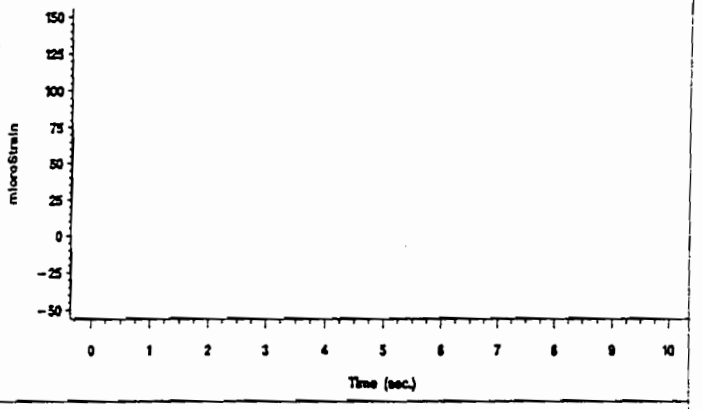

PAD #2: 034 PML-60

11850 lbs., 5 mph, approx. -0.58 ft, rep. 1

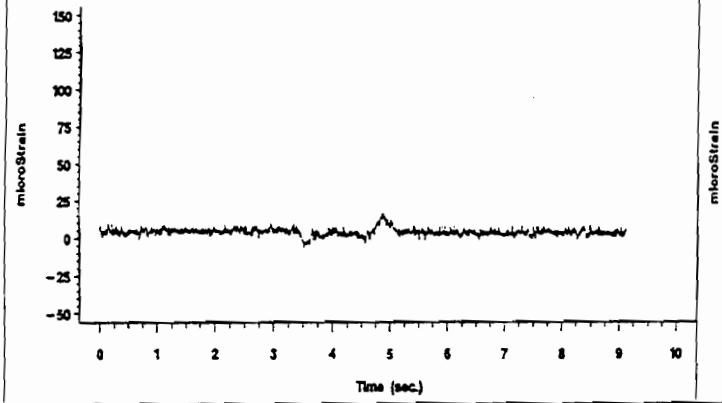

PAD #2: 040 PML-60

11850 lbs., 5 mph, approx. +0.58 ft, rep. 1

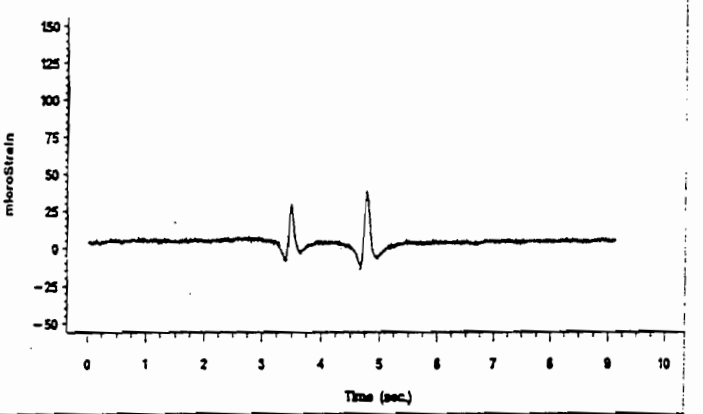

PAD #2: 035 PML-60

11850 lbs., 5 mph, approx. +1.33 ft, rep. 1

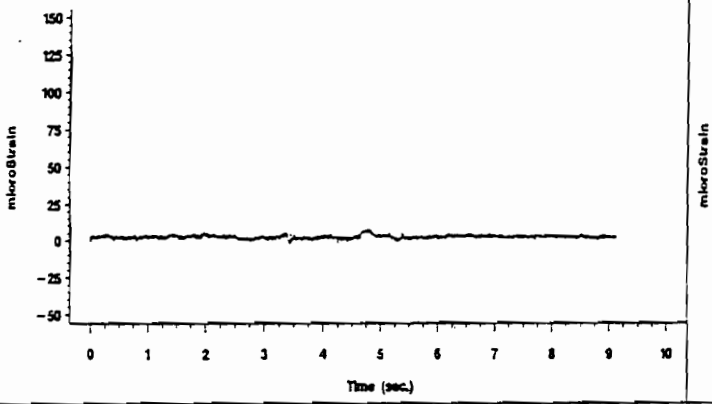

PAD #2: 041 PML-60

11850 lbs., 5 mph, approx. +0.58 ft, rep. 1

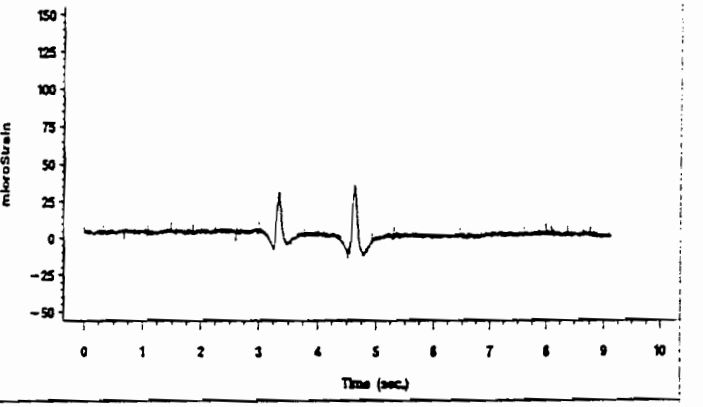

PAD #2: 036 PML-60

11850 lbs., 5 mph, approx. +0.58 ft, rep. 1

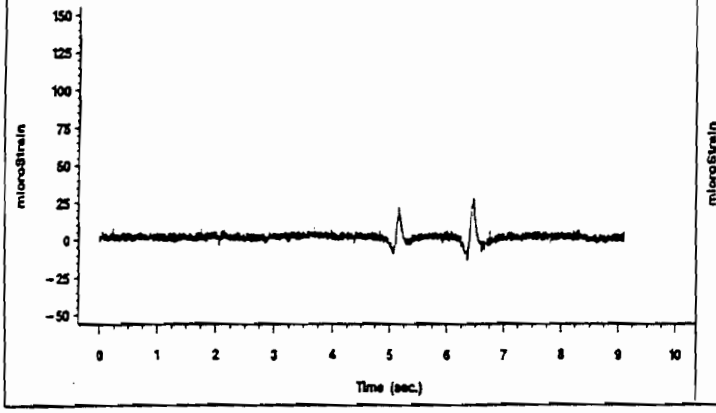

PAD #2: 043 PML-60

11850 lbs., 5 mph, approx. +0.00 ft, rep. 1

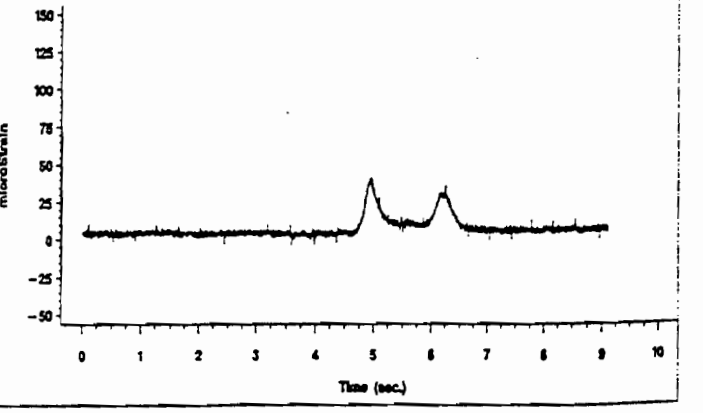

PAD #2: 044 PML-60

11850 lbs., 5 mph, approx. -1.33 ft, rep. 1

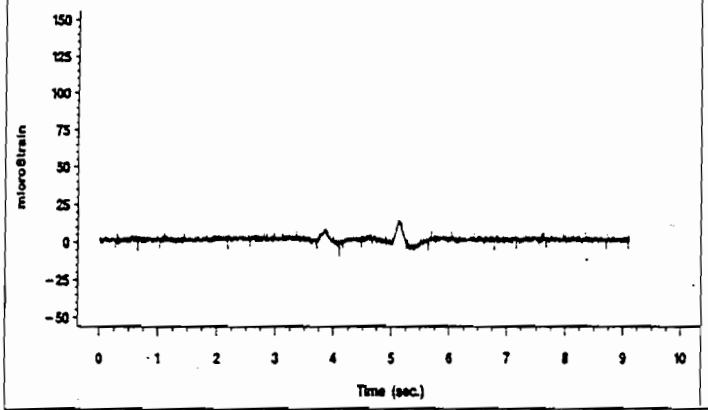

PAD #2: 061 PML-120

11850 lbs., 5 mph, approx. +1.33 ft, rep. 1

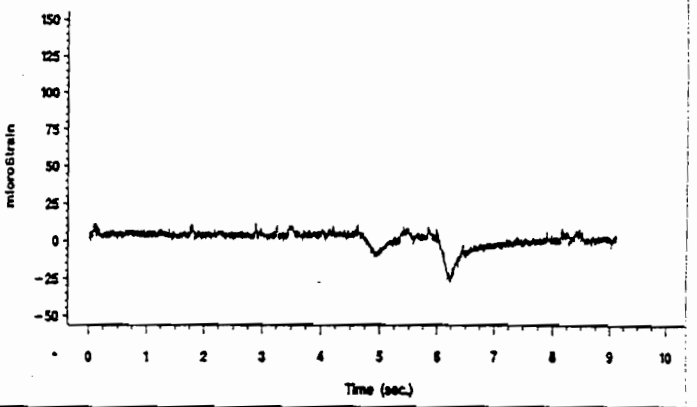

PAD #2: 045 PML-60

11850 lbs., 5 mph, approx. -1.33 ft, rep. 1

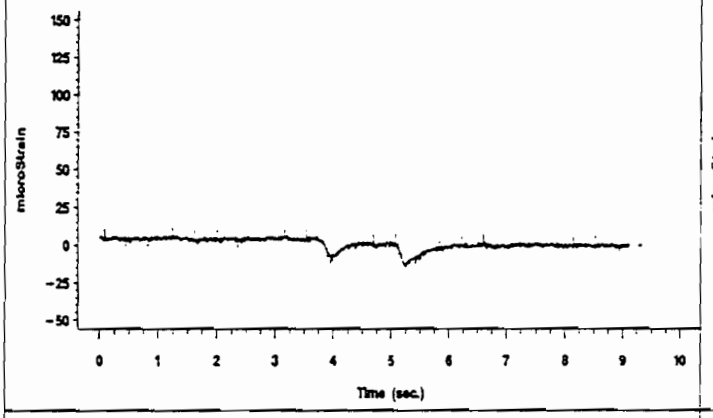

PAD #2: 080 Kyowa

11850 lbs., 5 mph, approx. +1.33 ft, rep. 1

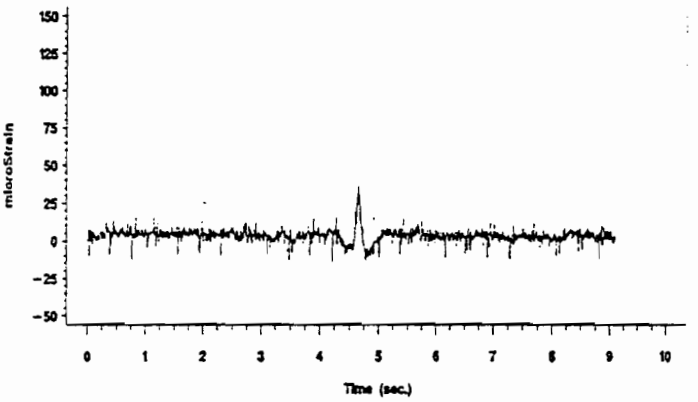

PAD #2: 046 PML-60

11850 lbs., 5 mph, approx. -1.33 ft, rep. 1

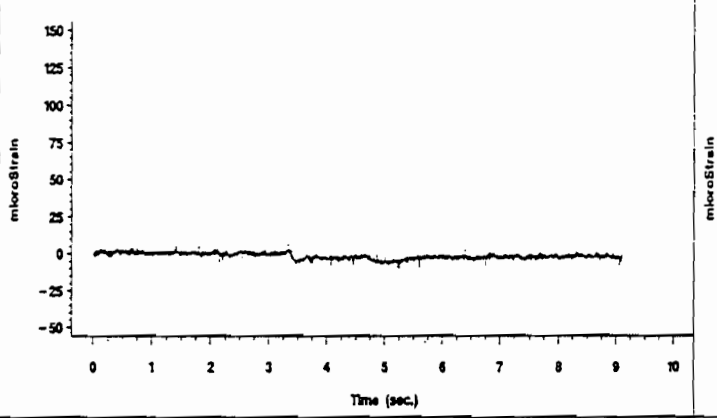

PAD #2: 082 Kyowa

11850 lbs., 5 mph, approx. +0.58 ft, rep. 1

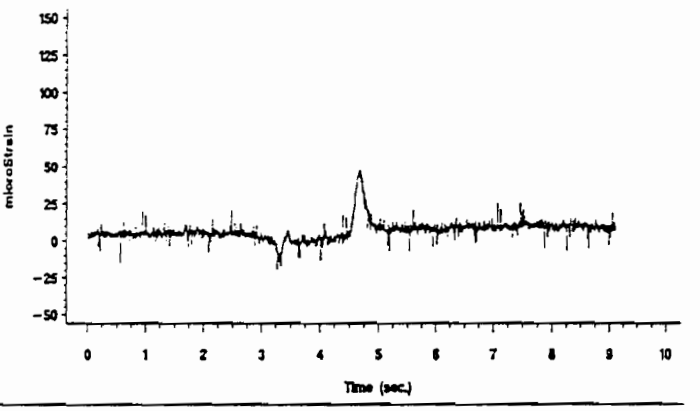

PAD #2: 049 PML-60

11850 lbs., 5 mph, approx. -1.33 ft, rep. 1

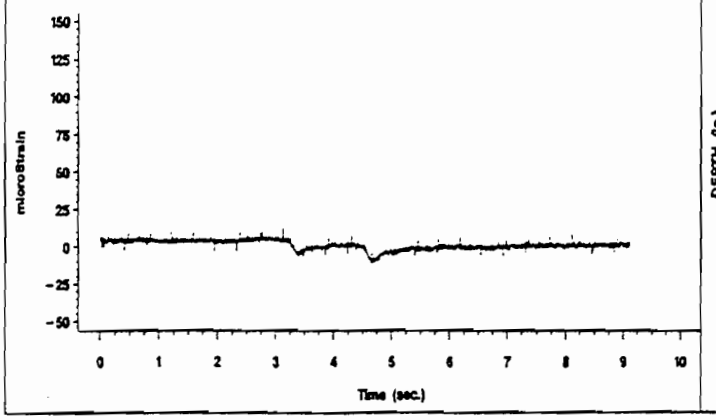

PAD #2: ThermoCouple Trees 1,3,4

11850 lbs., 5 mph, rep. 1

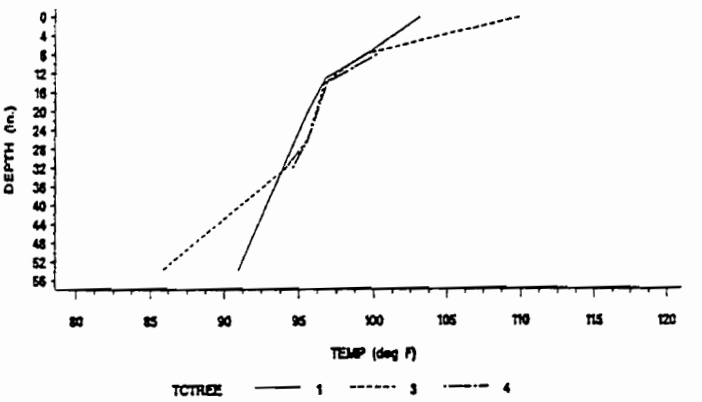

PAD #2: 181 hbm

11850 lbs. (rear axle), "Incr. static", approx. −0.58 ft

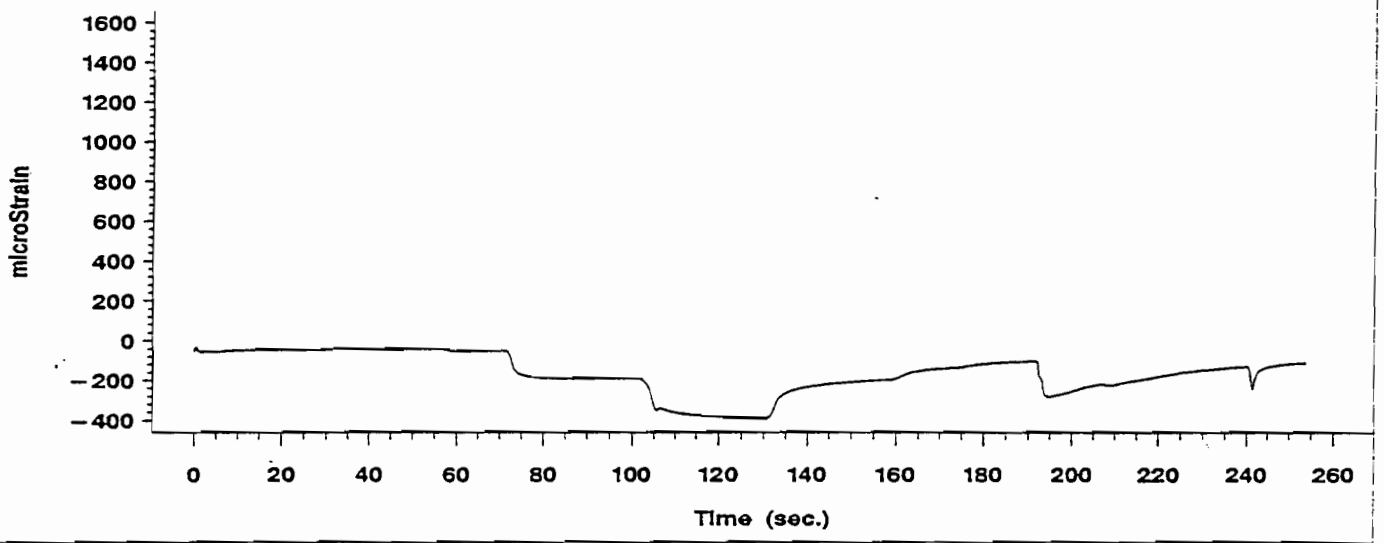

PAD #2: 183 hbm

11850 lbs. (rear axle), "Incr. static", approx. +1.33 ft

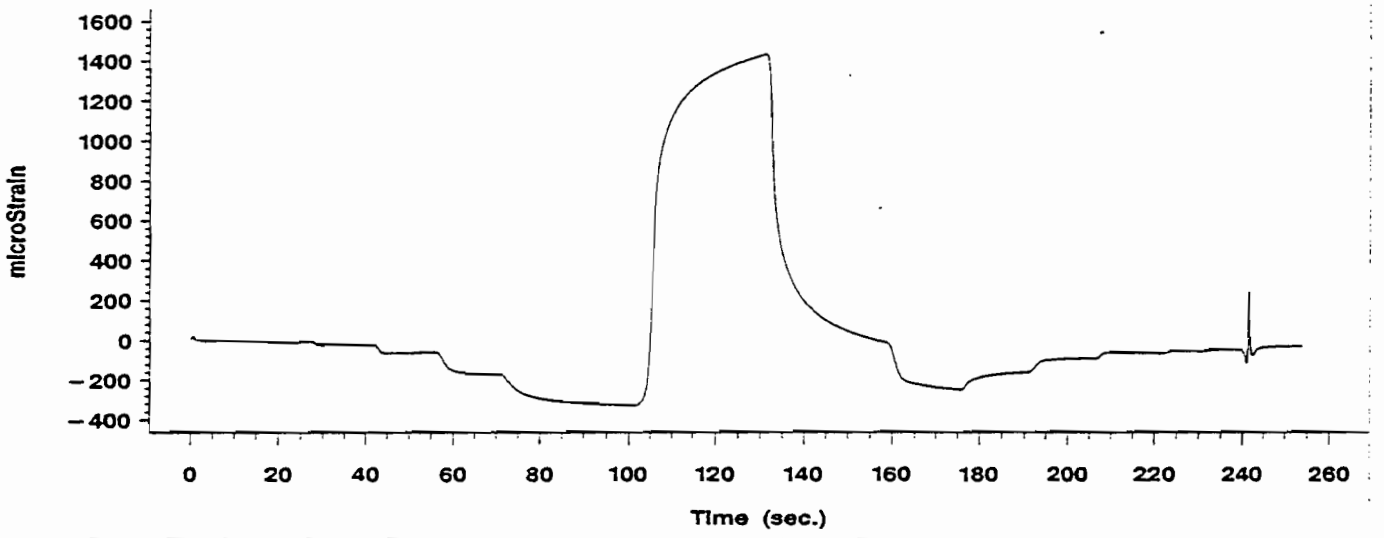

PAD #2: 184 hbm

11850 lbs. (rear axle), "Incr. static", approx. +0.00 ft